SCAFFOLDING FUNCTIONS OF MAGI-2 IN THE PTEN MEDIATED ATTENUATION OF THE PI3K/AKT SIGNALLING PATHWAY

A Thesis Submitted to the College of Graduate Studies and Research

in Partial Fulfilment of the Requirements for the Degree of

Master of Science

in the Department of Biochemistry

University of Saskatchewan

Saskatoon

by

Sharon Franceska Poland

PERMISSION TO USE

In presenting this thesis in partial fulfilment of the requirement for a Post graduate degree from the University of Saskatchewan, I agree that the Libraries of this University may make it freely available for inspection. I further agree that permission for copying of this thesis in any manner, in whole or in part, for scholarly purposes may be granted by my Post graduate supervisor, Dr. Deborah Anderson, or in her absence, by the Head of the Department of Biochemistry or the Dean of the College of Graduate Studies and Research. It is understood that any copying or publication, or use of this thesis or parts thereof for financial gain shall not be allowed without my written permission. It is also understood that due recognition shall be given to me and to the University of Saskatchewan in any scholarly use which may be made of any material in my thesis.

Request for permission to copy or to make other use of material in this thesis in whole or part should be addressed to:

Dr. Deborah Anderson

Saskatchewan Cancer Agency

Cancer Research Unit

20 Campus Drive

University of Saskatchewan

Saskatoon, Saskatchewan

S7N 4H4

Canada

ABSTRACT

Activated receptor tyrosine kinase (RTK), such as the epidermal growth factor (EGF) receptor (EGFR) and the platelet-derived growth factor (PDGF) receptor (PDGFR), recruit downstream signalling proteins, including phosphatidylinositol 3-kinase (PI3K). PI3K, composed of a regulatory p85 subunit and a catalytic p110 subunit, phosphorylates phosphatidylinositol 4,5-bisphosphate at the 3 position to generate phosphatidylinositol 3,4,5-trisphosphate. This lipid second messenger activates Akt, which promotes cell growth, cell cycle entry and progression, as well as cell survival and cellular migration. PTEN, a tumor suppressor protein, dephosphorylates phosphatidylinositol 3,4,5-trisphosphate at the 3 position, turning off Akt signalling. PTEN contains a C-terminal PDZ binding motif that binds to the PDZ2 domain of MAGI-2, a scaffolding protein that localizes signalling molecules to the plasma membrane. MAGI-2 has ten domains that potentially mediate multiple protein-protein interactions simultaneously. A PTEN associated-complex (PAC) has been described and may contain MAGI-2, PTEN and p85. The PAC is hypothesized to form at the plasma membrane at appropriate sites for PTEN to gain access to its lipid substrates, since the binding of PTEN to MAGI-2 has been shown to enhance the suppression of PI3K-mediated Akt signalling. In order to better understand the role of the PAC in attenuation of the Akt signalling pathway, regions of the MAGI-2 scaffolding protein were mapped to identify the interactions taking place in the PAC. MAGI-2, and its individual domains, were expressed as GST fusion proteins. These were immobilized onto beads and allowed to bind to cellular proteins including PTEN, p85, PDGFR and EGFR using a GST pull-down experiment. The proteins bound to GST-MAGI-2 were identified using an immunoblot analysis. *In vitro* pull-down experiments revealed that MAGI-2 PDZ2 and PDZ5 domains bind to PTEN, and both MAGI-2 WW domains were shown to bind to p85. EGFR and PDGFR did not bind to the PDZ domains of MAGI-2 under the conditions studied. In order to study protein-protein interactions in cells, immunoprecipitation assays were also performed. Full length MAGI-2 was expressed tagged to a Myc epitope. This was used in immunoprecipitation assays to determine if MAGI-2 could co-immunoprecipitate with proteins involved in the Akt signalling pathway, such as PTEN, p85, PDGFR and EGFR. MAGI-2 can co-immunoprecipitate with PTEN upon 5 min EGF stimulation however, this result was inconclusive because replicate experiments did not verify this initial observation. MAGI-2 does not co-immunoprecipitate with the EGFR nor p85, under the conditions tested.

We examined for these interactions after 5 min of growth factor stimulation and more experiments that test different time points after growth factor stimulation would reveal if these interactions are present at shorter time points. MAGI-2 has been shown to bind to PTEN and p85 *in vitro* and therefore has the potential to regulate the attenuation of the PI3K/Akt signalling pathway in response to activated EGFR and/or PDGFR.

ACKNOWLEDGMENTS

I would first and foremost like to thank my supervisor Dr. Deborah Anderson. Her patience and guidance throughout my project was truly appreciated. She is an incredible teacher who always finds time to consult with her students and is always ready to help in any way that she can. Her support and encouragement in my teaching was greatly appreciated.

I would also like to thank my advisory committee Dr. Khandelwal, Dr. Roesler, and Dr. Moore. The constructive critiques, ideas and encouragement I received throughout my research career were truly invaluable and it has taught me to keep an open mind when it comes to scientific learning and research. I would also like to extend my thanks to those supporting me in providing me with many teaching opportunities throughout my Masters career.

I would also like to thank the past and present members of the Anderson laboratory and the Cancer Research Unit at the Saskatchewan Cancer Agency. Thank you so much for your kindness and friendship, and making the laboratory a great place to work.

Last, but not least, I would like to thank my family and friends for all of their support throughout my studies at the University of Saskatchewan.

This work is dedicated to my family

who supported me through my entire University career:

Patricia Jones

Abraham Poland

Sherri-Lynn Poland

Jacob Poland

TABLE OF CONTENTS

LIST OF TABLES

Page

LIST OF FIGURES

Page

LIST OF ABBREVIATIONS

cDNA	complementary DNA
DMEM	Dulbecco's Modified Eagle Medium
dNTP	deoxyribonucleoside triphosphate
E. coli	*Escherichia coli*
EGF	epidermal growth factor
EGFR	epidermal growth factor receptor
FBS	fetal bovine serum
FL	full length (in reference to MAGI-2 only)
GARP	Gly, Ala, Arg and Pro domain of MAGI-2
GK	guanylate kinase
GST	glutathione S-transferase
HA	hemagglutinin (tag)
HNTG	HEPES, NaCl, Triton X-100 and glycerol containing wash buffer
HRP	horseradish peroxidase
IgG	immunoglobin G
IgG-AC	immunoglobin G agarose conjugated
IPTG	isopropyl-β-D-thiogalactopyranoside
KOD	*Thermococcus kodakaraensis*
LB	Luria Broth
LBA	Luria Broth containing ampicillin

MAGI	membrane associated guanylate-kinase inverted
MAGUK	membrane associated guanylate-kinase homologous
MBP	maltose binding protein
NEDD4	neural precursor cell expressed developmentally down-regulated 4
NHERF	Na^+/H^+ exchanger regulatory factor
PAC	PTEN-associated complex
PCR	polymerase chain reaction
PDGF	platelet-derived growth factor
PDGFR	platelet-derived growth factor receptor
PDZ	PSD-95, Disc-large, ZO-1 homologous
Pfu	*Pyrococcus furiosus*
$PI3,4P_2$	phosphatidylinositol (3,4) bisphosphate
$PI4,5P_2$	phosphatidylinositol (4,5) bisphosphate
$PI3,4,5P_3$	phosphatidylinositol (3,4,5) trisphosphate
PI3K	phosphatidylinositol 3-kinase
P/S	penicillin and streptomycin
PTEN	phosphatase with tensin homology on chromosome 10
RTK	receptor tyrosine kinase
RT-PCR	reverse transcriptase polymerase chain reaction
SDS	sodium dodecyl sulphate
SDS-PAGE	sodium dodecyl sulphate-polyacrylamide gel electrophoresis

SH	Src homology
TBST	Tris buffered saline with tween-20
YGK	yeast guanylate kinase

1.0 INTRODUCTION

1.1 Receptor tyrosine kinase activated PI3K/Akt signalling pathway

Receptor tyrosine kinases (RTKs) are cell surface receptors that are capable of receiving signals from outside the cell and transmitting these signals intracellularly to generate an appropriate, transient cellular response. RTKs are unique from other cell surface receptors in that they have intrinsic protein tyrosine kinase activity. RTKs share a similar domain structure composed of an extracellular ligand binding domain, a single α-helical *trans*-membrane domain and a cytoplasmic domain containing the intrinsic tyrosine kinase activity with autophosphorylation sites (reviewed in Ogiso *et al.,* 2002; Schlessinger, 2002). Upon binding of the ligand to its respective receptor, a conformational change occurs that promotes receptor dimerization (Garrett *et al.,* 1998, 2002; Ogiso *et al.,* 2002). Dimerization of the receptor induces a *trans* autophosphorylation event of the cytosolic domain (reviewed in Ferguson, 2008). The phosphorylated Tyr residues in the cytoplasmic domain of RTKs are docking sites for downstream signalling molecules that are recruited to the newly phosphorylated receptor, which are then activated and allows for further downstream signalling.

Two main families of RTKs are the epidermal growth factor receptor (EGFR) and the platelet-derived growth factor receptor (PDGFR). One of the many pathways that are activated by these receptors is the PI3K/Akt signalling pathway, which promotes cell cycle entry and progression, cellular survival, cellular migration and cell growth (Figure 1.1). Upon epidermal growth factor (EGF) stimulation, EGFR subunits dimerize and autophosphorylation occurs on the Tyr residues of the cytosolic domain (reviewed in Pawson and Scott, 2005). Phosphorylated receptor recruits the phosphatidylinositol 3-kinase (PI3K) complex to the plasma membrane through binding of an adaptor protein, growth factor receptor-binding protein 2 associated binder 1 (reviewed in Hirano and Nishida, 2003; Schlessinger, 2002). The PI3K complex is made up of the p85 regulatory subunit, bound to the p110 catalytic subunit (Ueki *et al.,* 2002). Binding of p110 to the p85 subunit of PI3K is required for p110 stability and proper PI3K function (reviewed in Geering *et al.*, 2007). Upon binding of the PI3K to EGFR, p85 inhibitory effects on p110 are relieved and p110 phosphorylates phosphatidylinositol (4,5) bisphosphate ($PI4,5P_2$) on the 3 position to generate

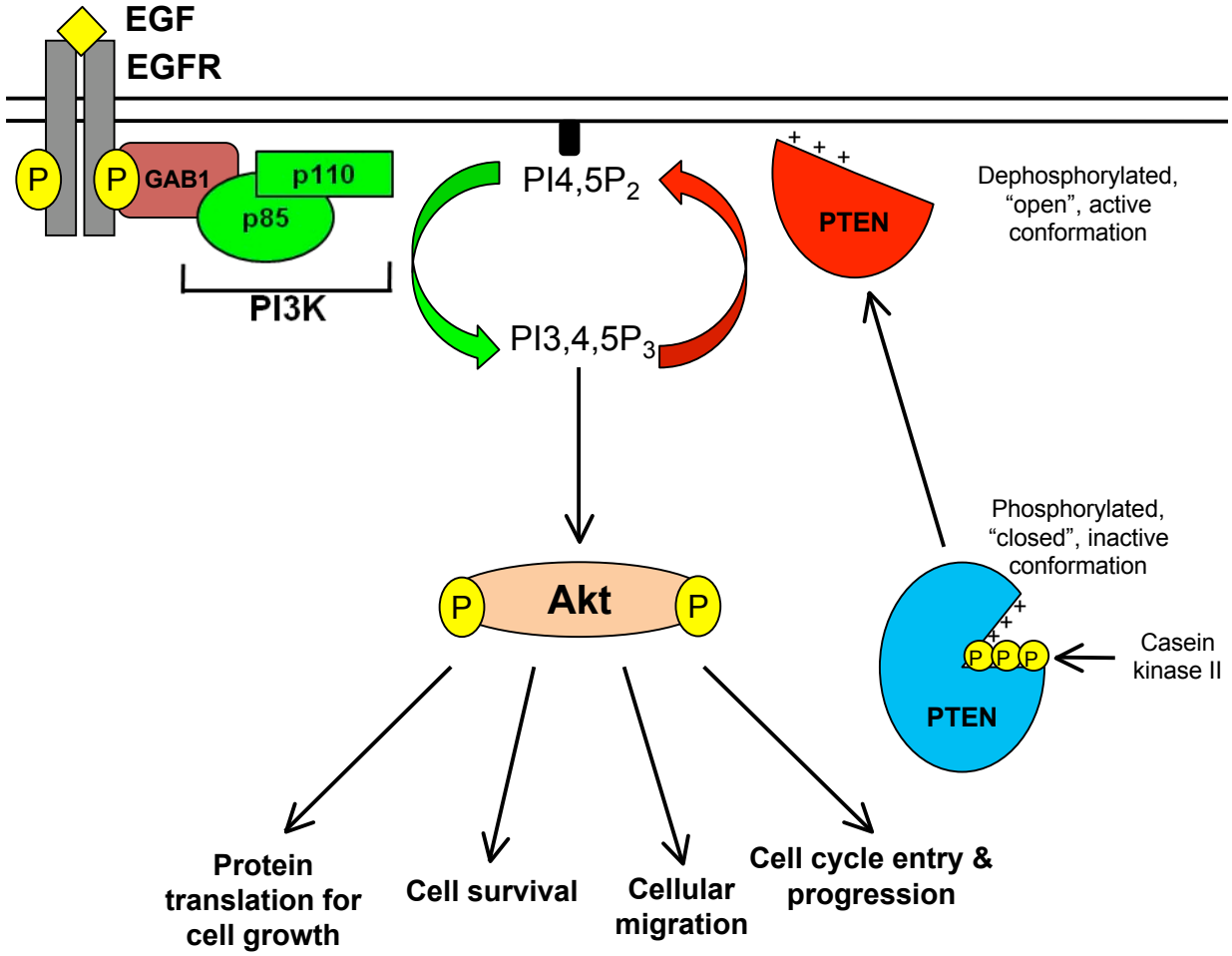

Figure 1.1: EGFR activates the PI3K/Akt signalling pathway that promotes cell cycle entry and progression, as well as cell survival. Upon EGF stimulation, EGFR subunits dimerize and autophosphorylation occurs on Tyr residues. Phosphorylated receptor recruits the PI3K complex to the plasma membrane by association to the (growth factor receptor-binding protein 2 associated binder 1) GAB1 adaptor protein. The PI3K complex phosphorylates $PI4,5P_2$ to $PI3,4,5P_3$. The lipid second messenger $PI3,4,5P_3$ is involved in the recruitment and activation of the Ser/Thr kinase Akt. Akt signalling regulates the phosphorylation of many downstream proteins, such as those that promote cell cycle entry, cell growth, cellular survival and cellular migration. In quiescent cells, PTEN is hypothesized to be in its closed, inactive conformation. Inactive PTEN is constitutively phosphorylated in the regulatory domain by casein kinase II. This closed conformation is hypothesized to mask the positively charged residues of the C2 domain and the PDZ binding motif. Upon growth factor stimulation, PTEN is dephosphorylated and in its open conformation. Positively charged residues and the PDZ binding motif are exposed and PTEN is localized to the plasma membrane, where its lipid phosphatase activity is turned on. At the plasma membrane, PTEN dephosphorylates $PI3,4,5P_3$ back to $PI4,5P_2$, counteracting PI3K activity, blocking cell growth and survival effects of the activated PI3K/Akt pathway.

phosphatidylinositol (3,4,5) trisphosphate ($PI3,4,5P_3$) (Ueki *et al.,*2002). The lipid second messenger $PI3,4,5P_3$ recruits and activates phosphoinositide-dependent protein kinase-1, which is responsible for the activation of the Ser/Thr kinase Akt (Ueki *et al.,* 2002). The Akt signalling pathway initiates the phosphorylation of many downstream proteins that promote anti-apoptotic signalling. Activation of EGFR results in the the phosphorylation and activation of the PI3K/Akt signalling pathway that leads to cellular survival, cell cycle entry and progression and protein translation for cell growth.

1.2 PTEN biological functions

1.2.1 PTEN attenuation of the Akt signalling pathway

PTEN (phosphatase with tensin homology on chromosome 10) is a lipid phosphatase that dephosphorylates $PI3,4,5P_3$ back to $PI4,5P_2$, counteracting PI3K activity and blocking cell growth and survival effects of the activated EGFR pathway (Figure 1.1) (reviewed in Cantley and Neel, 1999). PTEN has five domains: a $PI4,5P_2$ binding motif, a phosphatase domain, a lipid binding domain (C2) made up of positively charged residues that have been shown to interact electrostatically with the plasma membrane, a regulatory domain containing Ser/Thr residues that have been shown to be phosphorylated by casein kinase II, and a class I PSD-95, Disc-large ZO-1 homologous (PDZ) binding motif (GI**TKV**-COOH) at the C-terminus that has been shown to interact with many PDZ domains (Figure 1.2A) (Keniry and Parsons, 2008; Maehama and Dixon, 1999; Valiente *et al.,* 2005). A model has been proposed explaining PTEN regulation and localization to the plasma membrane (Rahdar *et al.,* 2009; Vazquez *et al.,* 2000, 2001). PTEN is present in the cytosol of quiescent cells in its phosphorylated, closed conformation due to constitutive phosphorylation by casein kinase II (Figure 1.2B) (Rahdar *et al.,* 2009; Torres and Pulido, 2001). This closed conformation may be responsible for masking the positively charged residues responsible for electrostatic interactions with the plasma membrane (Das *et al.,* 2003; Rahdar *et al.,* 2009; Ross and Gericke, 2009). Upon growth factor stimulation, PTEN is dephosphorylated and adopts an open conformation believed to expose its positively charged residues for plasma membrane interaction (Rahdar *et al.,* 2009; Ross and Gericke, 2009). The open conformation of PTEN is also hypothesized to expose the PDZ

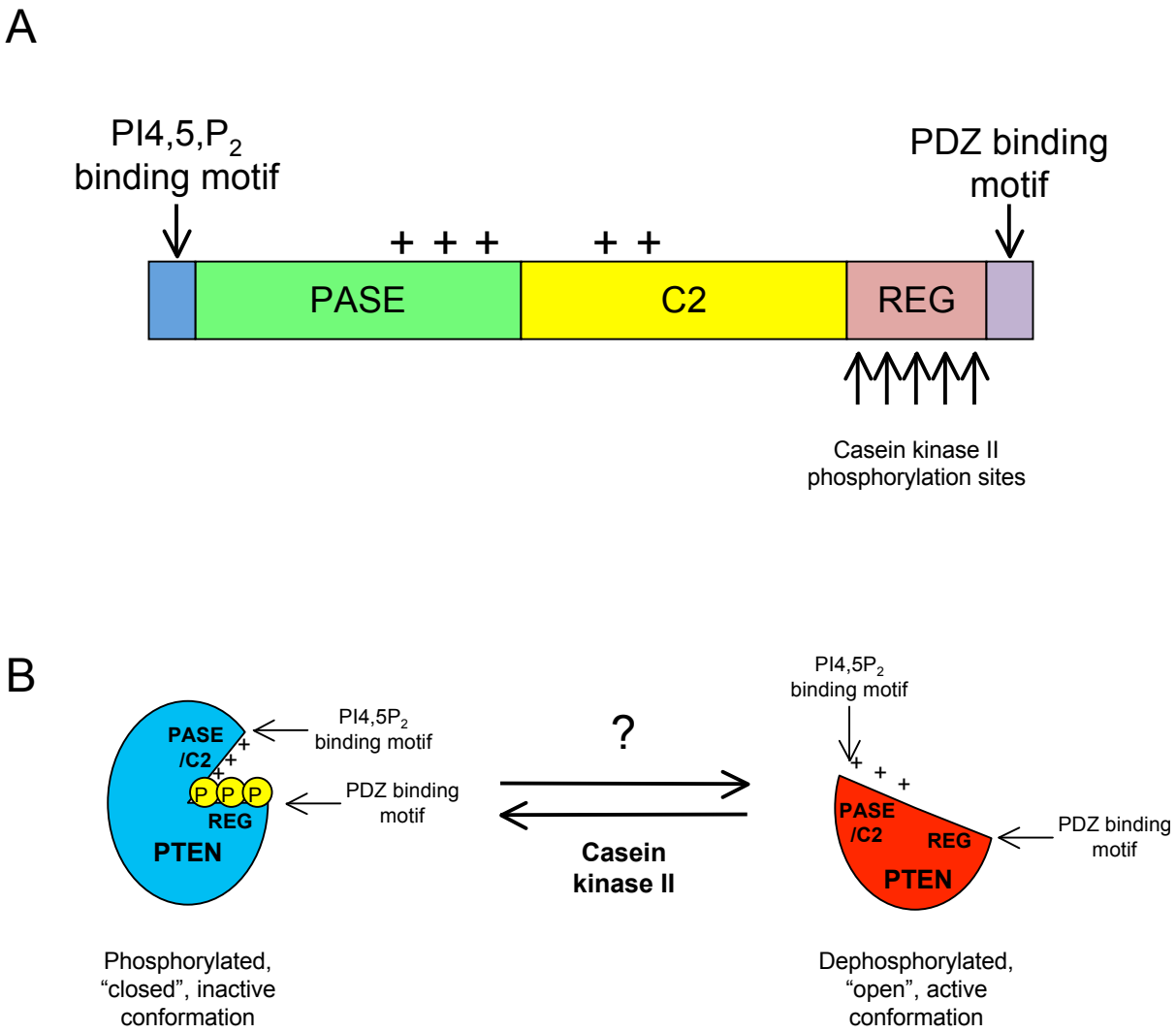

Figure 1.2: Schematic representation of the structure of the PTEN tumor suppressor protein. **A**, PTEN has five domains: a PI4,5P_2 binding motif, a phosphatase domain (PASE), a lipid binding domain (C2) made up of positively charged residues that have been shown to interact with the negatively charged plasma membrane; a regulatory domain (REG) composed of residues such as Ser/Thr residues that have been shown to be phosphorylated by casein kinase II, and a class I PDZ binding motif that has been shown to interact with several PDZ domains. **B**, Simplified representation of the closed and open conformation of the PTEN tumor suppressor protein (modified from Radhar *et al.*, 2009). Casein kinase II has been shown to phosphorylate PTEN, however an unknown phosphatase dephosphorylates PTEN.

binding motif for PDZ domain interactions (Vazquez *et al.,* 2000, 2001). The PDZ binding motif may localize PTEN to a PDZ domain scaffolding protein that is responsible for positioning PTEN in the correct membrane microdomain in order for it to gain access to PI3K lipid products for dephosphorylation.

PTEN has been shown to interact with many PDZ containing proteins including the Na^+/H^+ exchanger regulatory factor 1 (NHERF1) and NHERF2 (Kotelevets *et al.,* 2005; Takahashi *et al.,* 2006). PTEN has been shown to form a ternary complex with PDGFR and the NHERF scaffolding proteins (Figure 1.3) (Takahashi *et al.,* 2006). The NHERF family of proteins are scaffolding proteins that contain two PDZ domains (Reczek *et al.,* 1997). It is hypothesized that upon platelet-derived growth factor (PDGF) stimulation, NHERF1 PDZ1 and PDZ2 domains bind to both PTEN and PDGFR, respectively, in order to localize PTEN to the correct subcellular location at the plasma membrane in the cell to gain access to its lipid substrates. NHERF is located at the plasma membrane under physiological conditions and therefore may already be bound to PDGFR (Takahashi *et al.,* 2006). PTEN binding to NHERF is dependent on PDGF stimulation (Takahashi *et al.,* 2006). Proper localization allows PTEN to gain access to its lipid substrates and turn off PI3K/Akt signalling (Takahashi *et al.,* 2006). Therefore, the NHERF scaffolding protein places PTEN in close proximity of the PI3K lipid products in order for PTEN to efficiently attenuate Akt signalling.

1.2.2 PTEN stability

PTEN is a tumor suppressor protein that is mutated, deleted or has altered post-translational modifications that causes its loss of function in many types of cancer cells including those of the breast, prostate, lung, endometrium, brain, thyroid, skin, liver and lymphoid cancers (Pendaries *et al.,* 2003; Simpson and Parsons, 2001; Sulis and Parsons, 2003). A common mutation in PTEN is a truncated version of the protein that lacks its C-temrinal end, including the PDZ binding motif (Pendaries *et al.*, 2003; Sulis and Parsons, 2003). Mice with homozygous deletions of PTEN die in early embryogenesis, whereas heterozygous animals develop many malignancies (Suzuki *et al.,* 1998). Cultured mammalian cells that lack the PTEN tumor suppressor proliferate faster, resist apoptosis, have elevated activated Akt levels and migrate aberrantly (Dahia *et al.*, 1999; Hu *et al.*, 2007; Subauste *et al.*,

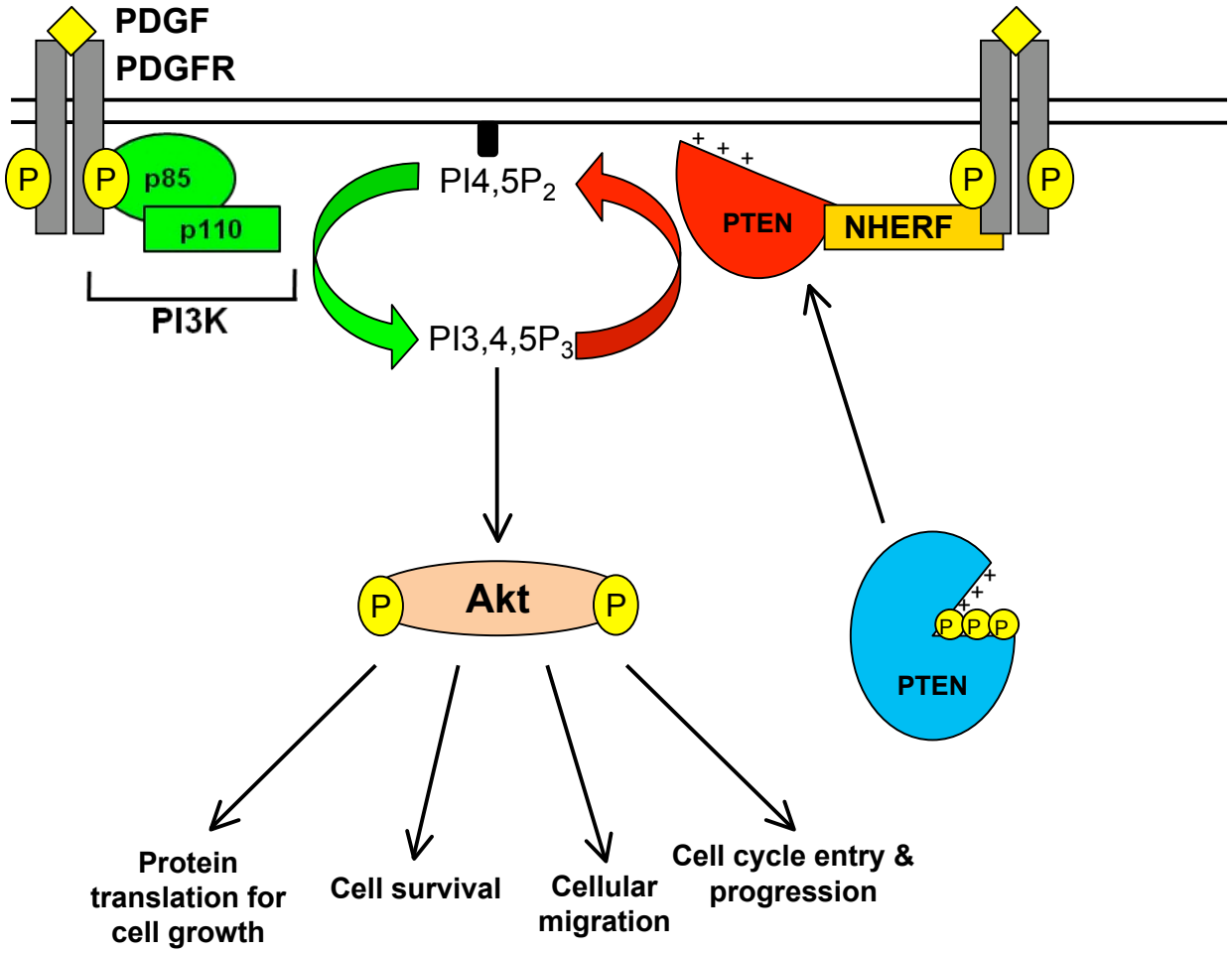

Figure 1.3: NHERF is a scaffolding protein that forms a ternary complex with PTEN and the PDGFR to attenuate Akt signalling (modified from Takahashi *et al.,* 2006). Upon PDGF stimulation, PDGFR subunits dimerize and autophosphorylation occurs on the Tyr residues. PI3K generates the lipid second messenger $PI3,4,5P_3$, which in turn activates Akt signalling. Upon growth factor stimulation, PTEN is dephosphorylated and recruited to the plasma membrane and binds through is PDZ binding motif to the PDZ1 domain of the NHERF scaffolding protein. NHERF is hypothesized to be responsible for bringing PTEN to the appropriate location at the plasma membrane where it can gain access to its lipid substrate, $PI3,4,5P_3$. Therefore, NHERF is a scaffolding protein that is able to localize the antagonistic PTEN protein to the PDGFR in order to rapidly attenuate PI3K/Akt signalling and ensure it is transient.

2005; Wang *et al.*, 2007). PTEN can be mono- and poly-ubiquitinated by neural precursor cell expressed developmentally down-regulated 4-1 (NEDD4-1) (Wang *et al.,* 2007), an E3 ubiquitin ligase (Blot *et al.,* 2004). Mono-ubiquitination of PTEN in the C2 domain leads to the translocation of PTEN into the nucleus, where it is involved in antagonizing nuclear Akt signalling (Trotman *et al.,* 2006) and plays a role in maintaining chromosomal integrity (Shen *et al.,* 2007). The focus of this work is the regulatory function at the plasma membrane, so these nuclear roles will not be discussed further. Poly-ubiquitination at the C-terminal end of PTEN leads to its rapid degradation by the proteosome (Wang *et al.,* 2007). Overexpression of NEDD4-1, which has been shown in some types of cancers, can lead to the post-translational suppression of PTEN (Wang *et al.,* 2007). A recent publication however, claims that PTEN does not associate with NEDD4-1, nor is the half-life of PTEN affected by NEDD4-1 ubiquitination (Fouladkou *et al.,* 2008). This study also found that PTEN nuclear localization is independent of NEDD4-1 mono-ubiquitination (Fouladkou *et al.,* 2008). Regardless of whether PTEN is mono- or poly-ubiquitinated by NEDD4-1, PTEN has been shown in previous studies to be ubiquitinated, which affects its redistribution in the cell and its degradation by the proteosome (reviewed in Wang and Jiang, 2008).

PTEN degradation is known to be mediated through C-terminal ubiquitination and proteosomal degradation. PTEN is poly-ubiquitinated at the C-terminal end (amino acids 352-403) and is quickly degraded by the proteosome (van Themsche *et al.,* 2009; Wang *et al.,* 2007). The C-terminal end of PTEN is also involved in intra- and intermolecular interactions with PDZ domains (Kotelevets *et al.,* 2005; Rahdar *et al.,* 2009; Takahashi *et al.,* 2006; Valiente *et al.,* 2005; Wu *et al.,* 2000a, 2000b). In the closed conformation of PTEN, these C-terminal residues are involved in an intramolecular interaction with its C2 domain (Rahdar *et al.,* 2009). PTEN residues involved in poly-ubiquitination may be unavailable for ubiquitination by the E3 ligase NEDD4-1 when PTEN is involved in these intramolecular interactions, explaining why PTEN is most stable in its cytosolic, closed conformation (Wang and Jiang, 2008). It is hypothesized that upon growth factor stimulation and simultaneous dephosphorylation, PTEN is recruited to the plasma membrane to a high molecular weight complex (the PAC) associated with a PDZ domain-containing scaffolding protein (Kotelevets *et al.,* 2005; Takahashi *et al.,* 2006; Valiente *et al.,* 2005; Vazquez *et al.,* 2001; Wu *et al.,* 2000a, 2000b). PTEN bound to a PDZ domain has been shown to have an increased half-life with

respect to a PTEN that cannot be recruited to a PDZ domain (Valiente *et al.,* 2005; Wu *et al.,* 2000a). When the PDZ binding motif of PTEN is interacting with a PDZ domain, the C-terminal residues are again unavailable for poly-ubiquitination, resulting in increased PTEN stability (Wang and Jiang, 2008). Therefore PTEN intra- or intermolecular interactions through its C-terminal end may prevent PTEN from poly-ubiquitination and subsequent degradation by the proteosome, thereby increasing the half-life of the tumor suppressor protein.

1.2.3 p85 regulation of PTEN

The p85 subunit of PI3K has been shown to have functions outside of the regulation of the p110 subunit of PI3K. p85 has been shown to positively regulate PTEN dephosphorylation of $PI3,4,5P_3$ back to $PI4,5P_2$ (Chagpar, 2004; Pastor, 2008). p85 is composed of 5 domains; an N-terminal Src homology 3 (SH3) domain, a breaking point cluster region homology domain flanked by two pro rich sequences, and two Src homology 2 (SH2) domains flanking the p110 binding site (Figure 1.4) (Harpur *et al.,* 1999). SH3 domains are known to bind to Pro rich sequences (Pawson, 1994). The breakpoint cluster region homology domain of p85 has been shown to have GTPase activating protein for Rab4 and Rab5 proteins *in vitro* (Chamberlain *et al.,* 2004). Rab4 and Rab5 are monomeric G-proteins involved in vesicle trafficking and fusion events during endocytosis and recycling of receptors (reviewed in van Ijzendoorn *et al.,* 2003). SH2 domains bind to phosphorylated Tyr residues and those of p85 have been shown to bind to phosphorylated Tyr residues of many RTKs (Harpur *et al.,* 1999; Hock *et al.,* 1998; Kubota *et al.,* 1998; Liu and Pawson, 1994; Pawson *et al.,* 1993; Pawson, 1994). p85 Pro rich regions have been shown to bind to the SH3 domains within the p85 protein itself and the SH3 domain of Lyn and Fyn, which are Src-family non-receptor tyrosine kinases (Harpur *et al.,* 1999; Pleiman *et al.,* 1994). These Pro rich regions have not been shown to bind to WW domains. Although p85 is known for its regulatory functions towards the p110 subunit of PI3K, it has been described complexed with other proteins and therefore has functions outside of the PI3K complex (Chagpar, 2004; Chamberlain *et al.,* 2004; Harpur *et al.,* 1999; Pastor, 2008; Pleiman *et al.,* 1994).

The p85 regulatory subunit of PI3K can bind directly to PTEN and positively regulate

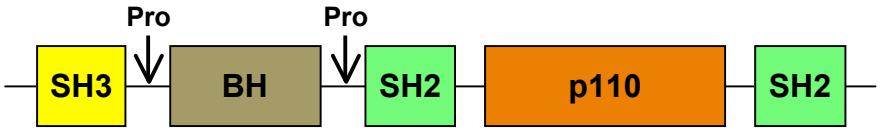

Figure 1.4: Schematic representation of the domain organization of the p85 protein. p85 is composed of an N-terminal SH3 domain, a breakpoint cluster region homology (BH) domain flanked by two Pro rich regions and two SH2 domains flanking the p110 binding site.

PTEN dephosphorylation of $PI3,4,5P_3$ back to $PI4,5P_2$ (Chagpar, 2004). Others have found that cells lacking p85 were deficient in PTEN attenuation of Akt signalling through dephosphorylation of $PI3,4,5P_3$ (Taniguchi *et al.,* 2007). Although cells had a decrease in PI3K levels (due to loss of p85), $PI3,4,5P_3$ and Akt levels were enhanced when compared to wild type cells (Taniguchi *et al.,* 2007). Therefore, p85 may be a critical regulatory component in PTEN attenuation of the Akt signalling signalling.

1.3 MAGUK and MAGI scaffolding proteins

Membrane associated guanylate kinase homologs (MAGUK) scaffolding proteins contain many protein binding domains capable of binding to multiple proteins simultaneously (Figure 1.5). Scaffolding proteins are multidomain proteins important in forming macromolecular protein complexes that regulate intracellular signalling pathways. Organizing signal transduction proteins into these complexes increases signalling efficiency by decreasing the distance over which signal transduction intermediates have to travel (Dimitratos *et al.,* 1999; Pawson and Scott, 1997). It is also hypothesized that scaffolding molecules may have the ability to orient signalling molecules with respect to each other, in order for more effective interactions to take place (Dimitratos *et al.,* 1999; Pawson and Scott, 1997). MAGUK scaffolding proteins share a common sequence similarity, placing them in this family of scaffolding proteins (Figure 1.5) (reviewed in Funke *et al.,* 2005). At the very C-terminal end of the protein is the guanylate kinase domain (GK) for which this family of proteins are named. These GK domains are typically catalytically inactive and are therefore thought to have evolved as protein binding domains, as opposed to a catalytically active enzyme (te Velthuis *et al.,* 2007). The GK domain is preceded by a single SH3 domain, which are known to bind to Pro rich sequences (Pawson and Schlessingert, 1993). At the N-terminal end of the protein, there are one or more copies of the PDZ domains. PDZ domains mediate protein-protein interactions with small polypeptide sequences usually found at the very C-terminal end of proteins (Doyle *et al.,* 1996; Kay and Kehoe, 2004; Morais-Cabral *et al.,* 1996). MAGUK scaffolding proteins share a common domain organization, with one or more PDZ domains followed by a single SH3 domain and a catalytically inactive GK domain.

One group of MAGUK proteins that does not follow the general domain architecture

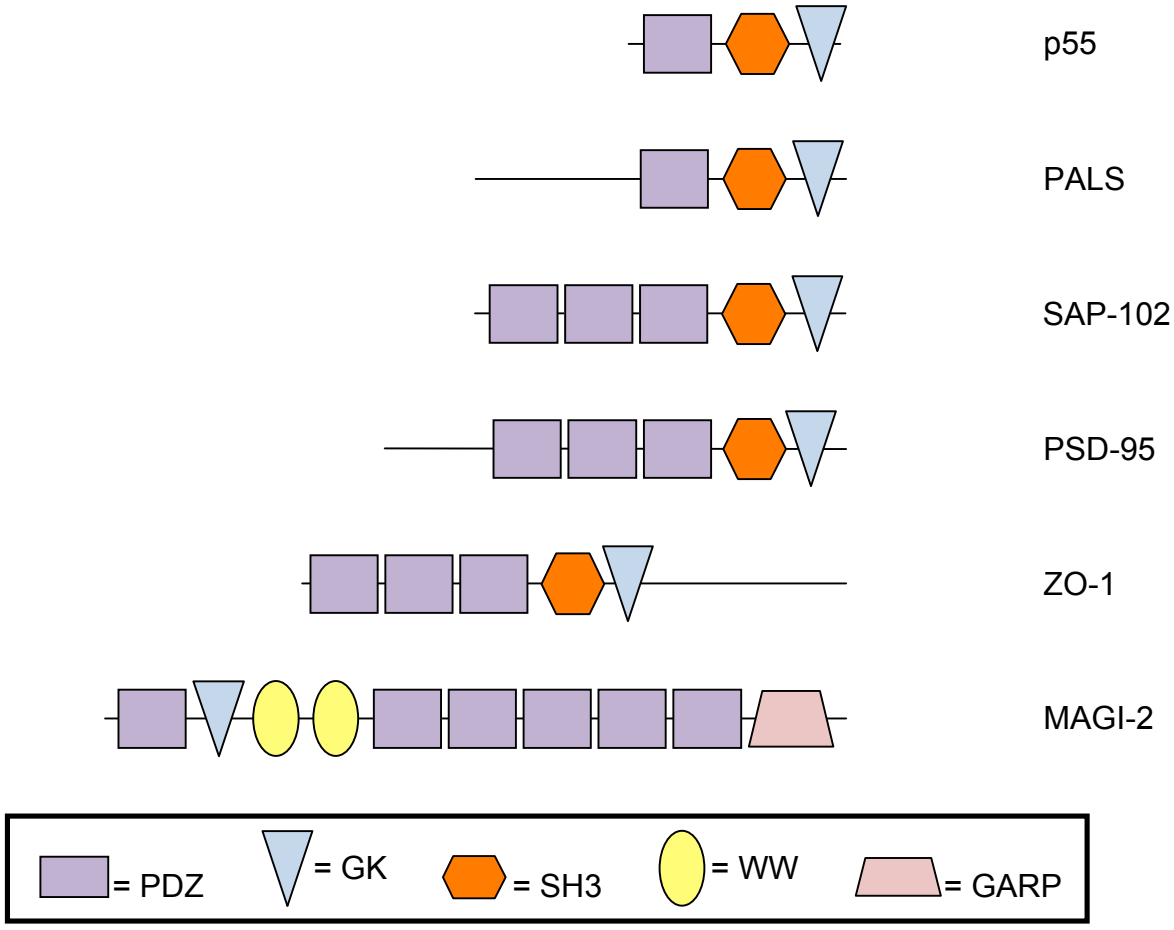

Figure 1.5: Protein domain organization of the MAGUK scaffolding proteins (modified from Funke *et al*., 2005). The N-terminal end of the protein contains one or multiple PDZ domains followed by a single SH3 domain. The C-terminal end of the protein contains the GK domain, for which this family of proteins are named. The MAGI family of MAGUK proteins contain identical or similar protein binding domains however, these have a different primary domain arrangement than its family counterparts. Its domain arragement is inverted with respect to the rest of the MAGUK family of scaffolding proteins. The MAGI family of proteins have one N-terminal PDZ domain, followed by the GK domain located at the N-terminal end of the protein. The GK domain is then followed by two tandem WW domains, followed by five more PDZ domains. The MAGI-2 protein contains an additional C-terminal region which is rich in Gly, Ala, Arg and Pro residues our laboratory has termed the GARP C-terminal sequence.

mentioned above, is known as the membrane associated guanylate kinase-inverted (MAGI) subfamily (Figure 1.5). MAGI protein domain organization is inverted with respect to the rest of the MAGUK scaffolding proteins, hence their nomenclature (Funke *et al.,* 2005; te Velthuis *et al.,* 2007). The MAGI group of scaffolding proteins has three members; MAGI-1, MAGI-2 and MAGI-3, which share extensivy sequence similarity (Figure 1.6). All MAGI proteins contain six PDZ domains (numbered 0-5), a single GK domain and two tandem WW domains (numbered 1 and 2, respectively). Overall, the sequence similarity of these domains is high, whereas the linker sequences between the domains are low (Wu *et al.,* 2000b). The MAGI group of scaffolding proteins have one N-terminal PDZ domain, followed by the GK domain, which is positioned N-terminally rather than C-terminally. The GK domain is followed by two tandem WW domains, which bind to Pro rich sequences, much like the SH3 domains (Macias *et al.,* 1996, 2000; Nguyen *et al.,* 1998). The WW domains are followed by five more PDZ domains. The MAGI group of scaffolding proteins share the same or similar protein-protein binding domains as the MAGUK scaffolding proteins however, the primary arrangement of these protein domains is inverted when compared to their MAGUK counterparts.

MAGUK scaffolding proteins are important in cell signalling pathways and they have been shown to be localized to areas important for cellular communication such as cell-cell junctions, adherens junctions, tight junctions and neuronal synapses (Deng *et al.,* 2006; Dobrosotskaya and James, 2000; Franklin *et al.,* 2005; Shoji *et al.,* 2000). MAGUK proteins have been found in all metazoans studied to date, however they are not present in fungi or other unicellular organisms, potentially indicative of their role in cell-cell communication and their importance in signal transduction pathways (te Velthuis *et al.,* 2007). MAGUK scaffolding proteins are also absent in plants, which contain cell walls and may require a different mechanism for cell-cell communication (te Velthuis *et al.,* 2007). MAGUK scaffolding proteins are ubiquitous throughout different tissues (Dobrosotskaya *et al.,* 1997; Godreau *et al.,* 2004; Laura *et al.,* 2002; Wood *et al.,* 1998; Wu *et al.,* 2000a, 2000b) where the most diversity of MAGUK scaffolding proteins occur in the brain (reviewed in Elias and Nicoll, 2007; te Velthuis *et al.,* 2007). The high incidence of MAGUK scaffolding proteins in the brain is appropriate because of the high incidence of neurons and neuronal synapses in these areas, thereby exhibiting a need for scaffolding proteins to regulate the many signal transduction

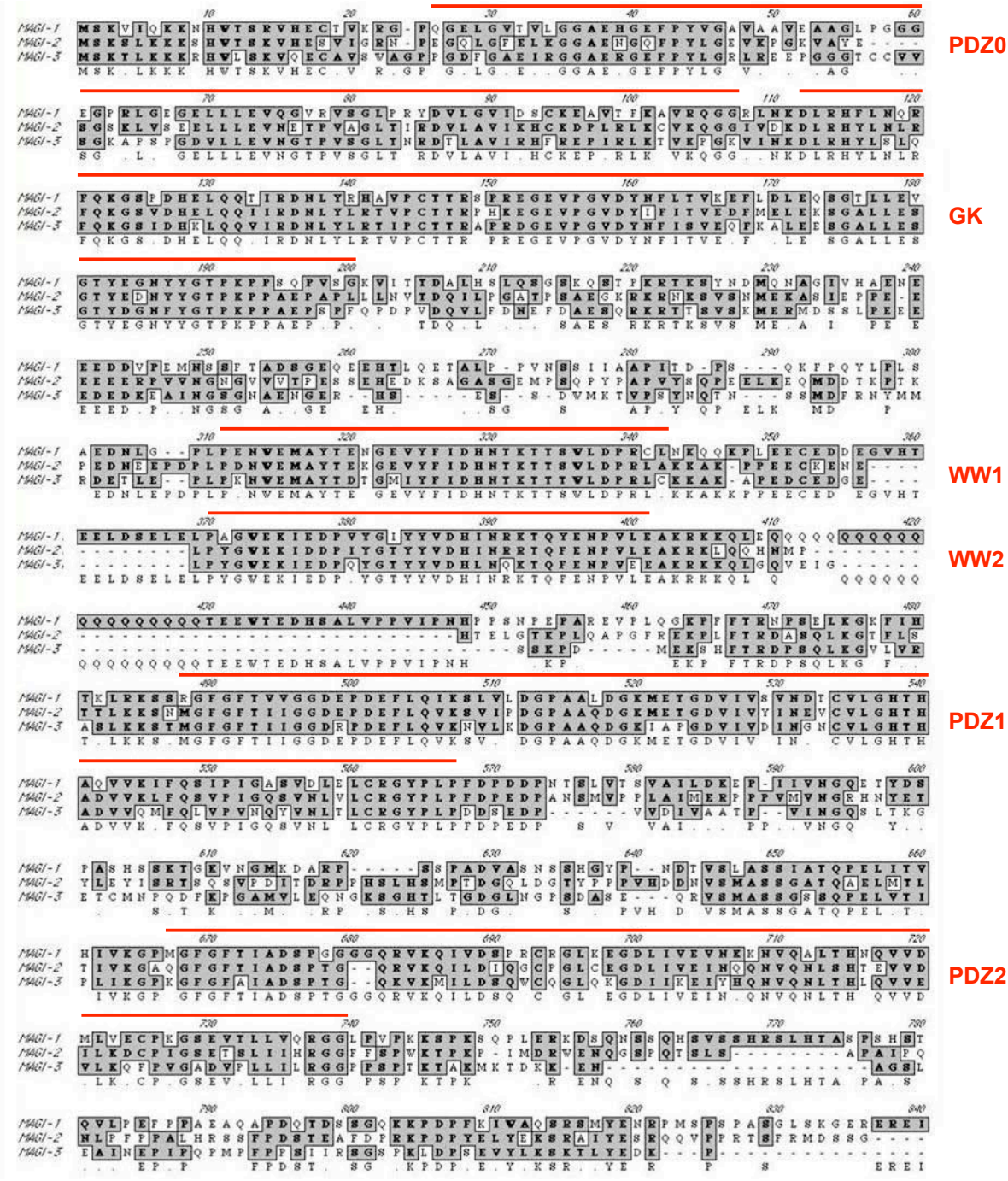

Figure 1.6: CUSTLAW sequence alignment of the MAGI family members (modified from Wu *et al.*, 2000b). Amino acids that are identical or similar are shaded in gray. All MAGI proteins contain the six PDZ domains (numbered 0-5), two WW domains and a GK domain. The homology of the domains remain high whereas the linker sequences between the MAGI domains are low. The red bars indicate the sequences representing the domains on the right. The MAGI sequences represented are the human proteins and their accession numbers are as follows: MAGI-1 NP_056335, MAGI-2 NP_036433 and MAGI-3 AF213259. The CUSTLAW sequence alignments were generated using MacVector software.

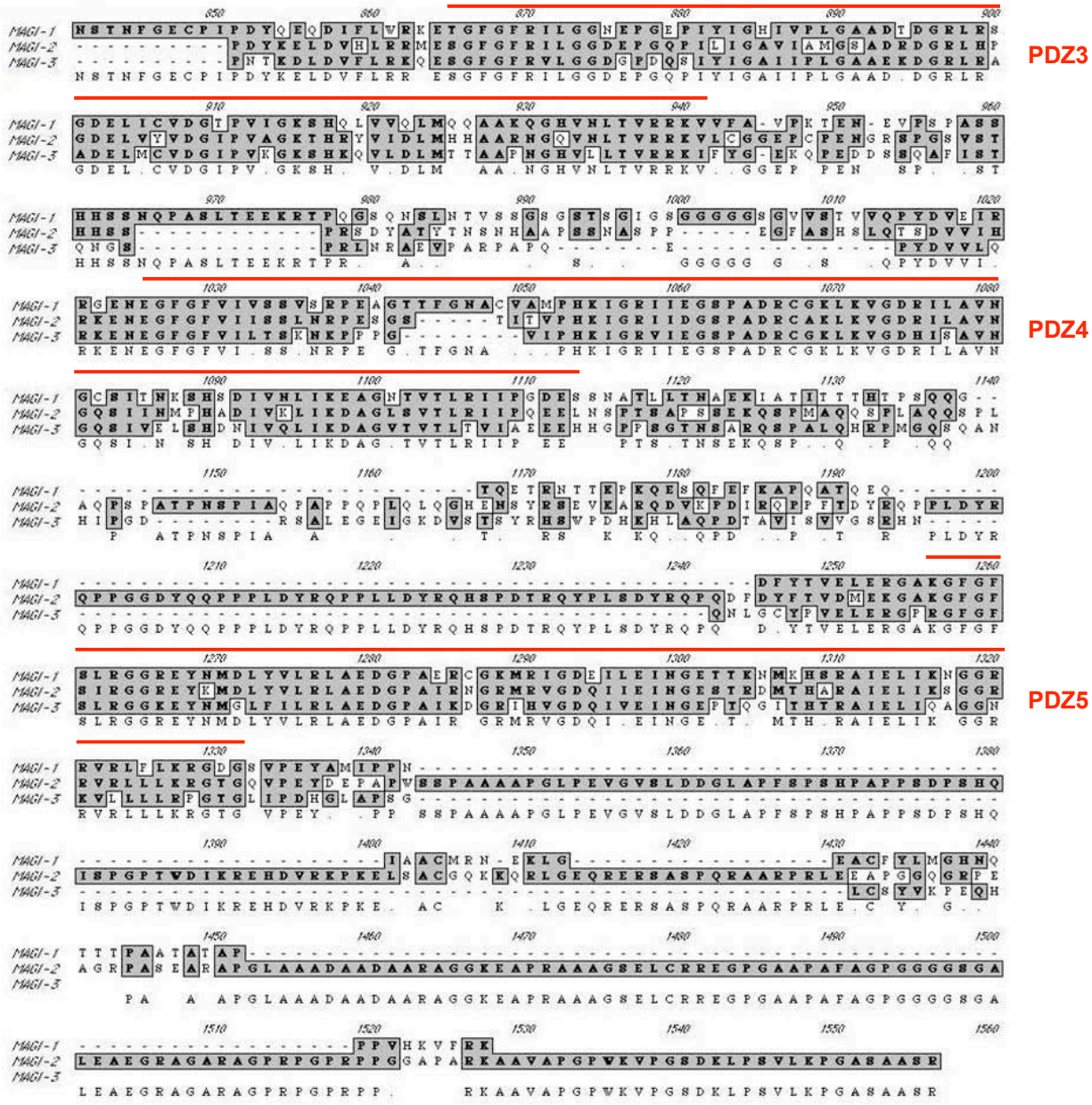

Figure 1.6: CUSTLAW sequence alignment of MAGI family members (continued from previous page).

pathways. Although MAGUK scaffolding proteins are known for their scaffolding functions at cell-cell communication sites, they also exhibit a wide variety of cellular functions such as establishment of cell polarity, tight junction formation, cell proliferation or apoptosis, cell differentiation and neuronal synapse transmission (Dobrosotskaya and James, 2000; Georgescu, 2008; Hirao *et al.,* 1998; Kaech *et al.,* 1998; Kornau, 2006; Lehtonen *et al.,* 2005; Subauste *et al.,* 2005; Tepass and Knust, 1993; Woods *et al.,* 1996). Mutations in MAGUK scaffolding proteins often cause defects in cell-cell adhesion, cell polarity and cell proliferation (Gregorc *et al.,* 2007; Hoover *et al.,* 1998; Kaech *et al.,* 1998; Tepass *et al.,* 1990; Woods and Bryant, 1991). MAGUK proteins can also be palmitoylated, phosphorylated or translocated to the nucleus (Bryant and Woods, 1992; Dobrosotskaya *et al.,* 1997; Hsueh *et al.,* 2000; Tanemoto, 2008; Topinka and Bredt, 1998). Although MAGUK scaffolding proteins are important in bringing together signal transduction intermediates, they have also been shown to play a role in other cellular functions.

MAGUK scaffolding proteins are important in bringing together proteins in a cell in close proximity to each other to increase the efficiency of cell signalling and signal transduction pathways. For example, the lethal protein 23 receptor, the EGFR homologue in *Caenorhabditis elegans*, is localized to the basolateral membranes of polarized vulval epithelial cells (Hoskins *et al.,* 1996). Lethal protein 23 has a C-terminal PDZ binding motif that binds to a PDZ domain in abnormal cell lineage 2, an interaction that is important for cellular proliferation and differentiation in *Caenorhabditis elegans* vulval cells (Kaech *et al.,* 1998). Abnormal cell lineage 2, a MAGUK scaffolding protein, also binds to adaptor proteins abnormal cell lineage 7 and abnormal cell lineage 10, vertebrate abnormal cell lineage homologs, and form a complex that allows lethal protein 23 basolateral localization in these epithelial cells (Kaech *et al.,* 1998). In order for vulval development to occur properly in *Caenorhabditis elegans*, abnormal cell lineage 3 (an EGF-like signal) is secreted into the basal extracellular space of vulval precursor cells and activates lethal protein 23 to cause cells to proliferate and differentiate into vulval cells (Hoskins *et al.,* 1996). A defect in the abnormal cell lineage complex formation disrupts basolateral localization of lethal protein 23, thereby preventing vulval induction (Kaech *et al.,* 1998). Similar results are seen upon of a loss of function mutant of the lethal protein 23 receptor (Kaech *et al.,* 1998). Therefore, MAGUK proteins are important scaffolding proteins responsible for mediating cell signalling at proper locations within cells.

1.4 Binding specificities and functions of MAGUK protein domains

1.4.1 GK:SH3 domains

The GK domain of most MAGUK proteins share 40% sequence similarity to yeast guanylate kinase (YGK) domains (Kistner *et al.,* 1995; Kuhlendahl *et al.,* 1998; Li *et al.,* 2002), whereas the GK domains of MAGI proteins share approximately 22% sequence identity to YGK (Figure 1.7). Previous studies have shown that the GK domain of MAGI proteins share only 11% sequence similarity however they did not show the sequences involved in the alignment, which could account for the discrepancy in sequence similarity reported here (Adell *et al.,* 2004). Another study has also reported a sequence similarity of 27% between the GK domain of MAGI-1 and YGK (Dobrosotskaya *et al.,* 1997). However, they compared the sequence of the first 100 amino acids of the YGK to approximately 100 amino acids of the MAGI-1 GK domain, whereas Figure 1.7 shows 160 amino acids.

Unlike authentic YGKs, the MAGUK GK domains are not enzymatically functional and are unable to catalyze ATP-dependent phosphorylation of GMP to GDP (Li *et al.,* 1996) with the exception of very few MAGUK proteins that do exhibit very weak catalytic activity (Dimitratos *et al.,* 1999). Although most GK domains of MAGUK proteins are capable of binding GMP (Kistner *et al.,* 1995; Kuhlendahl *et al.,* 1998; Li *et al.,* 2002) they are catalytically inactive because they are missing key residues important in the catalytic function of the GK domain (Figure 1.7) (Kuhlendahl *et al.,* 1998; Li *et al.,* 2002). For example, although MAGIs contain many of the residues important in binding the guanine ring (red triangles), residues that bind the phosphate (purple circles) and the Mg^{2+} (blue square) are less well conserved (Figure 1.7) (Dobrosotskaya *et al.,* 1997). Also, YGK contains a GMP binding pocket as well as an ATP binding area important for catalytic function (Li *et al.,* 1996). The ATP binding domain is no longer functional in MAGI GK domains due to the lack of key residues that make contact with ATP (Figure 1.7, bracket) (Dobrosotskaya *et al.,* 1997; Kistner *et al.,* 1995; Kuhlendahl *et al.,* 1998). Therefore, it is hypothesized that the GK domains of

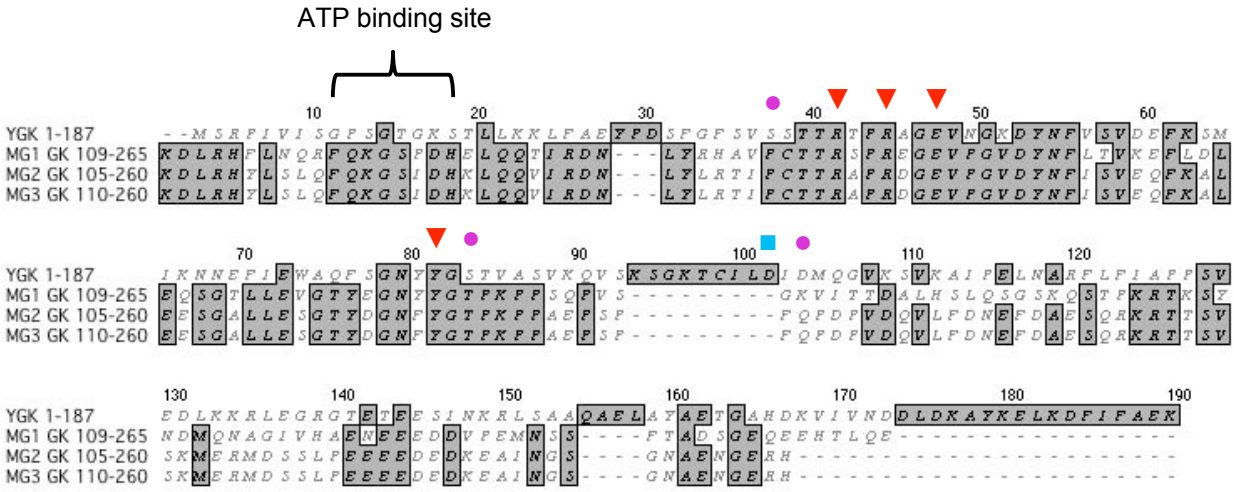

Figure 1.7: CUSTLAW sequence alignment of YGK and the GK domain of MAGI-1 (MG1), MAGI-2 (MG2) and MAGI-3 (MG3) (modified from Dobrosotskaya *et al.*, 1997). Amino acids in YGK that bind to ATP are indicated. GMP binding residues of YGK are indicated as follows; guanine ring (▼), phosphate (●) and Mg^{2+} (■). The YGK accession number is AAA34657 and the MAGI proteins are of the human origin and are of the same accession numbers described in Figure 1.6.

MAGUK proteins have evolved as protein-protein interacting modules, as opposed to catalytically active domains. GK domains have been shown to bind to a variety of proteins that do not necessarily share sequence similarity. Most of these proteins are localized at areas of the cell important in cell-cell communication (*e.g.*, guanylate kinase associated protein and P90/SD-95 associated proteins) (Kim *et al.,* 1997; Takeuchi *et al.,* 1997), or aid in the trafficking of proteins to these areas (*e.g.*, A kinase anchoring proteins and guanylate kinase associated kinesin) (Colledge *et al.,* 2000; Hanada *et al.,* 2000). These protein-protein interactions are independent of the GMP binding pocket. The ability of the GK domain of MAGUK scaffolding proteins to bind to a variety of proteins reinforces the hypothesis that the GK domain has evolved as a protein interaction module rather than a catalytically active domain.

One last unique binding partner of the GK domain of MAGUK proteins is an intramolecular interaction with the adjacent SH3 domain (Figure 1.8A) (McGee and Bredt, 1999; Nix *et al.,* 2000; Shin *et al.,* 2000; Tavares *et al.,* 2001). A Hook domain, located between the GK and SH3 domain, allows for the GK domain to fold over and make interactions with the SH3 domain (Paarmann *et al.,* 2002). The GK:SH3 interaction is unusual because SH3 domains are known to bind to Pro rich sequences (Pawson and Nash, 2003) of which the GK domain has none. It was later shown, however, that the Pro binding site of the SH3 domain is not involved in the intramolecular interaction with the GK domain (Tavares *et al.,* 2001). Mutations that disrupt the GK:SH3 intramolecular interaction can result in tumor formation, improper cellular adhesion and improper cell-cell junction scaffold formations (Lahey *et al.,* 1994; Woods and Bryant, 1991), causing loss of proper formation of cell-cell junctions and loss of cell signalling (Hoskins *et al.,* 1996; Woods *et al.,* 1996). The GK:SH3 interaction has also been shown to produce intermolecular interactions with other GK:SH3 domain containing MAGUK proteins (Figure 1.8B) (McGee *et al.,* 2001; Nix *et al.,* 2000). It is believed that these intermolecular interactions are important in forming an interlocked MAGUK scaffolding network localized at cell communication borders (McGee *et al.,* 2001). Although the GK:SH3 intra- and intermolecular interactions are not well understood, mutational analysis has shown that these interactions are important in the proper functioning of cell signalling pathways and proper cell junction formation in cells.

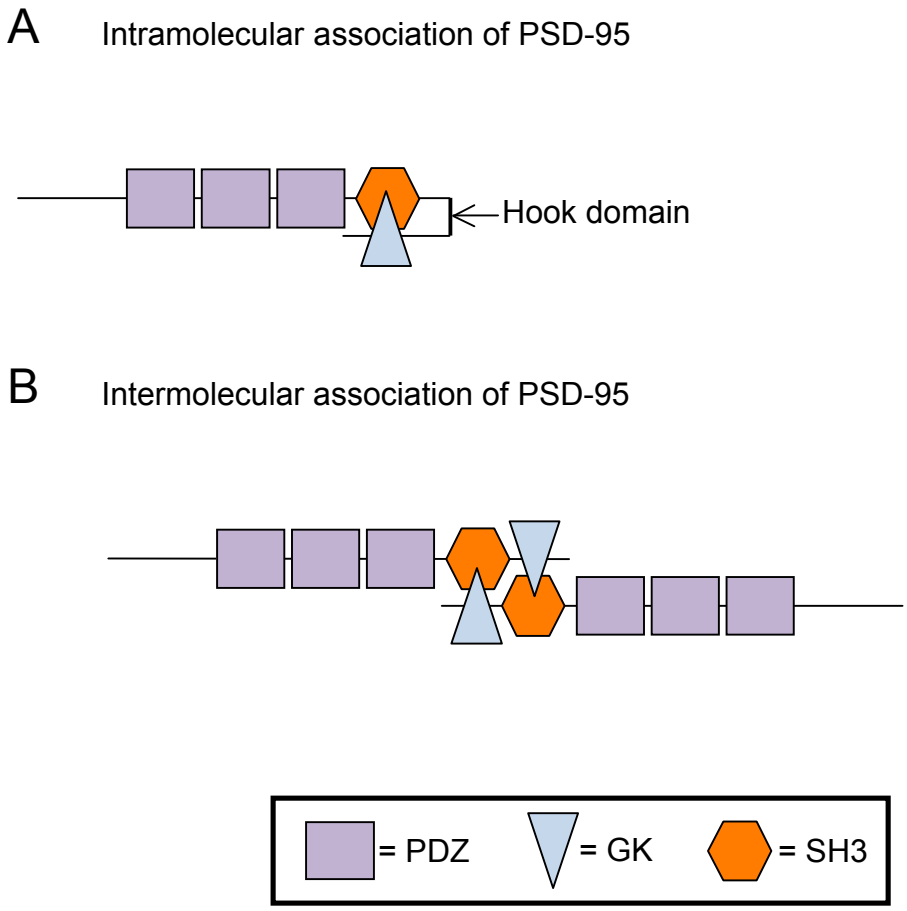

Figure 1.8: Schematic representation of the intramolecular and intermolecular association between the GK and SH3 domains of MAGUK scaffolding proteins. **A**, The intramolecular interaction of the GK:SH3 domains through the Hook domain. **B**, The intermolecular interaction of the GK:SH3 domains, which allows the formation of supramolecular scaffolds localized in areas of the cell important for intercellular communication.

1.4.2 SH3 and WW domains

Most MAGUK scaffolding proteins contain a single SH3 domain, however the MAGI group is the only MAGUK proteins that contain two tandem WW domains (reviewed in Funke *et al.,* 2005). Both of these protein domains bind to Pro rich sequences (Nguyen *et al.,* 1998). SH3 domains are usually present within a protein as a single copy and they fold as two orthogonal β-sheets which contains five anti-parallel strands assembled into a β-barrel (Figure 1.9A) (Hoelz *et al.,* 2006; Loll *et al.,* 2008; Martin-García *et al.,* 2007; Wisniewska *et al.,* 2005). Two loops, the RT loop (connecting β1/β2) and the Src loop (connecting β2/β3) have been shown to make additional contacts with the peptide (Hoelz *et al.,* 2006; Martin-García *et al.,* 2007). A shallow hydrophobic groove, lined with highly conserved aromatic residues, makes up the binding pocket that accommodates the Pro rich peptide (Figure 1.9B, gray) (Nguyen *et al.,* 1998). The peptide can also make contact with highly conserved residues in the RT loop, Src loop and the highly conserved acidic residues known to make contact with the basic Arg residue in the peptide (Figure 1.9B, red) (Hoelz *et al.,* 2006; Nguyen *et al.,* 1998). The Pro residues of the peptide pack against the aromatic residues of the SH3 domain, forming a hydrophobic buckle (Figure 1.9C) (Nguyen *et al.,* 1998). The SH3 domains recognize and bind to Pro rich sequences often bordered by an Arg residue (PXXPXR) (Figure 1.9C) (Nguyen *et al.,* 1998). Upon binding of the peptide to the SH3 domain, the peptide adopts a Type II polyproline helical conformation (Ogura *et al.,* 2006; Pisabarro *et al.,* 1998). Therefore, SH3 domains bind to Pro rich sequences flanked by an Arg residue, by forming a hydrophobic buckle against the aromatic residues found in the binding pocket of SH3 domains.

WW domains are protein interaction modules that also bind to Pro rich peptides. WW domains are usually present within a protein as two or more copies (Hofmann and Bucher, 1995) and they fold as stable, triple stranded, antiparallel β-sheets (Figure 1.9D) (Macias *et al.,* 1996). These domains are made up of approximately 30-40 amino acids and they usually contain two highly conserved aromatic residues (frequently Trp residues; Figure 1.9E, red) spaced approximately 20-22 amino acids apart (Chen and Sudol, 1995; Macias *et al.,* 1996; Schultz *et al.,* 2000). Again, a shallow hydrophobic groove, lined with highly conserved aromatic residues, makes up the binding pocket that accommodates the Pro rich peptide (Figure 1.9E, purple, blue and red) (Nguyen *et al.,* 1998). It has been shown that WW and SH3

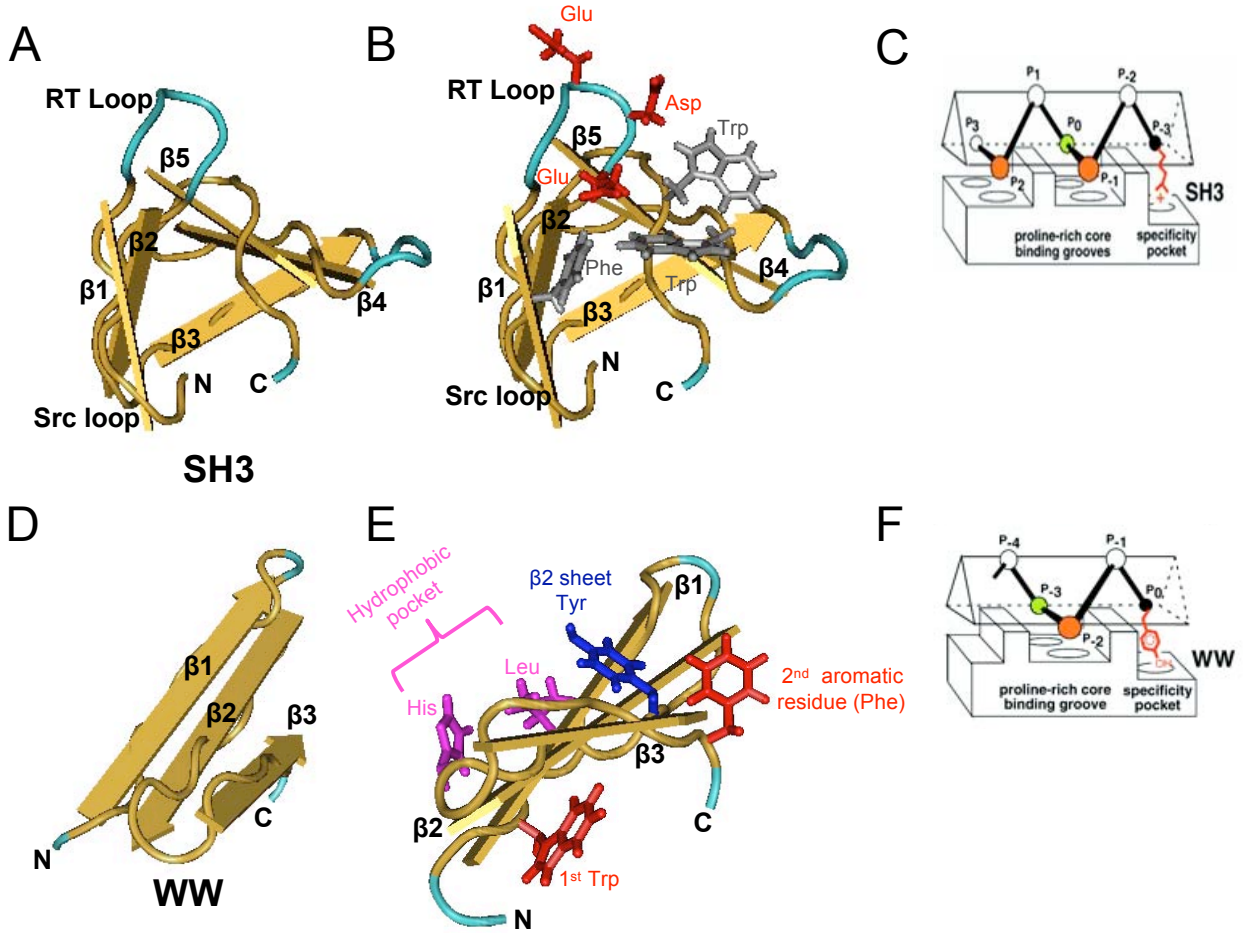

Figure 1.9: Comparison of the SH3 and WW domains. **A**, Crystal structure of the SH3 domain of the rat betaPIX, a protein involved in localization of p21-activated kinases [Protein databank identification number (PDB ID): 2D6F from Hoelz *et al.,* 2006]. SH3 domains contain two orthogonal β-sheets that contains five anti-parallel strands assembled into a β-barrel. **B**, SH3 domain highlighting the residues important in making contacts with the Pro rich peptide (peptide not shown). Acidic residues in the RT loop are highlighted in red. Aromatic residues making up the hydrophobic groove are highlighted in gray. **C**, Schematic representation of a Pro rich peptide binding to an SH3 domain (taken from Nguyen *et al.*, 1998). **D**, NMR solution structure of the third WW domain of Smurf2, a human E3 ubiquitin ligase (PDB ID: 2DJY from Chong *et al.,* 2006). WW domains are approximately 40 amino acids in length and are arranged as three anti-parallel β-sheets. **E**, WW domains highlighting residues important in binding to the proline rich peptide (peptide not shown). The conserved aromatic residues for which the domain is named are highlighted in red (Trp and Phe); the Tyr (center of the β2 sheet) is highlighted in blue; the residues forming the hydrophobic pocket (closely spaced His and Leu residues) are highlighted in purple. **F**, Schematic representation of a proline rich peptide binding to a WW domain (taken from Nguyen *et al.*, 1998). The gold arrows represent β-sheets and the blue tubes represent unstructured loops. Crystal structures were downloaded from the PDB and the figures were generated with Cn3D software.

domains can often compete for the same Pro rich binding motif (Sudol, 1996). WW domains often recognize a Pro rich sequence with an adjacent Tyr residue (PPXY, Figure 1.9F) (Nguyen *et al.,* 1998). The chemistry of the interaction between a WW domain is similar to that of an SH3 domain, where the Pros of the peptide pack against aromatic residues in the binding pocket of the WW domain, forming a hydrophobic buckle (Figure 1.9F) (Macias *et al.,* 1996; Nguyen *et al.,* 1998). Therefore, WW domains are found in the MAGI group of MAGUK scaffolding proteins and they bind to Pro rich sequences in a similar fashion to SH3 domains.

There are four different classes of WW domains that are based on the different peptide motifs that are recognized by individual WW domains (Table 1.1) (reviewed in Espanel *et al.,* 2003; Ingham *et al.,* 2005). Although the WW domains exhibit specificity for ligands, an individual WW domain has the ability to bind to more than one class of peptide, increasing the complexity of classifying these domains (Kato *et al.,* 2004; Wiesner *et al.,* 2002). There are four classes of peptide binding motifs, however the binding of WW domains to their different ligand classes is similar.

WW domains contain some highly conserved residues that are important in binding and making contacts with their respective ligands (Figure 1.10 and 1.11). The WW domain contains a shallow, hydrophobic surface that accommodates the Pro rich peptide (Figure 1.10A) (Macias *et al.*, 1996). This hydrophobic surface contains two Trp residues spaced 20-22 amino acids apart, for which the domain is named (Figure 1.10B and Figure 1.11A, red). Although the first Trp residue is absolutely conserved, the second can be replaced with a Tyr or Phe (Kanelis *et al.,* 2006; Kato *et al.,* 2006; Macias *et al.,* 1996; Pires *et al.,* 2005). WW domains also contain an absolutely conserved Pro near its C-terminal end (Figure 1.11, green). The absolutely conserved N-terminal Trp residue and C-terminal Pro residue are believed to support

Table 1.1: Table depicting the four different classes of WW domains and the short amino acid sequences they recognize (reviewed in Espanel *et al.,* 2003; Ingham *et al.,* 2005). X- denotes any amino acid. pS denotes a phosphorylated Ser and pT denotes a phosphorylated Thr.

Class	Peptide Motif
Class I	-P/L-P-X-Y-
Class II	-P-P-X-P-
Class III	-P-P-R-P-
Class IV	pS-P or pT-P cores

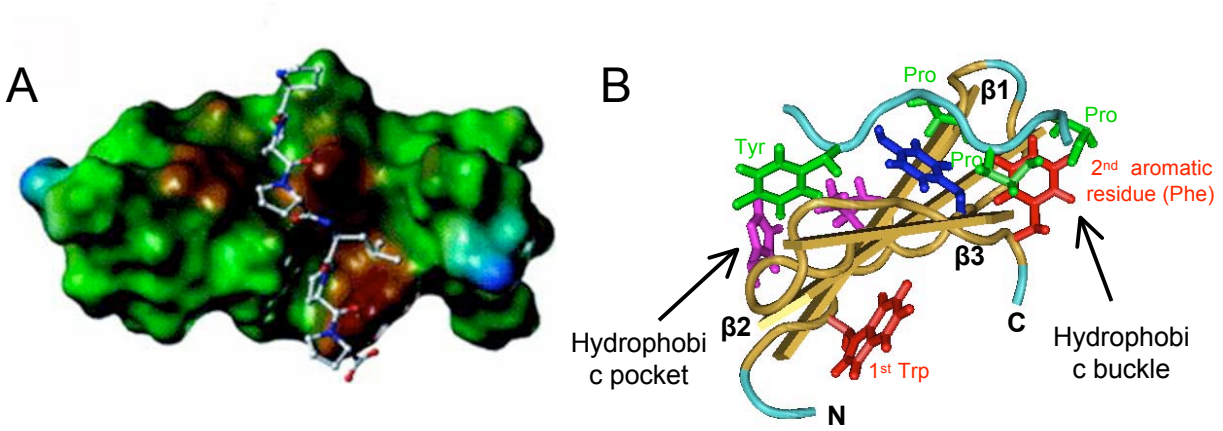

Figure 1.10: Peptide binding to a WW domain highlighting residues important in making contact with the Pro rich peptide. **A**, Space filled model of the first WW domain of human formin binding protein (NP_060362, used with permission from Pires *et al.*, 2005) showing the surface topology of the hydrophobic surface (red regions) on the WW domain that accommodates the proline rich peptide. **B**, NMR solution structure of the WW domain from Figure 1.19E (PDB ID: 2DJY from Chong *et al.*, 2006), highlighting key residues important in binding to the proline rich peptide. Peptide ligand (green residues) bound to the WW domain showing the important conserved contacts. The hydrophobic buckle is created upon binding of the Pro residues of the ligand to the second aromatic residue (Phe) on the surface of the WW domain.

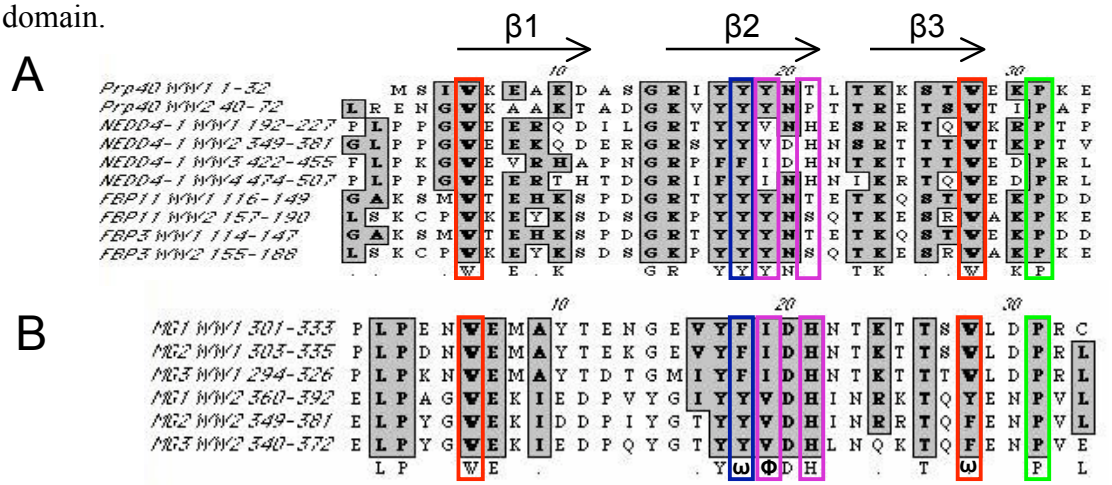

Figure 1.11: CUSTLAW sequence alignment of WW domains. **A**, Sequence alignment of ten individual WW domains. The human Prp40 protein (EAW58085) is a U1 snRNP involved in RNA splicing. The human NEDD4-1 protein (NP_006145) is an E3 ubiquitin ligase. The human formin binding protein (FBP, NP_060362) is involved in protein transport to the nucleus and may play a role in RNA splicing. The Trp residues, for which the domain is named, are boxed in red. A well conserved Tyr or aromatic residue in the center of the β2 strand, is highlighted in blue. The residues responsible for forming a small hydrophobic pocket are highlighted in purple. The always conserved Pro residue at the C-terminal end of the domain, is highlighted in green. **B**, Sequence alignment of the WW domains in MAGI-1 (MG1), MAGI-2 (MG2) and MAGI-3 (MG3). The second conserved Trp in the second WW domain of the MAGI proteins is replaced with a Tyr or Phe. The MAGI WW domains are more similar with respect to the homologous domains of the other MAGI proteins than they are with respect to the WW domains within an individual MAGI protein. **ω** represents an aromatic residue. Φ represents an hydrophobic residue.

the integrity of the tertiary structure of the domain, as mutations in these residues cause improper folding of the WW domain (Macias *et al.,* 2000). A highly conserved aromatic residue in the center of the β2 strand (Figure 1.10B and Figure 1.11, blue) makes contact with a center Pro residue in the peptide (Kanelis *et al.,* 2006; Kato *et al.,* 2006; Macias *et al.,* 1996; Pires *et al.,* 2005). In the class I WW domain, a hydrophobic pocket is formed in the β2/β3 loop region which makes contact with the aromatic ring of Tyr residue of class I peptides (Figure 1.10B and Figure 1.11, purple) (Huang *et al.,* 2000; Kanelis *et al.,* 2006; Kato *et al.,* 2006; Macias *et al.,* 1996). The residues making up this pocket are dependent on the class of the WW domain (reviewed in Espanel *et al.,* 2003; Ingham *et al.,* 2005). These highly conserved residues of the WW domain are important in making contact with their respective peptides.

The MAGI domains are hypothesized to bind to class I peptides as they contain the His and Ile/Val residues in the β2/β3 loop region (Figure 1.11B, purple). The first WW domain of the MAGI proteins contains both conserved Trp residues and the second Trp of the second WW domain is substituted with a Tyr or a Phe (Figure 1.11B, red). The WW domains of MAGI are more similar to the homologous domains of the other MAGI proteins, than they are with respect to the WW domains within the individual MAGI protein. Although MAGI WW domains bound to peptide complex have yet to be crystallized, it is hypothesised that it will bind to a class I peptide based on their primary amino acid sequences.

Additional binding energy and specificity is provided by contacts made outside the core region of the peptide and the WW domain (the β1/β2 and β2/β3 loops connecting the three β-strands) (Henry *et al.*, 2003; Kanelis *et al.,* 2006; Peng *et al.,* 2007; Pires *et al.,* 2005). For example, the epithelial Na^+ channel contains a -P-P-X-Y- motif that has been shown to bind to the third WW domain of NEDD4-2 (Henry *et al.*, 2003). The Ala-504 and Pro-505 residues within the β1/β2 loop of the NEDD4-2 WW3 domain has been shown to make contacts with the Pro rich region of the epithelial Na^+ channel, and a mutational analysis where these were mutated to His-504 and Thr-505 showed a 2-3 fold decrease in binding (Henry *et al.,* 2003). Although WW domains contain a consensus binding motif, additional binding may occur outside the binding pocket of the WW domain and increase specificity of the interaction, as well as binding affinities.

Mutations that can abolish binding of the WW domain to its respective ligand are important in order to study the importance of the interaction between cell signalling intermediates in signal transduction pathways. Mutations in the WW domain residues that form the hydrophobic pocket that makes contact with an internal Pro of the peptide, will eliminate binding to its respective class I ligand (Figure 1.11, purple) (Kanelis *et al.,* 2006; Macias *et al.,* 1996). Mutating the well conserved WW domain Tyr residue within the β2 stand (Figure 1.11, blue) to an Ala or Leu also eradicates peptide binding (Kato *et al.,* 2006; Macias *et al.,* 1996). Mutating the second Trp (or Tyr) in the WW domain to an Ala also abolishes peptide binding (Kato *et al.,* 2006; Macias *et al.,* 1996).

Mutations in the Pro rich peptides also eliminate binding to its respective WW domain. Replacing the center Pro residue of the peptide, which makes contact with the center β2 Tyr of the WW domain, with an Ala residue, can abolish binding to the WW domain (Macias *et al.,* 1996). Also, mutating the Tyr residue in the class I peptide has also been shown to eradicate binding to its respective WW domain (Kato *et al.,* 2006; Macias *et al.,* 1996). Mutational analysis that eliminates binding of the WW domain from its respective ligand is an important tool that can allow insight into the importance of interactions in specific signal transduction pathways.

1.4.3 PDZ domains

The third, and most prevalent protein binding domain found within MAGUK proteins are the PDZ domains. PDZ-containing proteins can be divided into two groups; the first group encompasses proteins that only contain PDZ domains, usually present in multiple copies within an individual protein (reviewed in Jeleń *et al.,* 2003). The second group of PDZ-containing proteins possess single or multiple PDZ domains, in combination with other functional domains (Jeleń *et al.,* 2003). MAGUK proteins belong to the latter group.

According to the simple modular architecture research tool, PDZ domains are one of the most common protein interaction modules (http://SMART.embl-heidelberg.de). The simple modular architecture research tool is a database that identifies and annotates genetically mobile domains and the analysis of domain architectures within proteins (Schultz *et al.,* 2000). PDZ domains contain approximately 80-100 amino acids which form two α-helices (α1 and α2) and six β-strands (β1-β6) (Figure 1.12A) (Doyle *et al.,* 1996; Morais-Cabral *et al.,* 1996). The

domain folds into a six stranded β-sandwhich (Doyle *et al.,* 1996; Morais-Cabral *et al.,* 1996). The peptide binds in a groove between the β2 strand and the α2 helix, forming an additional antiparallel β-strand with the PDZ domain, termed β-addition (Figure 1.12B and C) (Doyle *et al.,* 1996; Harrison, 1996). PDZ domains recognize short C-terminal peptide motifs of approximately 3-4 amino acids in length (nomenclature beginning with the C-terminal peptide 0, -1, -2, -3 and so on) (Doyle *et al.,* 1996), however is has been documented that residues up to -8 of the C-terminal peptide can also be significant for ligand binding specificity (Birrane *et al.,* 2003; Niethammer *et al.,* 1998; Songyang *et al.,* 1997). PDZ domains are known to interact with many cell surface receptors and can link these to their respective effector enzymes (Brône and Eggermont, 2005; Deng *et al.,* 2006; He, 2006; Morais-Cabral *et al.,* 1996), demonstrating the importance of PDZ domains in signal transduction pathways. Therefore, the presence of PDZ domains is integral to the scaffolding function of MAGUK proteins in signal transduction pathways.

PDZ domains are classified into four different classes based on the carboxy-terminal sequences to which they bind (Table 1.2). PDZ domains display overlapping specificity toward their different target ligands, thereby adding to the complexity of the classification of PDZ domains (Birrane *et al.,* 2003; Kang *et al.,* 2003; Nourry *et al.,* 2003; Pan *et al.,* 2007). A conserved carboxylate-binding loop (R/K-XXX-G-Φ-G-Φ or GLGF motif) is found in the loop connecting β1 and β2 (Figure 1.12A-B and Figure 1.13, red) (Doyle *et al.,* 1996). The carboxylate-binding loop creates a cavity and surrounds the hydrophobic C-terminal residue (at position 0) of the peptide ligand, which is most often a Val, however an Ile can also be tolerated here (Doyle *et al.,* 1996; Morais-Cabral *et al.,* 1996). The GLGF motif forms a cradle with the

Table 1.2: Classification of PDZ domains based on the C-terminal peptide to which they bind (reviewed in Dev 2004; Jeleń *et al.,* 2003; Nourry *et al.,* 2003). (X-any amino acid, Φ - hydrophobic, Ψ – basic, hydrophilic).

Class	C-terminal peptide
Class I	**-X-[S/T]-X-Φ**-COOH
Class II	**-X-Φ-X-Φ**-COOH
Class III	**-X-[D/E]-X-Φ**-COOH
Class IV	**-X-X-C**-COOH, **-X-Ψ-[D/E]**-COOH

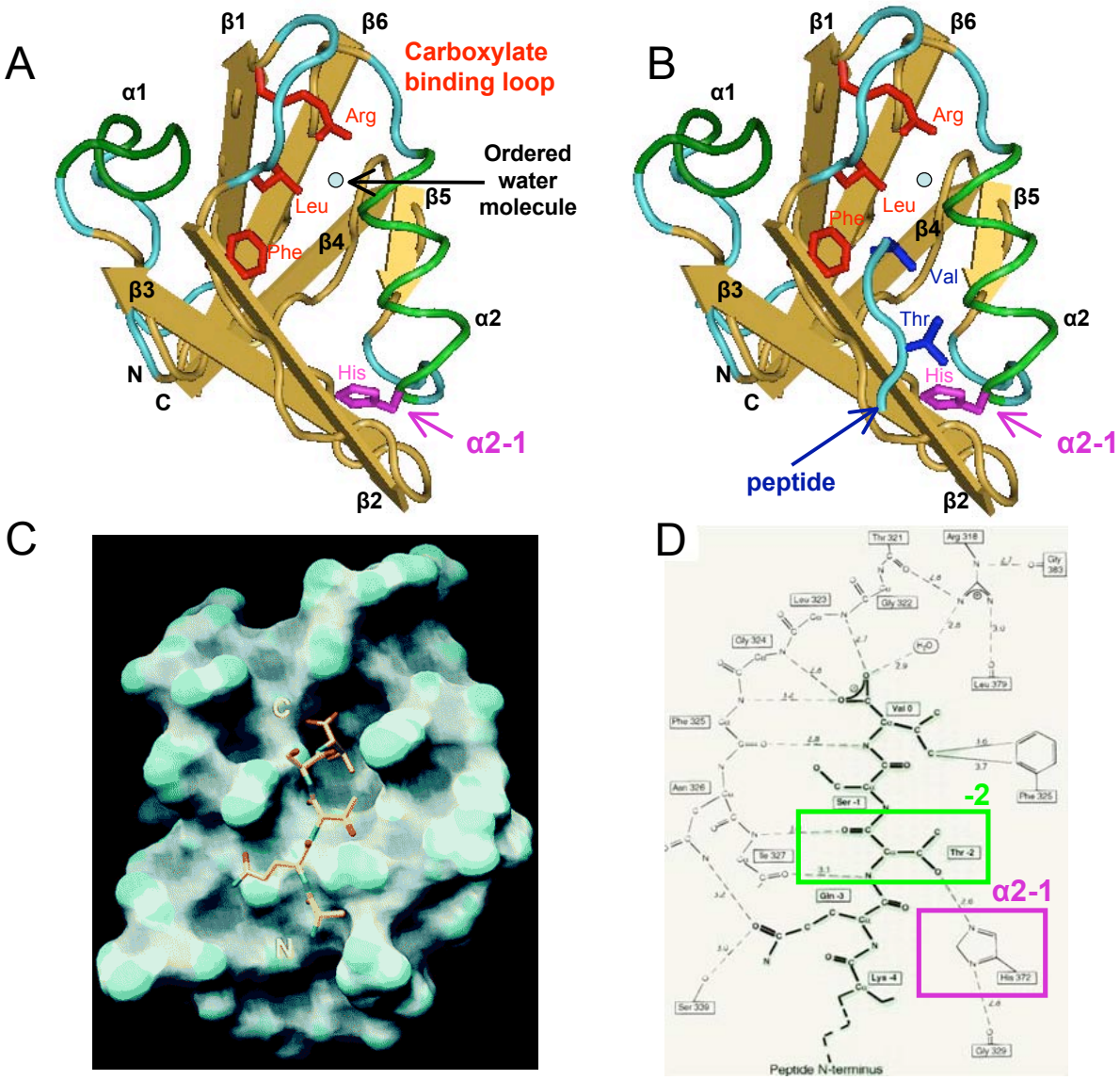

Figure 1.12: Structure of a PDZ domain. **A**, Ribbon diagram showing the structure of the third PDZ domain of the rat PSD-95, a MAGUK scaffolding protein (PTB ID: 1TP5 from Saro *et al.*, 2004). PDZ domains are made up of 80-100 amino acids which are arranged into two α-helices (α1 and α2), and six β-sheets (β1-β6). The basic Arg and the Leu and Phe, within the GLGF motif, forms the carboxylate binding loop, and are higlighted in red. The α2-1 residue (His), important in making contact with the -2 position of the peptide, is highlighted in purple. **B**, PDZ domain bound to a class I ligand with Val (0) and Thr (-2) residues highlighted in blue. **C**, Spacefill model depicting the surface topology of the PDZ domain bound to a C-terminal peptide, highlighting the peptide binding groove. For the short peptide (yellow), oxygen atoms are shown in red and nitrogen atoms are shown in blue (used with permission from Doyle *et al.*, 1996). **D**, Schematic representation of the contacts identified between the PDZ domain and its peptide. Darker black lines represent the peptide whereas the lighter black lines represent amino acids from the PDZ domain. Dashed lines represent hydrogen bonds. The green box indicates the -2 position of the peptide and the purple box indicates the His at position at α2-1 (used with permission from Doyle *et al.*, 1996).

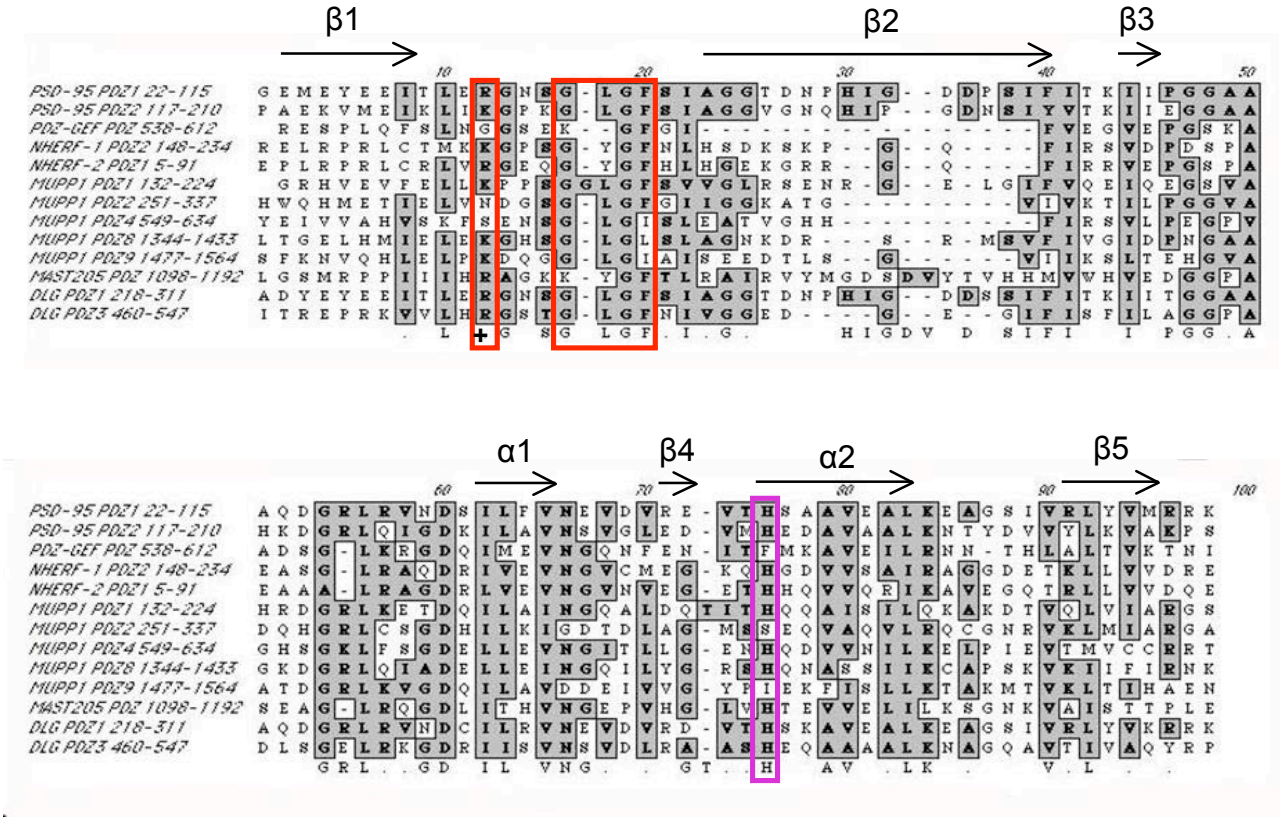

Figure 1.13: CUSTLAW sequence alignment of PDZ domains. Sequence alignment of thirteen PDZ domains of human origin representing the well conserved residues that are characteristic of a PDZ domain. PSD-95 (AAB07736) and DLG (NP_996407) are MAGUK scaffolding proteins. PDZ-GEF (NP_057424) is a guanine nucleotide exchange factor protein containing a PDZ domain. NHERF-1 and -2 (NP_004243 and NP_004776) and MUPP1 (ACC61870) are PDZ scaffolding proteins. MAST205 (BAB40778) is a Ser/Thr kinase. The well conserved basic residue and the GLGF motif with the carboxylate binding loop are boxed in red. The carboxylate binding loop forms a hydrophobic pocket that accommodates the 0 residue of the peptide. The α2-1 residue that makes contact with the -2 position of the peptide, is highlighted in purple.

three amides that hydrogen bond with the terminal carboxylate group of the peptide (Figure 1.12D). Also present in the carboxylate binding loop is a basic residue (Arg or Lys), which is conserved in approximately 85% of known PDZ domains and is found 3-4 amino acids from the GLGF motif (Doyle *et al.,* 1996; Morais-Cabral *et al.,* 1996). This basic residue coordinates a water molecule that in turn stabilizes the negative charge of the carboxylate group of the terminal residue of the peptide (Figure 1.12A-B-D) (Doyle *et al.,* 1996; Gee *et al.,* 2000; Harris *et al.,* 2003; Morais-Cabral *et al.,* 1996). A mutation in this basic residue to an Met or Ala often abolishes binding of the PDZ domain to its respective peptide (Chi *et al.,* 2006; Harris *et al.,* 2003). Therefore, the conserved carboxylate binding loop, containing the basic residue as well as the GLGF motif, are the hallmarks of a PDZ domain and are important in binding the terminal residue of its respective peptide ligand.

1.4.3.1 General binding characteristics of PDZ domains and their peptide ligands

PDZ domains undergo very little change in conformation upon binding to their peptide ligand (Doyle *et al.,* 1996; Morais-Cabral *et al.,* 1996). In addition, they demonstrate low affinities for their ligands ($K_d \leq$ 1-50 μM) (reviewed in Jemth and Gianni, 2007) which is indicative of the transient, reversible binding required for signal transduction pathways. Although PDZ domains exhibit specificity when binding peptides, an individual PDZ domain often has the ability to bind to different classes of peptide ligands (Birrane *et al.,* 2003; Kim and Sheng, 2004; Madsen *et al.,* 2005; Nourry *et al.,* 2003; Tonikian *et al.,* 2008; Vaccaro *et al.,* 2001). The side chains of the peptide at positions 0 (C-terminus) and -2 make direct contact with the PDZ domain, whereas the side chains at position -1 and -3 are solvent accessible (Novak *et al.,* 2002). The residues at positions -1 and -3 have few contacts with the PDZ domain, thus substitution mutations at these sites generally do not affect binding (Morais-Cabral *et al.,* 1996; Niethammer *et al.,* 1998; Pan *et al.,* 2007; Songyang *et al.,* 1997; Valiente *et al.,* 2005). The residue at position -2 is important in PDZ domain and ligand interactions because this residue is stabilized by hydrogen bonds with specific amino acids in the β2 and α2 regions of the PDZ domain (Figure 1.12D) (Dobrosotskaya, 2001; Doyle *et al.,* 1996; Songyang *et al.,* 1997). The first residue of the α2 domain (α2-1) of the PDZ domain is crucial in determining the specificity of that PDZ domain (Doyle *et al.,* 1996; Morais-Cabral *et al.,* 1996). For example, class I peptides contain a Ser/Thr residue at the -2 position of the peptide ligand

and this makes a hydrogen bond with the N-3 of the His positioned in the α2-1 of a class I PDZ domain (Figure 1.12B-D and Figure 1.13A, purple) (Doyle *et al.,* 1996; Nourry *et al.,* 2003; Novak *et al.,* 2002). For class II PDZ domains, a second hydrophobic pocket is created to accommodate the aromatic or hydrophobic residue at position -2 of the ligand (Table 1.2) (Nourry *et al.,* 2003). Therefore, α2-1 is a Val/Ile residue (Daniels *et al.,* 1998; Im *et al.,* 2003). For class III peptides, a Tyr residue is often present at the α2-1 position because a hydroxyl group is required to form hydrogen bonds with the negatively charged residue at position -2 of the ligand (Table 1.2) (Tochio *et al.,* 1999). Therefore, the residue positioned -2 of the peptide ligand are important in determining the specificity of binding to PDZ domains. In addition, residues more N-terminal of the peptide ligand are expected to play supplementary roles in fine-tuning the specificity of PDZ domain binding.

Class I and II PDZ domains are the most abundant classes, whereas the remaining classes are less common and often show conflicting binding properties (Bezprozvanny and Maximov, 2001). The last class of PDZ binding domains are not well defined as there are not many examples representing them. Additionally, many review articles claim that there are only three classes of PDZ domains (Jeleń *et al.,* 2003; Nourry *et al.,* 2003) and therefore class IV PDZ domains may be the exception rather than the rule. Class IV PDZ domains do not bind the traditional small hydrophobic residue such as the Val residue at position 0 found in class I, II and III ligands. Instead, they preferentially bind a terminal Cys or a hydrophilic residue (Table 1.2) (Borrell-Pagès *et al.,* 2000; Maximov *et al.,* 1999; Vaccaro *et al.,* 2001). Some examples of the class IV PDZ domains include the first PDZ domain in the Mint1 protein, which preferentially binds to the C-terminal end of N-type Ca^{2+} channel (-D**HWC**-COOH) (Maximov *et al.,* 1999). Although there is no crystal structure showing these interactions, it is believed that the Leu in position α2-1 is also important in providing specificity to ligand binding and makes contact with the -2 His of the peptide ligand (Maximov *et al.,* 1999). Crystal structures are needed for these PDZ domains complexed with ligands in order to further analyse their binding specificities.

MAGI PDZ domains are composed mainly of class I PDZ domains because most of them contain a His residue at position α2-1 (Figure 1.14, purple). The PDZ0 domain of the

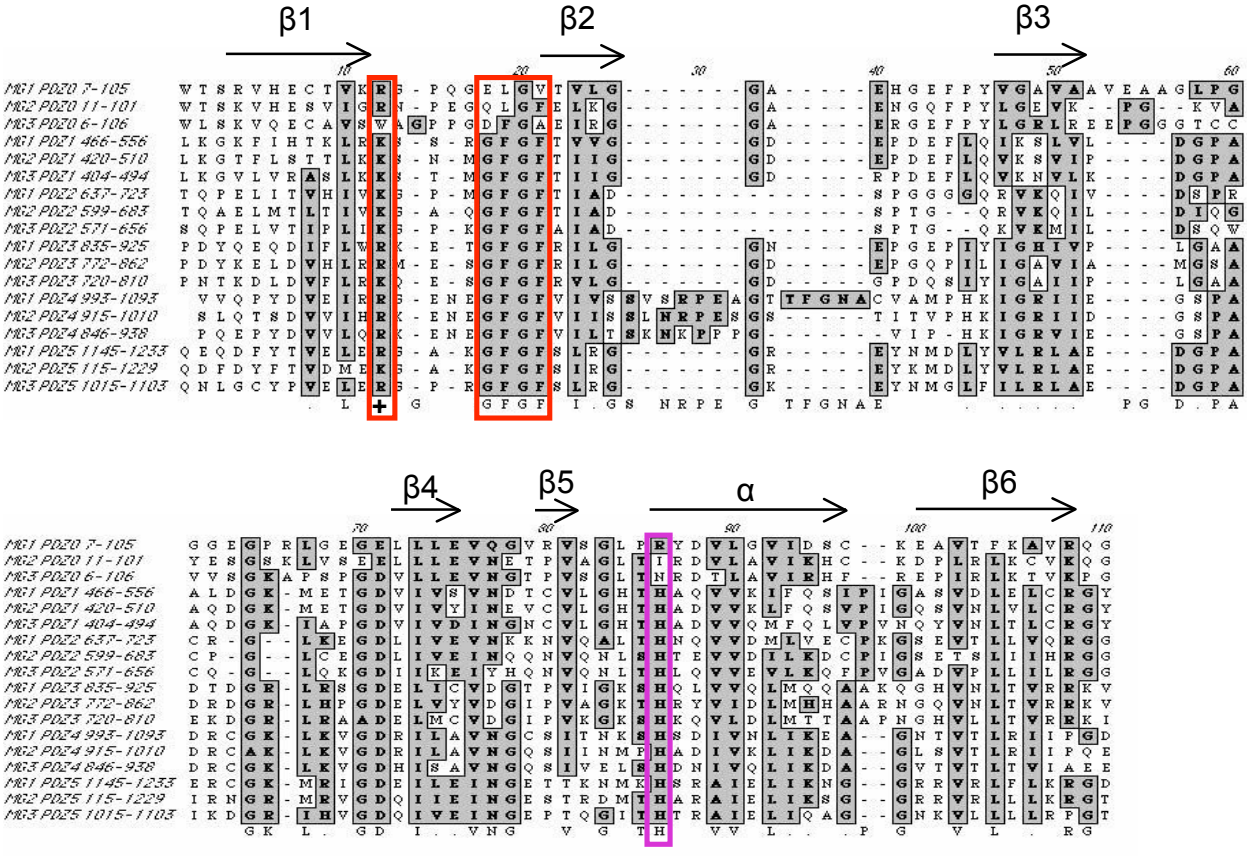

Figure 1.14: CUSTLAW sequence alignment of the MAGI PDZ domains. sequence alignment of the PDZ domains of MAGI-1 (MG1, NP_056335), MAGI-2 (MG2, NP_036433) and MAGI-3 (MG3, AF213259). Most of the PDZ domains of MAGI-2 are of class I with the anomaly being PDZ0. The MAGI PDZ domains are more similar with respect to homologous PDZ domains of other MAGI proteins than they are with respect to the PDZ domains within an individual MAGI protein. The well conserved basic residue, and the GFGF motif forming the carboxylate binding loop, are boxed in red. The carboxylate binding loop forms a hydrophobic pocket that accommodates the 0 residue of the peptide. The α2-1 His residue that makes contact with the -2 position of the peptide, is highlighted in purple.

MAGI proteins is quite different in sequence in that it has diverged from the GFGF motif when compared to PDZ1-PDZ5 of MAGI-2 (G-Ψ/Ω-L-G-Φ, where Ω-hydrophilic and Φ-hydrophobic) (Figure 1.14, red) and it has an Arg, Ile or Asn residue at position α2-1, respectively (Figure 1.14, purple). MAGI PDZ domains have been shown to bind a variety of class I peptides (Adamsky *et al.,* 2003; Deng *et al.,* 2006; Dobrosotskaya and James, 2000; Valiente *et al.,* 2005; Vazquez *et al.,* 2001; Wu *et al.,* 2000a, 2000b; Xu *et al.,* 2001) including the C-terminal PDZ binding motif of PTEN (I**TKV**-COOH), which has been shown to bind to the PDZ2 of all MAGI proteins (Dobrosotskaya *et al.*, 1997; Wu *et al.,* 2000a, 2000b). The PDZ domains of MAGI have not been shown to bind to any other classes of ligands. Also, no protein has been shown to bind to any of the PDZ0 domains. Therefore, binding of ligands to the MAGI PDZ domains are hypothesized to be to class I peptides, however other classes are also possible as PDZ domains often exhibit dual specificities.

Mutational analysis where PDZ domains are mutated as to abolish binding can give insight about the importance of specific interactions between PDZ domains and their respective peptide ligands. Class I PDZ domains contain a His residue, the first residue in the α2-1 PDZ domain, important for making contact with Ser/Thr at the -2 position of Class I peptides. This His residue is highly conserved amongst class I PDZ domains (Doyle *et al.,* 1996; Morais-Cabral *et al.,* 1996). The N-3 from the His residue makes hydrogen bonds with the hydroxyl groups of Ser/Thr -2 position of the peptide ligand (Doyle *et al.,* 1996; Morais-Cabral *et al.,* 1996; Novak *et al.,* 2002) (Figure 1.14D, purple). Previous studies have used mutation of this His to Leu to abrogate binding (Dobrosotskaya, 2001; Doyle *et al.,* 1996). Therefore a mutation of this residue should abolish binding to class I peptides. Similar contacts exist in most PDZ domains and therefore, similar point mutations can abolish binding while still maintaining the integrity of the tertiary structure of the PDZ domains.

Mutations in the C-terminal PDZ binding motif of the peptide ligand can also abolish binding. One of the most common mutations is of the terminal Val residue (0 position) to an Ala residue since this will often abolish binding of a Class I, II or III ligand to its PDZ domain (Jeleń *et al.,* 2003; Valiente *et al.,* 2005). Another residue in the ligand that is critical for making contact with the PDZ domain is the residue at the -2 position (a Thr/Ser in Class I ligands). A point mutation changing this residue to an Ala, or any residue that cannot maintain the hydrogen bond with the N3 of the highly conserved His residue at position α2-1 will abolish

binding (Dobrosotskaya, 2001; Jemth and Gianni, 2007). Discrete mutations that can abolish binding between PDZ domains and their respective ligands are useful in determining how loss of interactions can affect cell signalling.

1.4.3.2 PDZ domains also bind lipids

PDZ domains have recently been shown to have the ability to interact with phosphatidylinositol lipids and their phosphorylated derivatives (Izawa *et al.,* 2008; Kachel *et al.,* 2003; Mortier *et al.,* 2005; Pan *et al.,* 2007; Sugi *et al.,* 2008; Zimmermann, 2006). PDZ domain and lipid interaction has been implicated in receptor signal transduction, membrane trafficking, cytoskeleton remodelling and nuclear processes (Mortier *et al.,* 2005; Wu *et al.,* 2007; Zimmermann *et al.,* 2002, 2005). PDZ domain interaction with phosphorylated phosphoinositides not only provides a mechanism of protein localization to the plasma membrane, it may provide a mechanism to respond to sensing of phosphorylated phosphoinositide signalling (Wu *et al.,* 2007). The binding of PDZ domains to lipids is a novel interaction that is just now emerging.

Studies have suggested different mechanisms of interaction between PDZ domains and their lipids. The first mechanism involves positively charged residues located on the surface of the PDZ domain that are believed to interact electrostatically with the negatively charged lipids of the plasma membrane (Mortier *et al.,* 2005; Sugi *et al.,* 2008; Zimmermann *et al.,* 2002, 2005). This interaction often seems to compete with peptide ligand binding, leading to the suggestion that the lipid binding domain and peptide binding site overlap (Kachel *et al.,* 2003; Sugi *et al.,* 2008; Zimmermann *et al.,* 2002, 2005). Studies have found that the PDZ1 domain of syntenin-1 bound more strongly to phosphatidylinositol (3,4) bisphosphate ($PI3,4P_2$), and that the PDZ2 domain bound more strongly to the syndecan receptor, suggesting that syntenin-1 may be recruited to the membrane through binding of PDZ1 to the plasma membrane as well as through binding of PDZ2 to the receptor (Mortier *et al.,* 2005; Sugi *et al.,* 2008; Zimmermann *et al.,* 2002, 2005). This same study showed that PDZ binding to lipids is strongest when the PDZ domains of syntenin-1 are expressed in tandem (Mortier *et al.,* 2005). Also of importance, the PDZ domains of syntenin-1 have been shown to interact with the highest affinity for $PI3,4P_2$, and with less affinity towards other bisphosphorylated and trisphosphorylated lipids, and showed no binding of phosphatidylinositol or mono-phosphorylated phosphoinositides

(Mortier *et al.,* 2005). Therefore PDZ domains can interact with the lipids of the plasma membrane and do exhibit specificity when binding to lipids.

Recent structural studies of syntenin-1 revealed one mechanism of PI3,4P_2 binding to the first PDZ domains (Sugi *et al.,* 2008). Positively charged residues, and residues capable of forming hydrogen bonds, are positioned close to α2-helix of the PDZ domain (Sugi *et al.,* 2008). These residues are responsible for making contacts with negatively charged phosphates found in the lipids (Sugi *et al.,* 2008). The positively charged residues in syntenin-1 important in making interactions with the plasma membrane are Lys-214 and Lys-250, which are located in the β5/α2 (Figure 1.15A) (Sugi *et al.,* 2008). Mutations in these residues abolished PI4,5P_2 binding by syntenin-1 (Mortier *et al.,* 2005; Zimmermann *et al.,* 2005). The hydrophobic pocket of the PDZ domain, can bind the diacylglycerol moiety of PI4,5P_2 (Figure 1.15A) (Sugi *et al.,* 2008). Therefore, it is hypothesized that the diacylglycerol moiety can fit into the ligand binding groove, in agreement with the previous studies which show competitive binding between PI4,5P_2 and peptide ligands (Mortier *et al.,* 2005; Sugi *et al.,* 2008; Zimmermann *et al.,* 2005). These studies have shown that the PDZ domain of syntenin-1 has the ability to interact electrostatically with the plasma membrane and the membrane lipid can insert itself into the hydrophobic pocked of the PDZ domain, competing with peptide ligand interactions.

In a similar fashion, the PDZ domain of partitioning-defective protein-3 has been shown to bind to inositol phosphate (Wu *et al.,* 2007). Three positively charged residues in the PDZ2 domain of partitioning-defective protein-3 are important in binding to phosphoinositol (Wu *et al.,* 2007). These positively charged residues were located in the β1/β2 and α2/β6 loop, which is believed to be responsible for binding to the phosphoinositol 3-phosphate head group (Wu *et al.,* 2007). Also, a membrane insertion loop, containing hydrophobic residues (Leu-494, Pro-495, Ile-500) between the positively charged cluster and lipid head binding pocket, was capable of inserting in the plasma membrane (Wu *et al.,* 2007). These positively charged residues do not necessarily coincide with the positively charged residues found in syntenin-1 above and therefore may confer the specificity required to bind to phosphoinositol rather than PI4,5P_2.

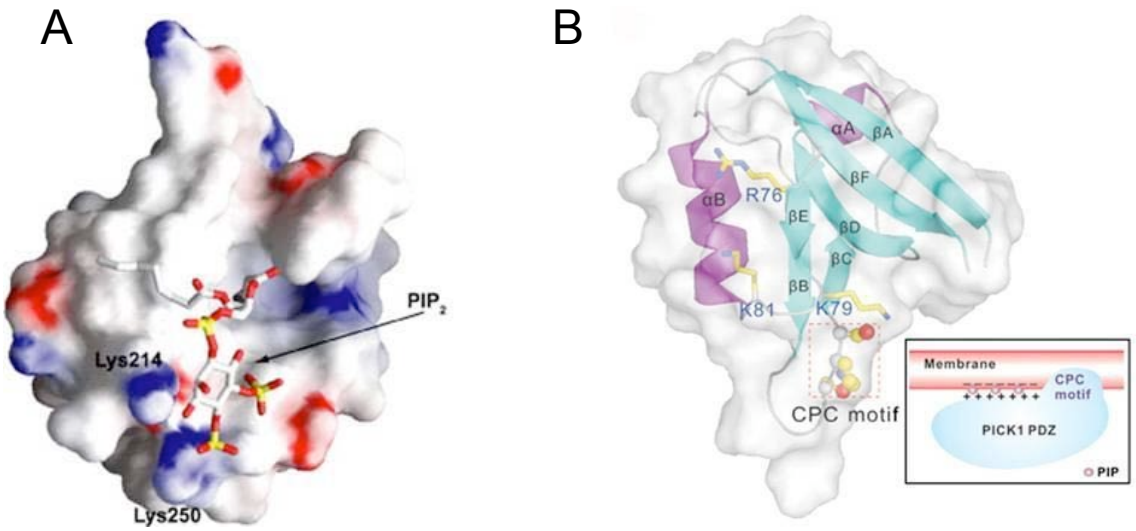

Syntenin-1 PDZ1 **PICK1 PDZ**

Figure 1.15: Mechanisms by which PDZ domains are able to interact with phospholipids. **A**, Spacefill model of the first PDZ domain of syntenin-1. Syntenin-1 PDZ1 domain can interact electrostatically through the positively charged residues on the surface of the PDZ domain and the negatively charged lipid heads. Phospholipids (PIP_2) can bind in the hydrophobic groove and compete for ligand binding. Blue indicates positively charged residues at the surface whereas red depicts negatively charged residues (used with permission from Sugi *et al.,* 2008). **B**, The PDZ domain of PICK1 is hypothesized to contain a Cys-Pro-Cys motif that embeds itself into the membrane, orienting positively charged residues on the surface of the PDZ domain to make contact with the negatively charged lipids within the plasma membrane (used with permission from Pan *et al.*, 2007). This interaction does not compete for the peptide binding groove.

A second PDZ-lipid binding mechanism involves a Cys-Pro-Cys motif that may insert into the plasma membrane, exposing a positively charged surface of the PDZ domain to interact with the plasma membrane (Figure 1.15B) (Pan *et al.,* 2007). Protein interacting with C kinase-1 is a protein that contains an N-terminal PDZ domain responsible for localization to the plasma membrane (Jin *et al.,* 2006; Pan *et al.,* 2007; Xu and Xia, 2006). The Cys-Pro-Cys motif interaction, in addition to several positively charged residues (Arg-76, Lys-79 and Lys-81) located in the β5 (βE) and β5/α2 (βE/αB) loop, are believed to be responsible for the localization of protein interacting with C kinase 1 to the plasma membrane (Pan *et al.,* 2007). The model proposes that the Cys-Pro-Cys motif, located in the β2/β3 (βB/βC) loop, inserts into the lipid membrane, while nearby positive residues on the PDZ domain interact with the negatively charged lipids (Pan *et al.,* 2007). Unlike the studies mentioned above, this lipid binding site does not overlap with the peptide ligand binding site because peptide binding can still occur (Pan *et al.,* 2007). The positively charged residues responsible for making contact with the plasma membrane are on a distant, opposite surface of the peptide ligand binding groove (Pan *et al.,* 2007). Cys residues are potential sites of palmitoylation (reviewed in Nadolski and Linder, 2007) and the authors did not rule out this option in the above model. Therefore, this model proposes that a Cys-Pro-Cys motif, in addition to positively charged residues on the surface of the PDZ domain, interact with the lipids within the plasma membrane.

In summary, PDZ domains can interact with lipids of the plasma membrane (Mortier *et al.,* 2005; Pan *et al.,* 2007; Wu *et al.,* 2007; Zimmermann *et al.,* 2002, 2005). These interactions have been shown to be important in protein localization to the plasma membrane and it has also been shown that PDZ domains can bind to a variety of phosphoinositides including inositol phosphate, phosphoinositol, mono-, bi- and triphosphorylated phosphoinositides. So far, studies have shown two mechanisms of localization to the plasma membrane; 1) through electrostatic interactions (Mortier *et al.,* 2005; Sugi *et al.,* 2008; Wu *et al.,* 2007; Zimmermann *et al.,* 2002, 2005) and 2) through Cys-Pro-Cys motif insertion (Pan *et al.,* 2007). Whatever the mechanism, PDZ domain interaction with the plasma membrane has been implicated in many important functions such as receptor signal transduction, membrane trafficking, cytoskeleton remodelling and nuclear processes (Mortier *et al.,* 2005; Pan *et al.*,

2007; Wu *et al.,* 2007; Zimmermann *et al.,* 2002, 2005). Therefore, PDZ domain interaction with the plasma membrane is a physiologically important interaction in cells.

1.4.4 GARP C-terminal sequence

The GARP C-terminal sequence, located at the C-terminal end of the MAGI-2 protein, is made up of 333 residues. Our laboratory has named this region the GARP C-terminal sequence because it is rich in Gly, Ala, Arg and Pro residues and it is unique to MAGI-2. Basic local alignment search tool is an algorithm for comparing primary amino acid sequences and matching these with other sequences that share homologies (Altschul *et al.,* 1990). According to a basic local alignment search sequence search, the GARP C-terminal sequence of MAGI-2 (amino acids 1233-1455) had no sequence homology with any other sequences nor does it contain any putative conserved domain sequences. Therefore, the GARP C-terminal sequence of MAGI-2 is unique and has no known function.

Zonnula occulens is a MAGUK scaffolding protein that is important in the maintenance of tight junctions and cellular polarity (Willott *et al.,* 1993). The last 994 residues are acidic and Pro rich. Although the C-terminal ends of *Zonnula occulens* proteins do not have characteristic protein binding domains, it has been shown to bind both cytosolic, cytoskeletal and transmembrane proteins, and disruption of these interactions has been shown to disrupt the integrity of tight junctions (reviewed in Gonzalez-Mariscal *et al.,* 2000). Also of note, the C-terminal end contains many PXXP motifs which have been shown to bind to selected SH3 domains (Katsube *et al.,* 1998). The C-terminal end of *Zonnula occulens* lacks a protein binding domain and is rich in Pro residues much like that of the GARP C-terminal sequence of MAGI-2. Therefore, the GARP C-terminal sequence may have similar functions as that of the C-terminal end of the *Zonnula occulens* MAGUK scaffolding proteins.

1.5 MAGI scaffolding proteins

MAGI is part of a subfamily of MAGUK scaffolding proteins which contains three members: MAGI-1, -2 and -3 (Dobrosotskaya *et al.,* 1997; Wu *et al.,* 2000b). As mentioned above, the MAGI family of proteins are inverted with respect to their family member counterparts. In addition to sharing great sequence similarity, these genes are alternatively spliced (Figure 1.16), adding another degree of complexity in distinguishing between these

protein variants (Dobrosotskaya *et al.,* 1997; Shoji *et al.,* 2000; Sierralta and Mendoza, 2004; Wood *et al.,* 1998). Much of the published literature have used antibodies that do not discriminate between the MAGI family, nor their individual splice variants (Subauste *et al.,* 2005; Wood *et al.,* 1998). Therefore the different MAGI proteins are difficult to discriminate. MAGI-1 has three alternatively spliced partners: MAGI-1a, -b and -c, all of which have different C-terminal ends (Figure 1.16A) (Dobrosotskaya *et al.,* 1997; Laura *et al.,* 2002). These splice variants have been shown to be both tissue specific and localized to different compartments of the cell (Dobrosotskaya *et al.,* 1997; Laura *et al.,* 2002). The MAGI-2 gene has also been shown to have three different promoters on distinct exons and their protein products have been named MAGI-2α, -β and -γ (Figure 1.16B) (Deng *et al.,* 2006). According to the RefSeq database, MAGI-3 has two isoforms which differ in the C-terminal ends (Figure 1.16C) (NP_001136254 and NP_690664, http://www.ncbi.nlm.nih.gov.cyber.usask.ca/RefSeq/). It is not uncommon for genes encoding PDZ domains to be alternatively spliced (Sierralta and Mendoza, 2004). Alternatively spliced genes allow for multiple mRNA to be formed from one gene which adds to the eukaryotic genetic diversity. Often, differentially spliced variants of a protein will be localized to specific tissues, restricted to discrete areas of the cell and may have different or similar functions than their spliced variants. Little is known about the mechanisms that control the specificity of MAGI expression in a cell or at a particular stage of development. There is also little known about the roles of the MAGI proteins encoded by these splice variants. The ability to discriminate between the different MAGI proteins and the different variants is important to distinguish which MAGI protein(s) are performing a given function at a given time.

MAGI proteins are expressed ubiquitously throughout mammalian tissues, with different expression profiles for each family member. Mammalian expression of MAGI-1 is found in the kidney, liver, lung, testis, heart, skeletal muscle and brain (Dobrosotskaya *et al.,* 1997; Laura *et al.,* 2002). MAGI-2 is expressed in the tissues in the brain and liver as well as in epithelial cells (Deng *et al.,* 2006; Hu *et al.,* 2007; Shoji *et al.,* 2000; Vazquez *et al.,* 2001; Wood *et al.,* 1998; Wu *et al.,* 2000a). MAGI-3 is expressed in most tissues with the exception

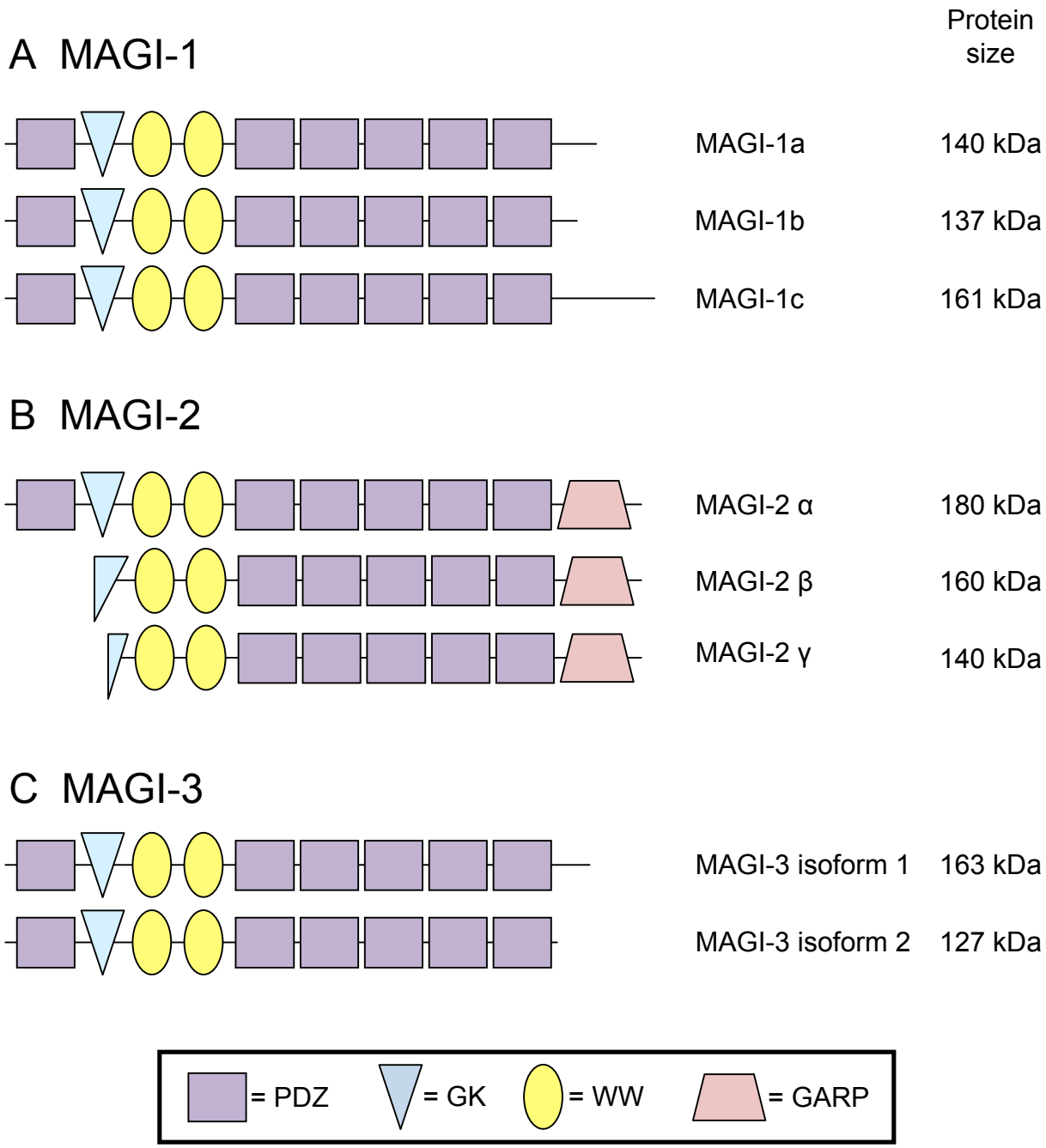

Figure 1.16: MAGI proteins encoded by alternative spliced mRNAs. **A**, MAGI-1 variants encoded by alternative splicing: MAGI-1a, b and c (modified from Laura *et al.*, 2002). **B**, MAGI-2 variants encoded by alternative splicing: MAGI-2 α, β and γ (modified from Deng *et al.*, 2006). **C**, MAGI-3 variants encoded by alternative splicing: MAGI-3 isoforms 1 and 2 (RefSeq Database).

of skeletal muscle, leukocytes and spleen (Franklin *et al.,* 2005; Wu *et al.,* 2000b). Therefore, MAGI proteins are collectively found throughout mammalian tissues.

Cellular localization of the MAGI proteins is prominent at the plasma membrane at areas of cell-cell communication, such as neuronal synapses and tight junctions (Laura *et al.,* 2002; Wu *et al.,* 2000a, 2000b). The MAGI family of scaffolding proteins have also been found to be present diffusely throughout the cytoplasm, as well as in the nucleus (Adamsky *et al.,* 2003; Deng *et al.,* 2006; Wu *et al.,* 2000a, 2000b). MAGI-2 has been shown to be localized mostly at the plasma membrane in the cell body, as well as in the dendrites and the synaptic area of neurons (Hirao *et al.,* 1998; Shoji *et al.,* 2000). Therefore, although the main purpose of the MAGI scaffolding proteins may be to act as scaffolding molecules at the plasma membrane, they may have additional scaffolding functions in the cytoplasm as well as the nucleus.

MAGI is not known to be lipid modified or strongly anchored to the plasma membrane, and the lack of strong anchorage to the plasma membrane allows for more rapid translocation within the cell in response to transient stimulation (Xu *et al.,* 2001). MAGI proteins interact directly or indirectly with many cell surface receptors and cytoskeletal components, which may provide a mechanism for MAGI localization to the plasma membrane (Adamsky *et al.,* 2003; Buxbaum *et al.,* 2008; He, 2006; Hirao *et al.,* 1998; Ide *et al.,* 1999; Kawajiri *et al.,* 2000; Shoji *et al.,* 2000; Wood *et al.,* 1998). For example, the PDZ1 domain of MAGI-3 has been shown to interact with the cell surface β1-adrenergic receptor (He, 2006). A mutation in the C-terminal PDZ binding motif of the receptor causes a redistribution of MAGI-3 to the nucleus (He, 2006). Therefore, binding of MAGI to a receptor at the cell surface may be a prominent mechanism by which MAGI proteins are localized to the plasma membrane. Also, studies have shown that all MAGI-1 splice variants are capable of localizing to the plasma membrane however, a truncated mutant containing only the sequences encoding PDZ0-WW2 was unable to localize to the plasma membrane (Laura *et al.,* 2002). The same study found that truncated proteins containing combinations of PDZ1 through PDZ5 were capable of localizing to the plasma membrane (Laura *et al.,* 2002). Therefore, the PDZ1-PDZ5 domains are necessary for MAGI-1 localization to the plasma membrane (Laura *et al.,* 2002). This finding is not surprising since it is well documented that PDZ domains interact with various cell surface receptors.

Another mechanism by which MAGI proteins could localize to the plasma membrane is through association with the phosphorylated phosphoinositides of the plasma membrane

through their PDZ domains. Glutathione S-transferase (GST) fused MAGI-3 has been shown to interact with PI3,4P_2 with low affinity (K_d of approximately 1 mM) (Mortier *et al.,* 2005). However, another study showed no interaction of MAGI-3 individual PDZ domains 3,4 and 5 with liposomes coated with PI3,4,5P_3 (Wu *et al.,* 2007), a different lipid than mentioned above. This last study was performed with individual GST fused MAGI-3 PDZ domains and perhaps this specific PDZ/lipid interaction requires the tandem expression of the MAGI-3 PDZ domains, which has been demonstrated in previous studies (Zimmermann *et al.,* 2002, 2005). Also, both studies cited above tested binding of MAGI-3 PDZ domains against two different types of lipids, and MAGI-3 PDZ domains may bind specifically to PI3,4P_2 and not PI3,4,5P_2 (Mortier *et al.,* 2005; Wu *et al.,* 2007). Therefore, MAGI PDZ domains may be responsible for localizing MAGI scaffolding proteins to the plasma membrane through interactions with cell surface receptors or by direct binding to the lipids of the plasma membrane.

MAGI proteins have been shown to share high sequence similarity (Figure 1.6) (Wu *et al.,* 2000b) and therefore bind to many of the same proteins (Figure 1.17). For example, the PDZ1 domain of MAGI-2 and MAGI-3 have both been shown to bind to the β1-adrenergic receptor, a cell surface receptor involved in neuronal signalling (He, 2006; Xu *et al.,* 2001). The PDZ5 domains of the MAGI proteins have been shown to associate with α- and β- catenin, cytoskeletal proteins (Kotelevets *et al.,* 2005; Subauste *et al.,* 2005). PTEN has also been shown to interact with all MAGI proteins through their PDZ2 domain (Kotelevets *et al.,* 2005; Wu *et al.,* 2000a, 2000b). In addition, MAGI proteins have been shown to interact with various cell surface receptors such as receptor tyrosine phosphatase β, the ErbB4 RTK and N-methyl-D-aspartate receptors, all of which mediate cell signalling pathways (Adamsky *et al.*, 2003; Buxbaum *et al.*, 2008; Hiaro *et al.*, 1998). Similar binding partners to MAGI domains is not always the case between MAGI proteins. For example, the PDZ1 domain of MAGI-2 and MAGI-3 has been found to bind to the C-terminal, cytoplasmic domain of the transforming growth factor-α precursor however, MAGI-1 does not (Franklin *et al.,* 2005). Therefore, determining the protein interactions of one of the MAGI proteins may generally function as a working model for the MAGI group of scaffolding proteins. In addition, the

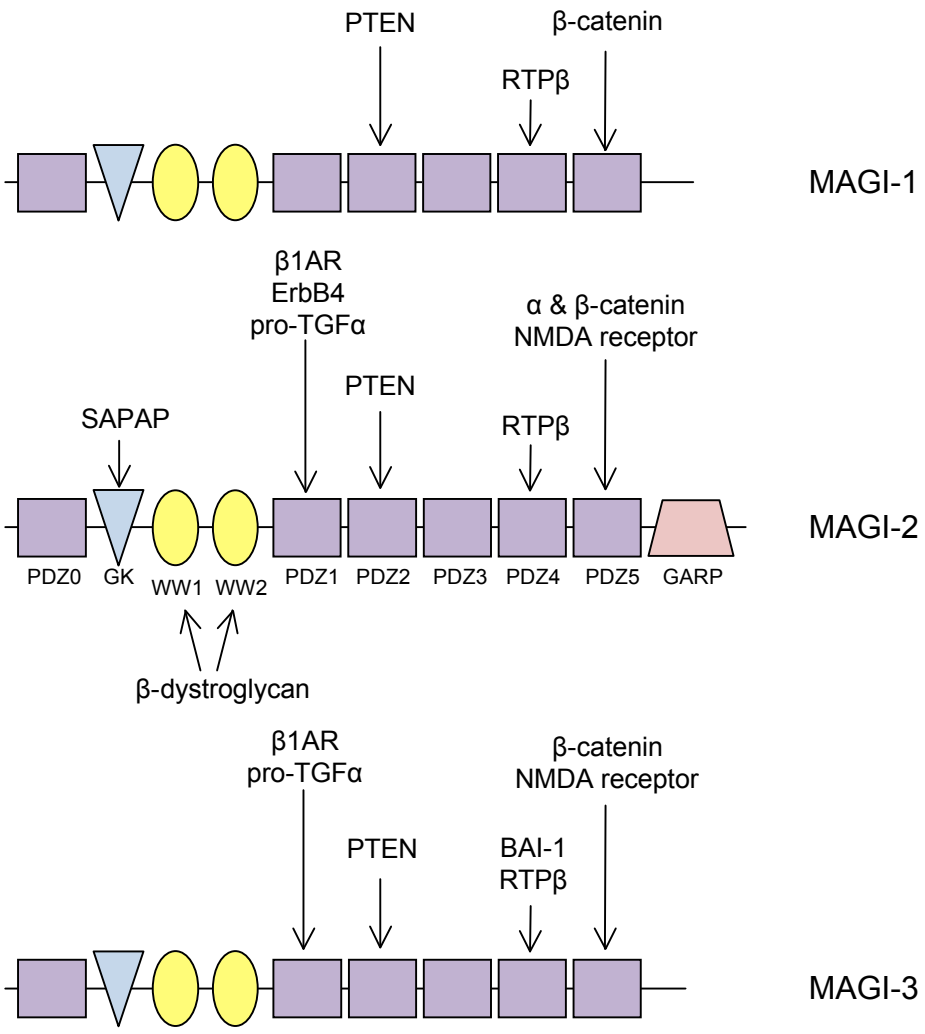

Figure 1.17: MAGI interacting partners. The MAGI family members share high sequence similarity and therefore bind to many of the same proteins, with some exceptions. The MAGI proteins have been shown to interact with various cell surface receptors such as the receptor protein tyrosine phosphatase (RPTP), ErbB4 RTK and N-methyl-D-aspartate (NMDA) receptor through their PDZ binding motifs. All of the PDZ5 domains of the MAGI proteins have been shown to associate with the cytoskeletal element β-catenin and MAGI-2 has been shown to also interact with α-catenin. MAGI-2 and MAGI-3 PDZ1 domains have been shown to bind brain angiogenesis inhibitor 1 (BAI-1), a protein involved in inhibiting brain angiogenesis. MAGI-2 and MAGI-3 PDZ1 domain has also been shown to bind to the cytoplasmic domain of the pro-transforming growth factor-alpha (pro-TGFα), which is important in localizing pro-TGFα at the proper location at the plasma membrane near its respective receptors. The GK domain of MAGI-2 has been shown to bind to SAP90/PSD-95-associated protein (SAPAP), a neuroglin that promotes the clustering of receptors and is known to associate with the plasma membrane. The WW domains of MAGI-2 have been shown to bind to β-dystroglycan, a cell adhesion molecule that plays a role in the organization of the neuronal synapses.

MAGI-2 GK domain has been shown to associate with SAP/PSD-95 associated protein, a neuroglin that is localized to the plasma membrane and is involved in the clustering of receptors (Deng *et al.*, 2006). The WW domains of MAGI-2 have also been shown to bind to β-dystroglycan, which are required for the structural integrity of neuronal synapses (Deng *et al.*, 2006). Therefore, MAGI proteins have been shown to bind to many of the same proteins similarly.

1.6 Regulation of PTEN by MAGI-2 proteins

MAGI proteins have already been identified as scaffolding molecules involved in many cell signalling pathways, localized in areas such as tight junctions in cells. PTEN has been found in two forms in cells; as a monomeric 65 kDa unit and in a high molecular weight complex of approximately 600 kDa (Vazquez *et al.,* 2001). This 600 kDa complex has been termed the PTEN-associated complex (PAC) and it is hypothesized that upon dephosphorylation and activation, PTEN is recruited to the plasma membrane to a high molecular weight protein complex, where it is believed to gain access to its lipid substrates (Valiente *et al.,* 2005; Vazquez *et al.,* 2001; Wu *et al.,* 2000a, 2000b). The PAC is believed to contain PTEN associated to a PDZ containing scaffold, such as MAGI-2, and the p85 protein (Vazquez *et al.,* 2001). It has been previously shown that p85 can bind directly to PTEN and positively regulate its lipid phosphatase activity towards $PI3,4,5P_3$ (Chagpar, 2004). This new regulatory function for p85 may be necessary in PTEN mediated attenuation of Akt signalling (Chagpar, 2004; Pastor, 2008). All MAGI proteins have been shown to co-localize with PTEN at tight junctions in epithelial cells, areas that are known to have activated Akt (Dobrosotskaya *et al.*, 1997; Wu *et al.,* 2000a, 2000b). Therefore, this suggests that MAGI-2, PTEN and p85 are able to co-localize at the plasma membrane, at appropriate sites in order to gain access to lipid substrates and attenuate PI3K/Akt signalling.

PTEN has been shown to bind to the PDZ2 domain of all MAGI proteins (Dobrosotskaya *et al.,* 1997; Wu *et al.,* 2000a, 2000b). In order for PTEN to interact with MAGI-2, PTEN must be dephosphorylated at Thr residues 382 and 383, thereby rendering it in its open, active conformation (Tolkacheva *et al.,* 2001; Vazquez *et al.,* 2000). Binding of PTEN to the PDZ domain of MAGI proteins has been shown to increase the half-life of PTEN (Georgescu, 2008; Valiente *et al.,* 2005; Wu *et al.,* 2000a, 2000b). This is probably due to the

fact that the C-terminal PTEN ubiquitination site is protected from ubiquitination when the nearby PDZ binding motif binds to the PDZ2 domain of MAGI (Wang and Jiang, 2008; Wang *et al.,* 2007). Also, a common PTEN mutation found in tumor cells is one that results in truncation of its C-terminal end, such that it lacks the PDZ binding motif (Vazquez *et al.,* 2000). This PTEN mutant has phosphatase activity, yet is unable to attenuate Akt effectively, probably due to an increase in ubiquitination thereby decreasing PTEN half-life (Vazquez *et al.,* 2000, 2001; Wang *et al.*, 2007; Wu *et al.,* 2000a, 2000b). Therefore, PTEN requires binding to a PDZ scaffolding protein, such as MAGI-2, for proper localization within the plasma membrane and protection against ubiquitination for effective attenuation of PI3K/Akt signalling.

MAGI-2 has been shown to be present at tight junctions, where it is present in the E-cadherin-β-catenin-α-catenin complex (Figure 1.18). Catenins play a pivotal role in E-cadherin function in that they link cadherins to cytoskeletal components of the cell, such as actin (Ozawa *et al.,* 1990). PTEN is hypothesized to be located at these tight junctions through binding of the PDZ2 domain of MAGI-2 (Subauste *et al.,* 2005; Wu *et al.,* 2000a). A cytoskeletal mutation that disrupts these tight junction complexes and causes improper localization of MAGI-2, showed elevated Akt activation and no PTEN protein expression, despite normal PTEN mRNA levels (Subauste *et al.,* 2005). These results suggest that PTEN is unable to bind to MAGI-2, thereby rendering PTEN ubiquitination sensitive such that it is quickly degraded by the proteosome (Subauste *et al.,* 2005). Many tumor cells have found mRNA levels of PTEN to be normal however, without any protein expression (Bastola *et al.,* 2002; Dahia *et al.,* 1999). It is thought that without proper localization of "open" and activated PTEN to a PDZ domain, PTEN is unstable and quickly degraded by the proteosome (Rahdar *et al.,* 2009; Subauste *et al.,* 2005; Vazquez *et al.,* 2000; Wu *et al.,* 2000a). Therefore, MAGI-2 is important in forming complexes at tight junctions to ensure the proper localization of PTEN upon its activation.

The p85 regulatory subunit has been shown to bind directly to β-catenin in a phosphorylation-dependent manner, and is present in the E-cadherin complex (Woodfield *et al.,* 2001). Also of significance is the fact that EGFR is present in an E-cadherin complex through direct binding to β-catenin upon EGF stimulation (Hoschuetzky *et al.,* 1994). It is well

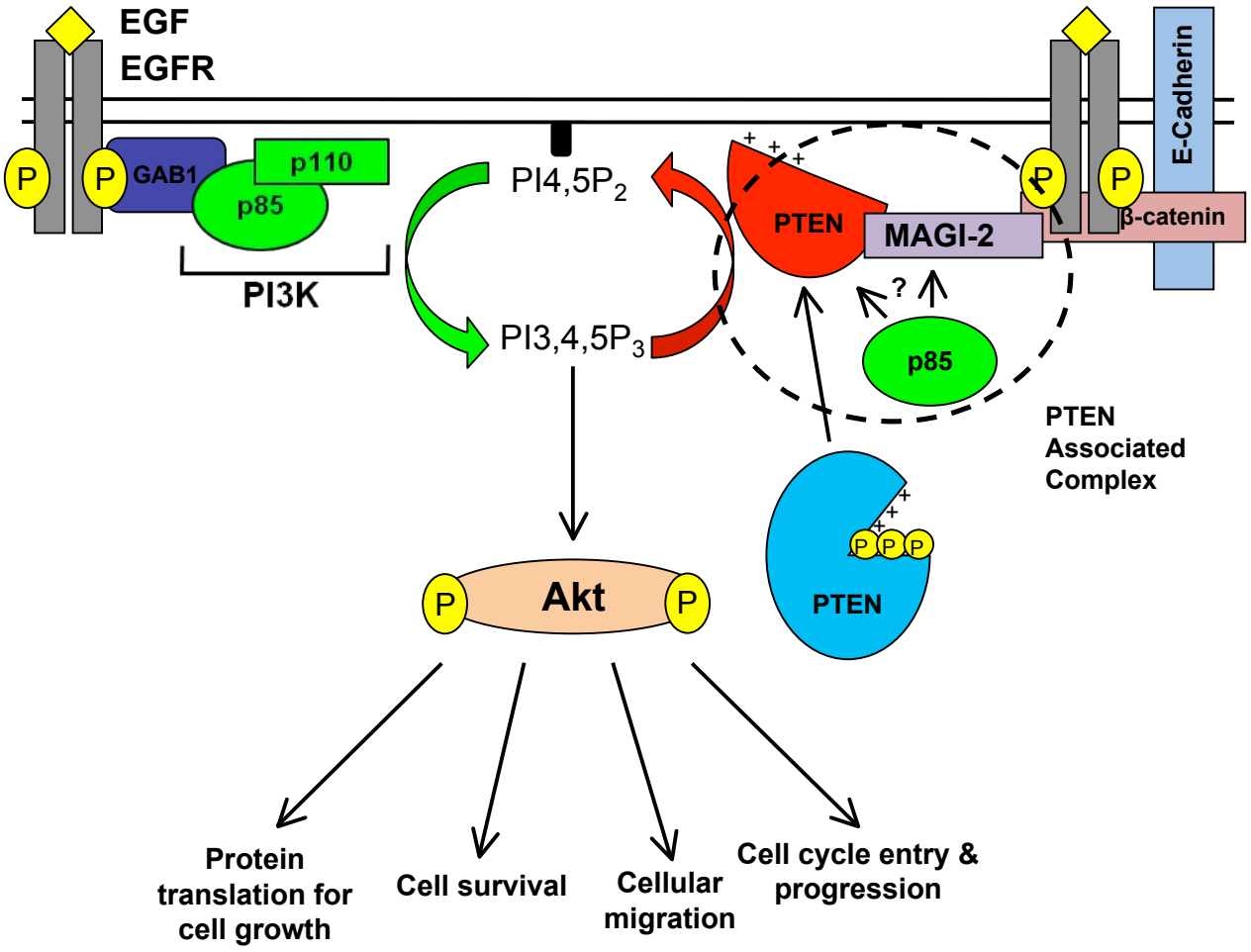

Figure 1.18: Proposed model of MAGI-2 scaffolding functions in the PTEN-mediated attenuation of PI3K/Akt signalling. The PAC has been speculated to redistribute PTEN to the plasma membrane at the proper location to gain access to its lipid substrates. MAGI-2 has been shown to be present at tight junctions, complexed with E-cadherin through β-catenin. EGFR and p85 have also been shown to bind to β-catenin and be present in the E-cadherin/β-catenin complex. Upon growth factor stimulation, EGFRs dimerize and phosphorylated receptor recruits the PI3K complex to the plasma membrane, generating $PI3,4,5P_3$. Lipid second messenger $PI3,4,5P_3$ recruits and activates Akt, which activates proteins that promote anti-apoptotic signalling, cell cycle entry, cellular migration and cellular survival. Upon growth factor stimulation, PTEN is believed to localize to the plasma membrane electrostatically and through association with the PAC. The PAC is believed to contain p85 and a PDZ scaffolding protein, such as MAGI-2. PTEN has been shown to associate through its C-terminal PDZ binding motif with the PDZ2 domain of MAGI-2. p85, a positive regulator of PTEN, may bind directly to PTEN, or to one of the WW domains of MAGI-2. Therefore MAGI-2 may act as a scaffolding protein, bringing together proteins responsible for the attenuation of the PI3K/Akt signalling pathway.

established that EGF treatment of epithelial cells causes destabilization of cadherin-based cell adhesion complexes, which leads to the reduction of intercellular adhesion and increased cell motility (Fujii *et al.,* 1996; Hazan and Norton, 1998). The human hepatocarcinoma tumor cell lines (MHCC-97H, BEL-7404, HepG2) lack MAGI-2 expression and also have elevated Akt and focal adhesion kinase signalling (Hu *et al.,* 2007), a phenotype reminiscent of PTEN null cells (Dahia *et al.,* 1999; Hu *et al.,* 2007; Subauste *et al.,* 2005). Akt and focal adhesion kinase signalling pathways are known to be downregulated by PTEN (reviewed in Hlobilková *et al.,* 2003). Once these MAGI-2 null cells were transfected with MAGI-2 cDNA, PTEN protein expression was restored, Akt and focal adhesion kinase signalling was attenuated, and cell migration was inhibited (Hu *et al.,* 2007). Therefore, the MAGI-2 complexes formed at tight junctions in cells plays a pivotal role in the ability of PTEN to downregulate Akt signalling in cells.

2.0 RATIONALE AND OBJECTIVES

We hypothesize that upon growth factor stimulation, PTEN is recruited to the PAC, which has been hypothesized to contain MAGI-2 and p85 (Vazquez *et al.*, 2000). The PAC may also contain EGFR and/or PDGFR, signalling molecules involved in the activation of the PI3K/Akt signalling pathway. Recruitment to the PAC may be important in bringing PTEN in close proximity to its lipids substrates in order to effectively attenuate Akt signalling. Therefore, the MAGI family of scaffolding proteins may improve the efficiency of PTEN signalling through the assembly of a high molecular weight complex at the plasma membrane at sites of RTK-mediated PI3K lipid product generation, where PTEN would have access to its substrates.

2.1 Hypothesis

MAGI-2 is the scaffolding protein responsible for bringing together proteins that both activate (RTKs and PI3K) and attenuate (PTEN and p85) Akt signalling, to ensure that cellular proliferation and cellular survival signals are transient.

2.2 Objectives

The goal of this thesis was to determine if the MAGUK scaffolding protein, MAGI-2, can interact with proteins involved in the PI3K/Akt signalling pathway, such as p85, EGFR, PDGFR, as well as to confirm PTEN binding. We chose MAGI-2 over MAGI-1 and MAGI-3 because it has been hypothesized to be present in the PAC (Vazquez *et al.*, 2000) and for ease of cloning.

1) To create clones of MAGI-2 full length (FL) and its respective domains tagged to a Myc epitope for eukaryotic protein expression.

2) To create clones of MAGI-2 FL and its respective domains fused to GST for bacterial protein expression.

3) Through pull-down experiments, determine if MAGI-2 domains can associate with proteins involved in the PI3K/Akt signalling pathway (PTEN, p85, EGFR and PDGFR).

A) First, to test whether the pull-down system is working properly, we would confirm PTEN binding to the PDZ2 domain of MAGI-2 (Valiente *et al.,* 2005; Vazquez *et al.,* 2000,

2001; Wu *et al.,* 2000a). PTEN contains a C-terminal binding motif (QI**TKV**-COOH, a class I ligand).

B) We hypothesize that one of the MAGI-2 PDZ domains could bind to the C-terminal PDZ binding motifs of PDGFR (ED**SFL**-COOH, a class I ligand) and/or EGFR (EF**IGA**-COOH, a class II ligand).

C) We hypothesize that p85 may bind through one of its two Pro rich regions [P1: amino acids 82-96 (S**PPTP**KPR**PPRP**LP, class II and III, respectively) and P2: amino acids 300-314 (ERQPAPAL**PPKPPKP,** both of which are class II) (Kapeller *et al.,* 1994)] to one or both of the WW domains of MAGI-2.

4) Through immunoprecipitation experiments, determine if Myc-MAGI-2 FL can associate with proteins involved in the activation and/or attenuation of PI3K/Akt signalling in cells (PTEN, p85, EGFR and PDGFR).

5) To create a MAGI-2 specific antibody that can distinguish MAGI-2 from its MAGI family counterparts.

The information obtained from these experiments will give us a better understanding of the role of the MAGI scaffolding proteins in the attenuation of PI3K/Akt signalling. From this data, we will be able to construct a more detailed model of PI3K/Akt signalling and its downregulation through PTEN. This model can then be used to explain how MAGI scaffolding proteins help in bringing together counteracting cell signalling proteins and how they can improve the efficiency of signal termination. Also, with a MAGI-2 specific antibody, future work can determine if the results obtained are specific for MAGI-2.

3.0 MATERIALS AND METHODS

All of the chemicals were of analytical grade or higher, and were purchased from VWR, Sigma-Aldrich or BDH, unless otherwise stated. The names and addresses of the distributors are listed in table 3.1. The list of commercially available kits is listed in table 3.2. All reactions were incubated at room temperature, unless otherwise stated.

Table 3.1: Names and addresses of reagent distributors.

Company Name	Address
American Type Culture Collection	Manassas, VA, USA
Applied Biosystems Canada	Streetsville, ON, Canada
BDH, Inc.	Toronto, ON, Canada
Bio-Rad Laboratories, Ltd.	Mississauga, ON, Canada
Cedarlane Laboratories, Ltd.	Burlington, ON, Canada
EMD Chemicals®, Inc.	Gibbstown, NJ, USA
Fermentas Canada, Inc.	Burlington, ON, Canada
GE Healthcare Bio-Sciences, Inc.	Baie d'Urfé, QC, Canada
HyClone	Logan, UT, USA
Invitrogen Canada, Inc.	Burlington, ON, Canada
MacVector, Inc.	North Carolina, USA
Millipore ™	Billerica, MA, USA
New England Biolabs, Ltd.	Pickering, ON, USA
Novagen	Mississauga, ON, Canada
PerkinElmer Life Sciences, Inc.	Boston, MA, USA
Qiagen, Inc.	Mississauga, ON, Canada
Santa Cruz Biotechnology, Inc.	Santa Cruz, CA, USA
Sigma-Aldrich Co.	Oakville, ON, Canada
VWR International	Mississauga, ON, Canada

Table 3.2: Commercially available kits.

Commercial Kit Name	Company	Catalogue Number
HiSpeed Plasmid Maxi Kit	Qiagen	12662
RNeasy Mini Kit	Invitrogen	74104
Superscript™ First Strand Synthesis System for RT-PCR	Invitrogen	11904-018
QIAprep Miniprep®Spin Kit	Qiagen	27106
QIAquick Gel Extraction Kit	Qiagen	28704
QIAquick PCR Purification Kit	Qiagen	27106

3.1 Bacterial strains and growth media

For DNA isolation, plasmid DNA was transformed into *Echerichia coli* (*E. coli)* TOP10 cells [F- *mcr*A Δ(*mrr-hsd*RMS-*mcr*BC) φ80*lac*ZΔM15 Δ*lac*X74 *rec*A1 *ara*D139 Δ(*araleu*)7697 *gal*U *gal*K *rps*L (StrR) *end*A1 *nup*G] (Invitrogen, Cat# C4040). These cells are deficient in endonucleases and are designed to allow for stable replication of a high copy number of plasmids. Cells were grown in Luria-Bertani (LB, EMD Chemicals®) broth [2.5% (w/v) per litre] containing 1% (w/v) bacto-trypone, 1% (w/v) NaCl and 0.5% (w/v) bacto-yeast extract, pH 7.0. All plasmids in this study contained the ampicillin resistance (amp^R) gene; therefore, TOP10 cells transformed with plasmids were grown in LB containing 0.1 mg/mL ampicillin (LBA).

For protein purification, plasmid DNA was transformed into *E. coli* BL21 cells [F^- *ompT hsdS*$_B$ (r_B^- m_B^-) *gal dcm* (DE3)] (Novagen, Cat# 69450). BL21 cells are deficient in proteases and facilitate protein overexpression and purification. BL21 cells were grown in the same conditions as TOP10 cells.

3.2 Cell lines and standard tissue culture conditions

African green monkey (*Cercopithecus aethiops)* kidney fibroblast-like cells (COS-1), mouse embryonic fibroblast cells (NIH 3T3) and human epithelial metastatic breast cancer cells (MCF-7) were obtained from American Type Culture Collection (CRL-1650, CRL-1658 and HTB-22, respectively). Cells were grown in Dulbecco's Modified Eagle Medium (DMEM, Invitrogen) pH 7.4, supplemented with 10% fetal bovine serum (FBS, Hyclone), 1% (v/v) penicillin G and streptomycin [(100 units/mL penicillin G and 100 µg/mL streptomycin) (P/S, Invitrogen)] in a humidified incubator at 37°C with 5% CO_2.

3.3 Molecular cloning of MAGI-2

3.3.1 Reverse-transcriptase polymerase chain reaction of MAGI-2 encoding inserts

In order to obtain the complementary DNA (cDNA) encoding MAGI-2 FL and MAGI-2 domains, we used reverse-transcriptase polymerase chain reaction (RT-PCR) of RNA isolated from eukaryotic MCF-7 cells. A sample of total RNA was isolated from MCF-7 cells using the RNeasy Mini Kit (Invitrogen), according to the supplier's instructions. In order to visualize the

extracted RNA from MCF-7 cells, the RNA was subjected to electrophoresis on an agarose gel containing 1% (w/v) agarose in 1.23 M formaldehyde in morpholinopropanesulfonic acid running buffer (20 mM morpholinopropanesulfonic acid, 5 mM sodium acetate and 1 mM ethylenediaminetetraacetic acid).

RT-PCR was performed with 0.5-5 µg total RNA, according to Superscript™ First Strand Synthesis System for RT-PCR (Invitrogen), using the supplied random primers, in a final volume of 20 µL.

PCR was performed with *Pyrococcus furiosus* (*Pfu*) DNA polymerase (Fermentas). For *Pfu* driven PCR, the 10x *Pfu* buffer containing $MgS0_4$, supplied with the enzyme was used, along with deoxyribonucleoside triphosphates (dNTPs) (Amersham Biosciences). Concentrations of the reaction components were determined by following the manufacturer's instructions. For the amplification of the PDZ0 domain of MAGI-2, the following components were used in the reaction: 2 mM $MgSO_4$, 0.2 mM dNTPs, a range of 0.1-0.3 µM of each 5' and 3' primer, 550 ng/µL dimethyl sulfoxide, a range of 5-15 µL of total RT product template DNA and 2.5 Units of *Pfu* DNA polymerase, to a final volume of 100 µL with *Pfu* buffer containing $MgSO_4$ and distilled water. PCR were carried out in a Geneamp 2700 thermocycler (Applied Biosystems) using an intial melting step of 95°C for 4 min, followed by a 30 cycles of : 95°C for 30 secs (melting), 45-70°C for 45 secs (annealing) and 72°C incubation for 30 secs (extension). Extension times varied depending on the size of the expected product; generally, *Pfu* driven extensions were determined using a 0.5 kb/min rule. The reaction ended with a 72°C for 7 min and was used immediately or stored at -20°C.

3.3.2 Polymerase chain reaction of MAGI-2 encoding inserts

The pcDNA3 plasmid, containing the cDNA for human MAGI-2 FL (NM_012301), was a generous gift from Dr. Sawyers (University of California, Los Angeles, CA). The human MAGI-2 cDNA was cloned into pcDNA3.3, as previously described (Wood *et al.,* 1998; Wu *et al.,* 2000a). In order to create clones encoding MAGI-2 FL and its respective domains, MAGI-2 was amplified by PCR using the pcDNA3-MAGI-2 plasmid as a template. PCR primers were designed using MacVector software (version 9.0, MacVector Inc.). Primers were designed to amplify MAGI-2 FL and to flank individual domains of MAGI-2, in order to cover all regions of the protein. Primers also introduced unique restriction sites to ease cloning; 5' primers

introduced a BglII restriction site, whereas the 3' primers introduced an EcoRI restriction site (Table 3.3).

PCR was performed with either *Pfu* DNA polymerase, or a recombinant form of *Thermococcus kodakaraensis* (KOD) DNA polymerase (Novagen). For *Pfu* driven PCR, the 10x *Pfu* buffer containing $MgS0_4$, supplied with the enzyme, was used, along with dNTPs. Concentrations of the reaction components were determined by following the manufacturer's instructions. For the amplification of the PDZ0 domain of MAGI-2, the following components were used in the reaction: 2 mM $MgSO_4$, 0.2 mM dNTPs, 0.2 μM of each 5' and 3' primer, 550 ng/μL dimethyl sulfoxide, 10 ng total template DNA and 2.5 Units of *Pfu* DNA polymerase to a final volume of 100 μL with 10x *Pfu* buffer containing $MgSO_4$ and distilled water. PCR were carried out in a thermocycler, using an intial step of 95°C for 4 min, followed by a 30 cycles of: 95°C for 30 sec, 58°C for 45 sec, and 72°C for 30 sec. Extension times varied depending on the size of the expected product; generally. The reaction was completed with an incubation of 72°C for 7 min and was used immediately or stored at -20°C.

KOD DNA polymerase was used for the PCR of MAGI-2 FL because we could not get a PCR product with *Pfu* DNA polymerase. KOD DNA polymerase was chosen, over other DNA polymerases, because it had a higher fidelity than *Pfu* DNA polymerase. In addition, KOD DNA polymerase is documented to work well with long sequences (up to 6 kb) and with GC rich regions (the nucleotides encoding to the GARP C-terminal sequence were up to 78% GC in areas). For KOD driven PCR, the 10x KOD Buffer #1 was utilized, along with dNTPs supplied with the enzyme. Concentrations of the reaction components were determined by following manufacturer's instructions. For MAGI-2-FL PCR, the following components were used in the reaction: 1.5 mM $MgCl_2$, 0.2 mM dNTPs, 0.4 μM of each 5' and 3' primer, 4 ng total template DNA and 1 Unit of KOD DNA polymerase, to a final volume of 50 μL with 1x KOD Buffer #1 and distilled water. KOD driven PCR were carried out using an initial step of 97°C for 15 sec, followed by a 25 cycles of: 98°C for 15 sec (melting), 65°C for 5 sec (annealing) and 72°C for 4 sec (extension). Extension times varied depending on the size of the expected product;

Table 3.3: PCR primers designed to amplify cDNA of MAGI-2 FL and respective domains. All primers were designed with MacVector software. Primers were designed to introduce a unique restriction site at the 5' and 3' ends, to ease cloning: a BglII site was introduced at the 5' end (A▼GA TC▲T), whereas an EcoRI site was introduced at the 3' end (G▼AA TT▲C). The nucleotide number refers to the first and last nucleotides that bind to the 5' and 3' primer, respectively. Primers were designed based on the MAGI-2 NM_012301 nucleotide sequence, where nucleotide #1 is the A in the first ATG of the MAGI-2 nucleotide sequence.

MAGI-2 PCR product	PCR primers (5'–3')	Primer name	Nucleotide number	Size of PCR product (bp)
MAGI-2	GCA AGA TCT ATG TCC AAG AGC TTG AAA AAG	5'MG2-PDZ0new	1-4395	4395
	CCA GAA TTC CGG GCG GGT TGG CCG TGG CC	3'MG2-GC		
PDZ0	GCA AGA TCT ATG TCC AAG AGC TTG AAA AAG	5'MG2-PDZ0new	1-312	312
	CCA GAA TTC AAC AAT TCC TCC TTG CTT GAC	3'MG2-PDZ0		
GK	GCA AGA TCT GAT AAA GAC CTT CGT CAC TAC	5'MG2-Guk	313-891	578
	CCA GAA TTC GTC TTC AGG TTT AGT TGG C	3'MG2-Guk		
WW1	GCA AGA TCT AAT GAG GAA CCA GAC CCA TTG	5'MG2-WW1	892-1020	128
	CCA GAA TTC TTT AGC TTT TTT CGC AAG TCG	3'MG2-WW1		
WW2	GCA AGA TCT CCT CCA GAA GAG TGC AAA G	5'MG2-WW2	1021-1209	188
	CCA GAA TTC CTG CAG GGG CTT TGT TCC AAG	3'MG2-WW2		
PDZ1	GCA AGA TCT GCC CCA GGT TTC CGA GAA AAA C	5'MG2-PDZ1	1210-1673	463
	CCA GAA TTC AAC TGA CTG TGA GGT CCG AG	3'MG2-PDZ1		
PDZ2	GCA AGA TCT CCA GAT ATA ACA GAT CGG C	5'MG2-PDZ2	1674-2199	525
	CCA GAA TTC CTC TGT TGA GTC AGG AAA GG	3'MG2-PDZ2		
PDZ3	GCA AGA TCT GCC TTT GAC CCA CGG AAG CCT G	5'MG2-PDZ3	2200-2691	491
	CCA GAA TTC GTT GCT GTT GGT GTA GGT TGC	3'MG2-PDZ3		
PDZ4	GCA AGA TCT CAC GCT GCC CCC AGT AGC AAT G	5'MG2-PDZ4	2692-3249	557
	CCA GAA TTC GAT GTC TGG TTT CAC ATC TTG	3'MG2-PDZ4		
PDZ5	GCA AGA TCT CGA CAG CCT CCA TTC ACA GAC	5'MG2-PDZ5	3250-3696	446
	CCA GAA TTC GAC CTG TCC CGT GCC TCT CTT G	3'MG2-PDZ5		
GARP	GCA AGA TCT CCA GAA TAT GAC GAA CCC GCC	5'MG2-GCnew	3697-4395	698
	CCA GAA TTC CGG GCG GGT TGG CCG TGG CC	3'MG2-GC		

generally, KOD driven extensions were determined using a 6 kb/min rule. The reaction ended with a final temperature of 72°C for 7 min and the sample was used immediately or stored at -20°C. An aliquot (5 µL) of each PCR product was resolved by agarose gel electrophoresis to determine if the correct sized PCR product was successfully generated (section 3.3.3).

3.3.3 Agarose gel electrophoresis

Agarose gels, and low melt agarose gels, consisted of 1-1.5% agarose (w/v) in Tris-acetate electrophoresis buffer (2 mM ethylene diamine tetraacetic acid disodium in 40 mM Tris-acetate) containing approximately 1% (w/v) ethidium bromide. DNA was loaded with bromophenol blue (Bio-Rad) or xylene cyanole (Bio-Rad) loading dyes, depending on the size of the DNA fragment (bromophenol blue was used with fragments larger than 1 kb and xylene cyanol was used with fragments smaller than 1 kb). Generally, 1 µL of loading dye was used with 10 µL volume of DNA solution and loaded into the individual wells of the agarose gel. Electrophoresis was performed for at least 20 min at 100 volts (V). The gel was subjected to ultraviolet light in order to visualize the DNA. The gel was photographed using a Gel-Doc 2000 system and Quantity One Software (Bio-Rad).

3.3.4 Restriction enzyme digestion of MAGI-2 PCR products

All PCR products were purified using the QIAquick PCR purification Kit (Qiagen) according to supplier's instructions, in order to remove enzymes, nucleotides, salts, primers and other impurities. PCR cleaned products were eluted in 25 µL of distilled water, passed through the column twice to maximize the amount of DNA extracted through the column.

PCR products of MAGI-2 FL or individual domains were digested with BglII (Fermentas) and EcoRI (New England Biolabs). Generally, the entire volume of the PCR cleanup product from above (25 µL) was digested with a total of 20 units of each restriction enzyme. The reaction proceeded in 1x One-Phor-All buffer (Amersham Biosciences) in a final volume of 40 µL, at 37°C for 1 hr. In order to remove enzymes, salts, and other impurities, the digested product was purified according to the QIAquick PCR Purification Kit protocol. The digested PCR product was eluted in 17 µL of distilled water, passed through the column three times.

3.3.5 Restriction enzyme digestion of the pMyc3 vector

The pMyc3 vector (2 μg) was digested with BglII and EcoRI as described for the MAGI-2 PCR products, and reactions were similarly subjected to a cleanup. The pMyc3 vector is based on the pRc/CMV2 vector (Invitrogen, Cat# V750-20) (Chamberlain *et al.*, 2004).

3.3.6 DNA ligation of the MAGI-2 PCR products into the pMyc3 vector

The BglII and EcoRI digested MAGI-2 PCR products were ligated into the similarly digested pMyc3 vector. DNA ligations were performed using Quick T4 DNA ligase (New England Biolabs) and the supplied buffer, according to manufacturer's instructions. Generally, ligation reactions were performed using 5-10 fold molar excess of MAGI-2 PCR product insert than pMyc3 vector, in a final volume of 20 μL. For example, 200 ng of the 5.7 kb vector was ligated with 60-120 ng of the 350 bp insert. The reaction proceeded for 15 min at room temperature.

3.3.7 Preparation of competent cells for transformations

E. coli TOP10 cells were inoculated in 5 mL LB, shaking overnight at 37°C. The next day, the 5 mL culture was poured into 100 mL LB and incubated in 37°C shaking incubator until an absorbance of 0.4 (550 nm) was reached. The 100 mL culture was collected and centrifuged at 2500 x g for 15 min. The supernatant was removed and cells were resuspended in 30 mL of cold, sterile RF1 buffer [100 mM RbCl, 50 mM $MnCl_2$, 10 mM $CaCl_2$, 15% (w/v) glycerol in 30 mM potassium acetate, pH 7.5] and placed on ice for 15 min. Cells were pelleted as before and the supernatant was removed. Cells were resuspended in 7.2 mL cold, sterile RF2 buffer [10 mM RbCl, 75 mM $CaCl_2$ and 15% (w/v) glycerol in 10 mM morpholinopropanesulfonic acid, pH 6.8] and placed on ice for 15 min. Two hundred μL of the competent *E. coli* cells were aliquoted into 1.5 mL sterile tubes and frozen quickly with liquid nitrogen and stored at -80°C until ready to use.

Competent *E. coli* TOP10 cells were transformed with half (10 μL) of the above ligation reaction mixture. Transformed cells were placed on ice for 30 min and heat shocked at 42˚C for 2 min. Cells were placed on ice for 10 min and 800 μL of LB was added. Cells were incubated at 37°C for 45-60 min to allow expression of the antibiotic resistant gene (amp^R). Following incubation, the cells were centrifuged at 2500 x g, and the entire cell pellet was

plated onto LBA agar plates [1.5% (w/v) agar] to select for transformed *E. coli* cells. Plates were incubated overnight at 37°C.

3.3.8 Isolation of plasmid DNA from bacterial cells

For plasmid DNA isolation from bacterial cells, individual bacterial colonies were selected and incubated in 5 mL (small preparations) or 250 mL (large preparations) LBA broth, shaking overnight at 37°C. Small and large plasmid purification preparations were performed with the QIAprep® Spin Miniprep Kit or the HiSpeed Plasmid Maxi Kit (Qiagen), respectively, according to the manufacturer's instructions. Successful ligations were verified by a restriction enzyme digestion, followed by agarose gel electrophoresis, to verify that the expected size of insert and plasmid DNA were present. The integrity of the MAGI-2 PCR inserts were verified by DNA sequencing once the PCR products had been inserted into a vector (National Research Council Canada, Plant Biotechnology Institute, Saskatoon, SK or DNA Sequencing Facility, The Center for Applied Genomics, Hospital for Sick Children, Toronto, ON).

3.3.9 Subcloning of MAGI-2 inserts from pMyc3 into the pGEX6P1 vector

MAGI-2 inserts from above were subcloned into the pGEX6P1 vector, in order to create glutathione S-transferase (GST)-MAGI-2 plasmids. Four µg of pMyc3-MAGI-2 DNA were digested with BglII and EcoRI to release the MAGI-2 insert. The digested product was electrophoresed on a low melt agarose gel and the MAGI-2 insert DNA was excised. The MAGI-2 DNA fragment was purified using the QIAquick Gel Extraction Kit (Qiagen), according to the supplier's instructions except that the DNA was eluted in 20 µL distilled water and passed through the column three times.

Two µg of pGEX6P1 vector were digested with BamHI (New England Biolabs) and EcoRI. The digested product was subject to purification, as described previously.

The MAGI-2 insert was ligated into the pGEX6P1, as described previously (section 3.3.6). BamHI and BglII restriction sites have compatible sticky ends; however, the BamHI/BglII restriction sites are destroyed upon ligation of the insert into the vector. Successful ligations were verified by a single restriction enzyme cut, followed by gel electrophoresis. A comparison of the size difference between pGEX6P1 plasmid containing

MAGI-2 insert was compared to the empty vector. Positive clones were sequenced through the splice site between the GST and MAGI-2 encoding regions at the above mentioned facilities.

3.4 Coomassie blue stained gels and immunoblot analysis

3.4.1 Sodium dodecyl sulfate-polyacrylamide gel electrophoresis

Proteins were resolved by sodium dodecyl sulfate-polyacrylamide gel electrophoresis (SDS-PAGE) (Laemmli, 1970) for protein staining or for immunoblot analysis. Gels were cast using the Mini-PROTEAN Tetra Electrophoresis System (Bio-Rad) using a 1 mm spacer. The polyacrylamide gels consisted of two parts, the resolving gel (bottom) and the stacking gel (top). The resolving gel contained between 7.5-15% (w/v) acrylamide/bisacrylamide solution (29.2:0.8 acrylamide to bisacrylamide) in 375 mM Tris-HCl, pH 8.8, and 0.1% (w/v) SDS. Polymerization of the gel was initiated upon the addition of 0.06% (w/v) ammonium persulfate and 0.1% (v/v) N,N,N',N'-tetra-methylethylenediamine. The resolving gel was poured in between the two glass plates and allowed to polymerize for at least 40 min. Water saturated butanol was added to the surface of the resolving gel in order to prevent oxygen free radicals, generated by the ammonium persulfate, from escaping into the air. The stacking gel consisted of 4.5% acrylamide/bisacrylamide solution containing 125 mM Tris-HCl, pH 6.8, and 0.1% (w/v) SDS. Polymerization of the stacking gel was initiated upon the addition of ammonium persulfate and N,N,N',N'-tetra-methylethylenediamine, as described above. After removing the butanol, the stacking gel was poured on top of the resolving gel and a comb containing 10 or 15 wells was inserted to form the wells. The stacking gel was allowed to polymerize for at least 8 min.

Protein samples were resuspended in SDS sample buffer [10% (w/v) glycerol, 5% (v/v) β-mercaptoethanol, 2.3% (w/v) SDS and 0.05% (w/v) bromophenol blue, pH 6.8], boiled at 100°C for 5 min and loaded into each well. The unstained protein standards were used for Coomassie blue stained gels and consisted of the following molecular weights in kDa: 200, 150, 120, 100, 85, 70, 60, 50, 40, 30, 25, 20, 15 & 10 (Fermentas, Cat# 0661). Prestained protein standards were used for immunoblot analysis and consisted of the following molecular weights in kDa: 170, 130, 100, 70, 55, 40, 35, 25, 15 &10 (Fermentas, Cat# 0671).

The gel was electrophoresed in running buffer [25 mM Tris-HCl, 192 mM glycine and 0.1 % (w/v) SDS] at 180 V until the bromophenol blue ran off the bottom of the gel (Laemmli, 1970).

3.4.2 Coomassie blue stain analysis

SDS-PAGE gels were stained in Coomassie blue stain [0.14% (w/v) Coomassie blue-250, 41.4% (v/v) methanol and 5.4% (v/v) glacial acetic acid] for at least 20 min and were destained in destaining solution [41.4% (v/v) methanol and 5.4% (v/v) glacial acetic acid] until the protein bands could be visualized. Pictures of the gels were taken with the Gel-Doc 2000 system using Quantity One software (Bio-Rad).

3.4.3 Immunoblot analysis

For immunoblot analysis, SDS-PAGE gels were incubated in transfer buffer [20% (v/v) methanol, 0.58% (w/v) glycine and 0.038% (w/v) SDS in 48 mM Tris-HCl, pH 9.2] for 15-20 min. Concurrently, 6 pieces of 3 MM filter paper (Whatman) was soaked into the transfer buffer and a nitrocellulose membrane (Whatman) was hydrated in distilled water. Both the 3 MM and nitrocellulose membrane were sized according to the dimensions of the gel (8.2 x 5.4 cm). The transfer system used was an Owl Panter™ Semi-Dry Electroblotter (VWR, Cat# 27372-374). Three 3 MM papers were layered on the base of the apparatus, followed by the SDS-PAGE gel and the pre-soaked nitrocellulose membrane. Three more 3 MM papers were layered on top, to complete the transfer sandwich. Air bubbles were rolled out of the layers and the proteins were transferred from the gel onto the nitrocellulose membrane at a constant current of 400 mA for 15 min per gel.

The membrane was blocked in blocking solution [0.1 M Tris-HCl, pH 8.0, 150 mM NaCl and 0.05% (v/v) Tween-20 (TBST), supplemented with 5% (w/v) Carnation skim milk powder] for 1 hr at room temperature or overnight at 4°C. Primary antibodies were diluted in the blocking solution according to manufacturer's recommendations (Table 3.4). Secondary antibodies, conjugated to horseradish peroxidase (HRP), were diluted 1:2000 in the blocking solution (Santa Cruz, sc-2004 anti-rabbit and sc-2005 anti-mouse). Primary antibodies were incubated for 1 hr at room temperature or overnight at 4°C. The nitrocellulose membrane was washed three times with TBST (5 min each). The membrane was incubated in secondary

antibody for 1-6 hr at room temperature and washed as described before. The membrane was incubated for 1 min in Western Lightning enhanced chemiluminescence reagent (PerkinElmer) and exposed to X-Omat Blue XB-1 film (Kodak) for up to 10 min in a darkroom. The film was developed in a Kodak M35A X-Omat processor.

Table 3.4 Primary antibodies used for immunoblot (IB) and immunoprecipitation (IP) experiments.

Antibody	Company	Catalogue number	Species	Application	Concentration (IB) or Amount (IP)	Figure
EGFR	UBI	05-104	Rabbit	IB	1 µg/mL	3.9A,
				IP	10 µg	3.10B,C & 3.11B
FLAG	Sigma-Aldrich	F3165	Mouse	IB	5 µg/mL	3.8B
				IP	12.5 µg	3.11C
GST	Santa Cruz	sc-138	Mouse	IB	0.5 µg/mL	3.3B,C
HA	Santa Cruz	sc-7392	Mouse	IP	10 µg	
PDGFR	New England Biolabs	3175	Mouse	IB	1 µg/mL	3.9B
PTEN-HRP	Santa Cruz	sc-7974-HRP	Mouse	IB	1 µg/mL	3.8A
Myc	Santa Cruz	sc-40	Mouse	IB	1 µg/mL	3.7, 3.10A, 3.11A & 3.12D
Myc	Santa Cruz	sc-789	Rabbit	IP	10 µg & 12.5 µg	3.10A & 3.11A
GARP	Anderson, affinity purified (to amino acids 1233-1455)	N/A	Rabbit	IB	1:100	3.12C

To re-probe the nitrocellulose membrane with a different primary and secondary antibody, the membrane was washed in TBST and incubated in stripping buffer [2% (w/v) SDS and 100 mM β-mercaptoethanol in 62.5 mM Tris-HCl, pH 6.8] at 80°C for 30 min. The membrane was then rinsed in TBST, blocked and re-probed with primary and secondary antibodies, as previously described.

3.5 Induction and purification of GST-MAGI-2 proteins from bacterial cells

Bl21 *E. coli* cells were transformed with pGEX6P1-MAGI-2 DNA, as previously described for TOP10 cells. Transformed cells were grown in LBA, in a shaking incubator at 37°C until an absorbance of 0.5 (600 nm) was attained, indicating that the cells were in log phase. Protein expression was induced with 0.3 mM isopropyl β-D-thiogalactopyranoside (IPTG) overnight at room temperature. Bacterial cells were pelleted and lysed enzymatically with lysozyme [10 mg/mL in phosphate buffered saline (PBS, 137 mM NaCl, 2.7 mM KCl, 4.3 mM Na_2HPO_4, 1.4 mM KH_2PO_4, pH 7.3)] on ice for 30 min and mechanically through sonication (3x 10 sec at a setting of 1.5). Triton X-100 were added to a final concentration of 1% (v/v) and the cells were centrifuged at 21,920 x g to remove insoluble debris (pellet). Soluble cell lysate was filtered through a 0.8 micron filter to remove particulate. GST-fused MAGI-2 proteins were bound to glutathione-Sepharose 4B beads (Amersham Pharmacia, Cat# 27-4574). The immobilized GST-MAGI-2 proteins were washed in PBS to remove unbound protein. An aliquot of the purified GST-fusion protein suspension was resolved by SDS-PAGE and the protein was either stained with Coomassie blue or transferred to nitrocellulose and immunoblotted with anti-GST mouse monoclonal (anti-GST^{Ms}, Santa Cruz, Cat# 138) (Table 3.4). The quality and purity of the GST-fused MAGI-2 proteins were assessed by visualizing the size of the fused proteins compared to that of the expected protein size and the number of additional proteins and/or degradation products.

3.6 Limited trypsin digestion

3.6.1 Eluting the GST-MAGI-2 proteins from the glutathione-Sepharose beads

In order to elute GST-MAGI-2 proteins from glutathione-Sepharose beads, immobilized GST-MAGI-2 proteins were centrifuged at 2500 x g and excess PBS supernatant was removed. The beads were incubated for 30 min in reduced glutathione buffer (15 mM reduced glutathione in 50 mM Tris-HCl, pH 8.0). The beads were then centrifuged again at 2500 x g and the supernatant containing the eluted protein was kept. An aliquot of the supernatant containing the eluted GST-fusion protein was resolved by SDS-PAGE and stained with Coomassie blue. The amount of protein present was determined using bovine serum albumin protein standards of known concentration.

3.6.2 Limited trypsin digest of GST-MAGI-2 proteins

A limited trypsin digest was performed on all GST-MAGI-2 proteins to determine if the portions of the MAGI-2 proteins were folded properly while fused to GST. A 1:1000 protease to protein ratio was used for the limited protein digestion of the GST-MAGI-2 proteins. The reaction proceeded in the following mixture at 37°C: 400-600 µg GST-MAGI-2 protein, 1 mM β-mercapthoethanol and 0.4-0.6 µg of trypsin (L-1-Tosylamide-2-phenylethyl chloromethyl ketone treated, Sigma-Aldrich, Cat# T-8642) in 20 mM Tris-HCl, pH 8.0, to a final volume of 1 mL. A 10 µL aliquot was taken from the reaction mixture before the addition of the trypsin. Once the trypsin was added, 10 µL aliquots were taken at the following time points: 0, 5, 10, 20, 30, 40, 60 min and overnight. These aliquots were added directly to SDS sample buffer and boiled for 5 min in order to inactivate the trypsin. These were resolved by SDS-PAGE and stained with Coomassie blue.

3.7 Cell culture techniques

3.7.1 Growth factor stimulations

NIH 3T3 and COS-1 cells were grown in DMEM + 10% FBS + 1% P/S at 37°C in a 5% CO_2 incubator. These were grown to approximately 60-70% confluency and starved of FBS for 24 hrs in DMEM containing 0.5 % FBS.

Growth factor stimulations in NIH 3T3 cells were performed with PDGF-BB (Cedarlane, Cat# 220-BB-050) since these cells endogenously express PDGFR. PDGF-BB was resuspended in PDGF dilution buffer [10 mM acetic acid and 2 mg/mL bovine serum albumin, (BSA)] and further diluted in spent starving media to a final concentration of 50 ng/mL. PDGF stimulations proceeded for the different times indicated in each experiment.

Growth factor stimulations in COS-1 cells were performed with EGF (Sigma-Aldrich, Cat# E-9644) since these cells endogenously express EGFR. EGF was resuspended in 10 mM acetic acid, and then further diluted in EGF dilution buffer [2% (w/v) BSA in PBS]. EGF was then further diluted in spent starving media to a final concentration of 80 nM. EGF stimulations proceeded for the different times indicated in each experiment.

3.7.2 Transient transfection of COS-1 cells

In order to test whether the newly generated plasmids encoding Myc-MAGI-2 proteins had the ability to express in eukaryotic cells, pMyc3-MAGI-2 DNA was transiently transfected into COS-1 cells. Transient transfections were performed using lipofectAMINE™ (Invitrogen, Cat# 18324) according to the manufacturer's instructions. Briefly, on day 1, COS-1 cells (85-90% confluent) were trypsinized and re-seeded on 10 cm culture plates in a 1:10 dilution and grown overnight in DMEM + 10% FBS + 1% P/S. On day 2, cells were approximately 25-30% confluent and were transfected with 6 µg DNA Myc-MAGI-2 FL, or its respective domains. Briefly, solution A [600 µL of Opti-MEM®I reduced serum medium (Invitrogen, Cat# 31985-062) containing 6 µg DNA] and solution B (600 µL Opti-MEM®I reduced serum medium containing 18 µL lipofectAMINE™ reagent) were mixed and incubated at room temperature for 15 min. Each 10 cm plate of cells was washed with warm serum-free DMEM. To each 10 cm plate of cells, 4.8 mL of serum free DMEM and the combined solutions A and B were

added and cells were incubated at 37°C and 5% CO_2 for 5 hr. Six mL of DMEM containing 20% FBS were added to the existing transfection media on each plate and the cells were incubated overnight at 37°C and 5% CO_2. On day 3 transfection medium was replaced with DMEM + 10% FBS + 1% P/S. On day 5 cells were approximately 80-90% confluent and were washed and lysed in 1 mL of lysis buffer (described in section 3.7.4). Ten µL aliquots were mixed with SDS sample buffer and resolved by SDS-PAGE and transferred to nitrocellulose and immunoblotted with anti-Myc mouse monoclonal (anti-Myc^{Ms}) (Santa Cruz, Cat# sc-40) (Table 3.4).

In order to generate cell lysates for pull-down experiments, COS-1 cells transiently transfected with FLAG-p85 (Chamberlain *et al.,* 2004) or HA-PTEN-C124S (phosphatase dead mutant of PTEN) (Chagpar, 2004) were transfected according to the protocol above. These were lysed in 1 mL lysis buffer, and prepared for pull-down or immunoprecipitation assays (described in section 3.7.4).

3.7.3 EGF stimulation of transiently transfected COS-1 cells

EGF stimulations were performed on transiently transfected COS-1 cells, which were used in the immunoprecipitation assays (see section 3.9). On day 1, COS-1 cells with a confluency of 85-90%, were trypsinized and re-seeded on 10 cm culture plates, in a 1:10 dilution. Cells were left to grow on day 2. On day 3, cells were approximately 50-60% confluent and were transfected with 3 µg or 6 µg DNA total (Myc-MAGI-2, HA-PTEN-C124S or FLAG-p85) as described above. On day 4, cells were approximately 80-90% confluent and were starved with starving media for 6 hours. Cells were left unstimulated, or stimulated for 5 min with EGF, as previously described. Cells were washed and prepared immunoprecipitations assays, as described in section 3.7.4.

3.7.4 Cell lysate preparation

To prepare cell lysates for pull-down or immunoprecipitation assays, 10 cm plates of cells (of approximately 85-90% confluency) were placed on ice and washed once with cold PBS. Each 10 cm plate of cells was scraped into 1 mL lysis buffer [50 mM N-(2-hydroxyethyl) piperazine-N'-(2-ethanesulfonic acid), pH 7.5, 150 mM NaCl, 10% (v/v) glycerol, 1% (v/v) triton X-100, 1.5 mM $MgCl_2$, 1 mM ethylene glycol-bis (B-aminoethylether) N,N,N,N,

tetraacetic acid, 10 mM sodium pyrophosphate, 100 mM sodium fluoride, containing 10 µg/mL aprotinin, 10 µg/mL leupeptin and 1 mM aminoethyl, 2-benzenesulfonyl (protease inhibitors) and 1 mM sodium orthovanadate]. Cells were incubated on ice for at least 10 min and centrifuged at 21,920 x g for 10 min, in order to remove insoluble cellular debris (pellet). Lysates were used immediately or stored at -80°C.

3.7.5 Whole cell lysate preparation

Whole cell lysates were solubilised in SDS sample buffer. Briefly, one plate of 85-90% confluent cells was washed in PBS, scraped into warm 300 µL SDS sample buffer and passed through a 27 gauge needle several times to reduce viscosity. Whole cell lysates were boiled at 100°C for 5 min and used immediately or stored at -80°C.

3.8 Pull-down experiments

In order to test protein-protein interactions *in vitro*, a pull-down assay was employed. GST and GST-MAGI-2 fusion protein (10 µg each) were immobilized on glutathione-Sepharose beads and incubated with 100-200 µL of COS-1 cell lysates (10-20% of a 85-90% confluent 10 cm plate) expressing HA-PTEN-C124S or FLAG-p85, mixing for 1 hr at 4°C. To confirm whether PTEN could bind to the PDZ domains of MAGI-2, COS-1 cell lysates expressing HA-PTEN-C124S were mixed with 10 µg of GST, GST-MAGI-2 FL, GST-PDZ domains, as well as the GST-GARP C-terminal sequence of MAGI-2. To test whether p85 could bind to the WW domains of MAGI-2, COS-1 cells expressing FLAG-p85 were mixed with 10 µg of GST and GST-fused WW domains.

To test whether MAGI-2 PDZ domains associated with EGFR, COS-1 cells (expressing endogenous levels of EGFR) were either left unstimulated, or stimulated with EGF for 5 min. Cell lysates were lysed in lysis buffer (1 mL of lysate; 100% of a 85-90% confluent 10 cm plate) were mixed with 10 µg GST and GST-PDZ domains of MAGI-2, mixing for 1 hr at 4°C. To test whether MAGI-2 PDZ domains associated with PDGFR, NIH 3T3 cells (expressing endogenous levels of PDGFR) were tested similarly, however these were left unstimulated or stimulated with PDGF-BB for 5 min.

Protein complexes immobilized on glutathione-Sepharose beads were centrifuged at 2500 x g for 1 min and washed three times with 500 µL wash buffer [20 mM N-(2-

hydroxyethyl) piperazine-N'-(2-ethanosulfonic acid), pH 7.5, containing 150 mM NaCl, 0.1% (v/v) triton X-100 and 10% (w/v) glycerol] wash buffer containing the aforementioned protease inhibitors and sodium orthovanadate. Samples were resuspended in 20 µL of SDS sample buffer, heated at 100°C for 5 min and resolved by SDS-PAGE. The protein was transferred to a nitrocellulose membrane and immunoblotted for the protein of interest. The antibodies used in these experiments were anti-PTEN^{Ms}-HRP (1 µg/mL, Santa Cruz, Cat# sc-7974-HRP), anti-FLAG^{Ms} (5 µg/mL, Sigma-Aldrich, Cat# F3165) to detect p85, anti-EGFR^{Ms} (1 µg/mL, UBI, Cat # 05-104) or anti-PDGFR^{Ms} (1 µg/mL, New England Biolabs, Cat# 3175) according to manufacturer's instructions (Table 3.4).

3.9 Co-immunoprecipitation experiments

In order to test protein-protein interactions in cells, a co-immunoprecipitation assay was employed. All co-immunoprecipitation experiments were performed with COS-1 cell lysates derived from cells transfected with plasmids encoding proteins of interest.

To determine if MAGI-2 formed complexes in cells with PTEN, a co-immunoprecipitation was performed with Myc-MAGI-2 and HA-PTEN-C124S. COS-1 cells were co-transfected with 3 µg DNA encoding Myc-MAGI-2 FL and 3 µg of DNA encoding the phosphatase dead mutant of PTEN (HA-PTEN-C124S). Cells were left unstimulated or stimulated with EGF for 5 min and lysed in 1 mL lysis buffer. Cell lysates used in an immunoprecipitation experiment were pre-cleared once to remove residual protein that may bind non-specifically with rabbit or mouse antibodies and/or beads. Five µg of rabbit IgG agarose conjugated (Rb IgG-AC, Santa Cruz, Cat# 2345) and 5 µg of mouse IgG agarose conjugated (Ms IgG-AC, Santa Cruz, Cat# 2343) and 50 µL of a 50% suspension of protein G beads (Sigma-Aldrich, Cat# P-7700) were mixed with 875 µL cell lysates, mixing at 4˚C for 1 hr. These were centrifuged at 21,920 x g and the supernatant was removed and used in the immunoprecipitation assay. One hundred and twenty five µL of these lysates (12.5% of a 85-95% confluent 10 cm plate) were used in an co-immunoprecipitation assay where 5 µg of rabbit IgG and 5 µg of mouse IgG, 10 µg of anti-Myc rabbit polyclonal (anti-Myc^{Rb}, Santa Cruz, Cat# 789) to immunoprecipitate MAGI-2 or 10 µg of anti-HA mouse monoclonal (anti-HA^{Ms}, Santa Cruz, Cat# sc-7392) to immunoprecipitate PTEN, along with an excess of protein G beads (20 µL of a 50% suspension) were mixed for 1 hr at 4˚C. Samples were washed as for pull-down

experiments and resuspended in 20 µL SDS sample buffer. The samples were resolved by SDS-PAGE and transferred to a nitrocellulose membrane. The nitrocellulose membrane was cut in half at the 100 kDa marker. Using an immunoblot approach, the top of the membrane (containing ≥ 100 kDa proteins) was probed with anti-Myc^{Ms} (1 µg/mL, Santa Cruz, Cat# sc-40) to detect Myc-MAGI-2. The bottom portion of the immunoblot (containing ≤ 100 kDa proteins) was probed with anti-PTEN^{Ms} conjugated to HRP (Table 3.4).

The result obtained in this Myc-MAGI-2/HA-PTEN co-immunoprecipitation experiment above could not be replicated. First, we had non-specific binding, which were eventually eliminated by pre-clearing the cell lysates 2x for 1 hour, as described above. A range of co-transfections of HA-PTEN-C124S (1, 3 and 5 µg) and Myc-MAGI-2 (1, 3, 5 and 10 µg) was also used to determine which ratio of transfections could give optimal expression. We also used a range of cell lysate volumes from 50-500 µL (5-50% of a 85-90% confluent 10 cm plate). Unfortunately, the results seen in the first experiment were never seen again.

In order to determine if MAGI-2 formed complexes in cells with EGFR, an immunoprecipitation was performed where Myc-MAGI-2 and EGFR could co-immunoprecipitate. COS-1 cells were transfected with 3 µg of DNA encoding Myc-MAGI-2 FL. Cells were left unstimulated or stimulated with EGF for 5 min and lysed in lysis buffer. Cell lysates used in co-immunoprecipitation assays were pre-cleared to remove residual protein that may bind non-specifically with rabbit antibodies. Ten µg of Rb IgG-AC and 50 µL of a 50% suspension protein A beads (Sigma-Aldrich, Cat# P-3391) were mixed with 2.8 mL cell lysate mixing at 4°C for 1 hour. These were then centrifuged at 21,920 x g and the pre-clear was repeated on the supernatant once more. Four hundred µL of these lysates (40% of a 85-90% confluent 10 cm plate) were used in an immunoprecipitation assay where 10 µg of rabbit IgG, anti-Myc^{Rb} (Santa Cruz, Cat# sc-789) to immunoprecipitate Myc-MAGI-2 or anti-EGFR^{Rb} (UBI, Cat# 06-847) along with an excess of Protein A beads (20 µL of a 50% suspension) were mixed for 1 hr at 4°C. Samples were washed as for pull-down experiments and resuspended in 20 µL SDS sample buffer. The samples were resolved by SDS-PAGE and transferred to a nitrocellulose membrane. The membrane was first immunoblotted for MAGI-2 with anti-Myc^{Ms} (1 µg/mL, Santa Cruz, Cat# sc-40), then stripped and re-probed with anti-EGFR^{Rb} (1:1000, UBI, Cat# 06-847) (Table 3.4).

To determine if MAGI-2 and p85 formed complexes in cells, an immunoprecipitation experiment was performed to determine if MAGI-2 and p85 could co-immunoprecipitate along with EGFR. COS-1 cells were co-transfected with 3 µg of DNA encoding Myc-MAGI-2 FL and 3 µg of DNA encoding FLAG-p85. Cells were left unstimulated or stimulated with EGF for 5 min and lysed in lysis buffer. Cell lysates were pre-cleared once using 10 µg of Rb IgG-AC and 50 µL of a 50% suspension protein A beads mixed with 2.8 mL cell lysate mixing at 4°C for 1 hour. These were then centrifuged at 20,920 x g. Two hundred µL of the supernatants (20% of a 85-90% confluent 10 cm plate) were used in an immunoprecipitation assay where 12.5 µg of rabbit IgG-AC and 12.5 µg mouse IgG-AC, anti-Myc^{Rb} antibody (Santa Cruz, Cat# sc-789) to immunoprecipitate MAGI-2, or FLAG antibody (Sigma-Aldrich, Cat# F3165) to immunoprecipitate p85, along with 20 µL of a 50% suspension Protein G beads were mixed for 1 hr at 4°C. Samples were washed and immunoblotted. The membrane was cut at the 100 kDa mark and the upper membrane (containing $\geq$ 100 kDa proteins) was probed with anti-Myc^{Ms} (1 µg/mL, Santa Cruz, Cat# sc-40) to detect MAGI-2. This membrane was stripped and re-probed with anti-EGFR^{Rb} (1:1000, UBI, Cat# 06-847). The bottom portion of the blot was probed with anti-FLAG^{Ms} (5 µg/mL, Sigma-Aldrich, Cat# F3165) to detect p85 (Table 3.4).

3.10 MAGI-2 rabbit polyclonal antibody

A MAGI-2 polyclonal antibody was created to distinguish MAGI-2 from other MAGI proteins. The anti-MAGI-2 antibody was raised against a portion of the MAGI-2 protein containing amino acids 1233-1455 (GARP C-terminal sequence, Table 3.3), a region unique to MAGI-2. The GST-GARP protein antigen was generated as described above. Briefly, the C-terminal end of MAGI-2 was subjected to PCR amplification of the region encoding amino acids 1233-1455. The GARP region was subcloned into the pGEX6P1 vector which was transformed into BL21 cells and induced with IPTG to overexpress the GST-GARP protein. BL21 cells were lysed and GST-GARP protein was immobilized on glutathione-Sepharose beads and washed. The GARP protein was cleaved from the immobilized GST using PreScission protease (Amersham Biosciences), following the manufacturer's recommendations.

One hundred µg of purified GARP protein was injected into a rabbit and the rabbit was allowed to generate polyclonal antibody against the protein for 3 weeks. A test bleed was performed where a sample of approximately 10 mL of blood was taken from the rabbit. The

crude serum was used to probe an immunoblot containing COS-1 lysates expressing Myc-MAGI-2 and compared to a control Myc immunoblot.

4.0 RESULTS

4.1 MAGI-2 expression in eukaryotic and prokaryotic cells.

4.1.1 Myc-MAGI-2 expression in eukaryotic cells

The DNA encoding MAGI-2 FL and its individual domains were amplified through PCR and cloned into the pMyc3 vector (Figure 4.1). These plasmids encoding Myc-MAGI-2 FL and individual domains were transfected into COS-1 cells. Lysates from these transfected cells were confirmed to express Myc-MAGI-2 fusion proteins, as determined using an immunoblot analysis with anti-Myc antibodies (Figure 4.2). Sizes of the Myc-tagged MAGI-2 proteins were estimated using MacVector software based on the amino acid sequence (Table 4.1). The bands representing Myc-MAGI-2 FL and its respective domains were of the apparent molecular weight indicated in Table 4.1, confirming that Myc-tagged MAGI-2 proteins are expressed in eukaryotic cells from these newly generated plasmids. A schematic representation of the tagged MAGI-2 proteins is shown in Figure 4.3. Therefore, these Myc-tagged MAGI-2 proteins could be used in immunoprecipitation experiments.

Table 4.1: Estimated protein sizes of MAGI-2 FL and its individual domains: alone or fused to either a triple Myc epitope or GST. The size of the Myc tag is 4.1 kDa and the GST protein is 26.5 kDa. Protein sizes were estimated using MacVector software, based on the amino acid sequence.

MAGI-2 domains	Amino acids	Protein size (kDa)	Myc-MAGI-2 protein size (kDa)	GST-MAGI-2 protein size (kDa)
MAGI-2 FL	1-1455	159	163	185
PDZ0	1-104	11	15	38
GK	105-297	22	26	48
WW1	298-340	5	9	32
WW2	341-403	8	12	34
PDZ1	404-558	17	21	44
PDZ2	559-733	19	23	45
PDZ3	734-827	11	15	37
PDZ4	828-1083	27	31	54
PDZ5	1084-1232	17	21	44
GARP	1233-1455	22	26	49

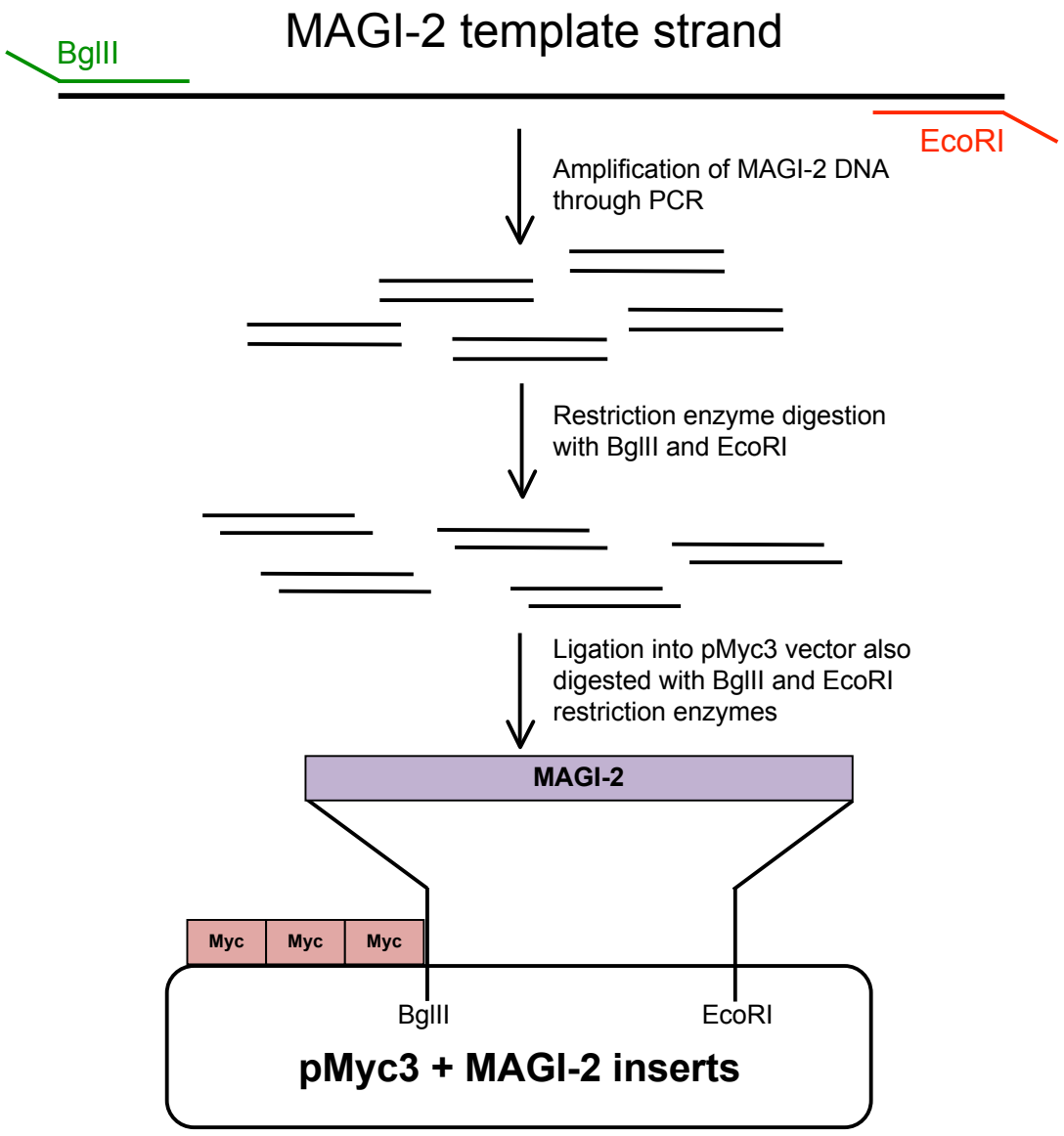

Figure 4.1: Cloning strategy of MAGI-2 FL and its respective domains into the pMyc vector. PCR primers were designed to introduce restriction enzyme sites BglII at the 5' end and EcoRI at the 3' end of the PCR product. Briefly, DNA encoding MAGI-2 FL and individual domains were amplified through PCR. PCR products were digested with BglII and EcoRI and ligated into the similarly digested pMyc3 vector. Successful cloning was determined by digesting the resulting plasmid with BglII and EcoRI, to assess if the insert of the appropriate size was present. The pMyc3-MAGI-2 plasmid inserts were sequenced to verify that no mutations were introduced during PCR and that the correct reading frame was maintained between the Myc and MAGI-2 encoding regions.

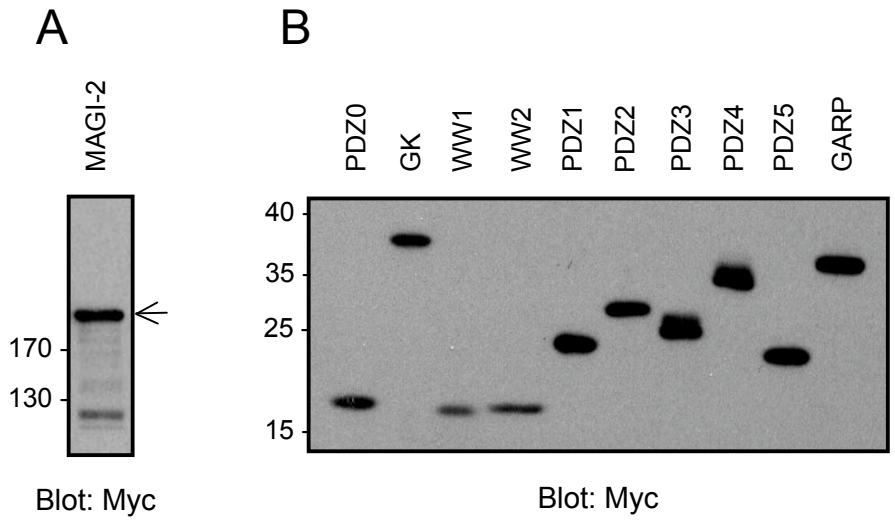

Figure 4.2: Expression and detection of Myc-MAGI-2 proteins in eukaryotic COS-1 cells. COS-1 cells were transfected with 6 µg of DNA encoding MAGI-2 FL or individual MAGI-2 domains. Cell lysates (10 µL) were resolved by SDS-PAGE, transferred to nitrocellulose and the resulting immunoblot was probed with anti-Myc antibodies. Secondary antibodies linked to HRP were used to probe the immunoblot and chemiluminescence was used to visualize the bound antibodies. **A**, Lysate from COS-1 cells, transfected with Myc-MAGI-2 FL (arrow). **B**, Lysates from COS-1 cells, transfected with Myc-MAGI-2 domains, as indicated. The molecular weights of standards are indicated in kDa.

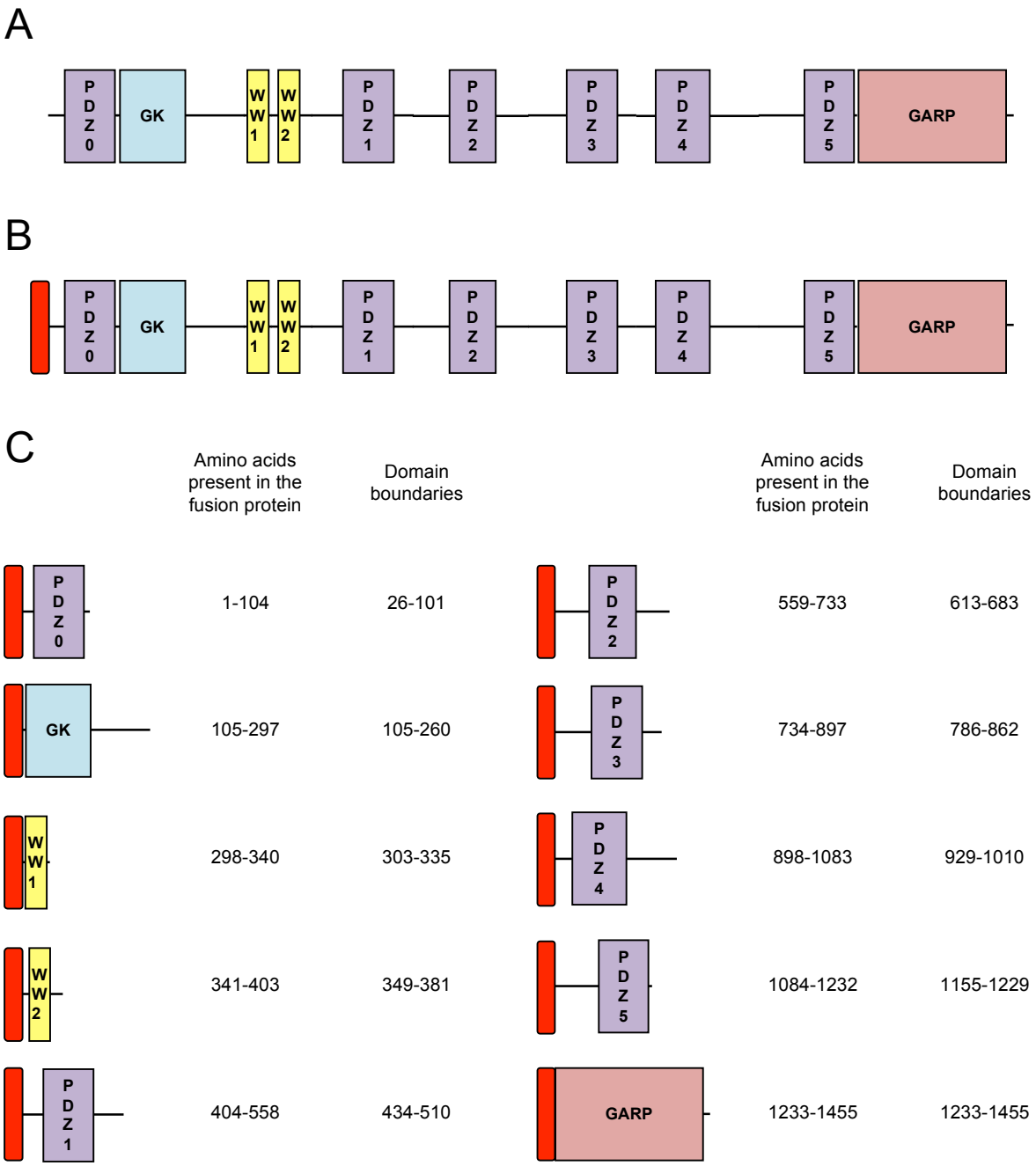

Figure 4.3: Schematic representation of the tagged (GST or Myc) MAGI-2 fusion proteins. A, Schematic representation of the MAGI-2 structure. **B and C**, Myc or GST fusion proteins were created as described in the methods. Briefly, MAGI-2 FL and its respective domains were cloned into the pMyc3 or pGEX6P1 vectors, encoding Myc or GST tags, respectively. The amino acids present in each fusion protein of MAGI-2 are indicated, as well as the MAGI-2 domain boundaries. A red box indicated the Myc or GST fusion, the purple boxes represent the PDZ domains, a blue box represents the GK domain, yellow boxes represent the WW domains, a pink box represents the GARP domain.

4.1.2 GST-MAGI-2 expression in prokaryotic cells

DNA encoding MAGI-2 FL and individual domains were subcloned into the pGEX6P1 vector (Figure 4.4). *E. coli* BL21 cells were transformed with pGEX6P1-MAGI-2 plasmids and protein expression was induced with IPTG. A schematic representation of the GST-MAGI-2 proteins is shown in Figure 4.3. GST-MAGI-2 proteins were immobilized on glutathione-Sepharose beads, and the purified proteins were resolved by SDS-PAGE. The SDS-PAGE gel was either stained with Coomassie blue (Figure 4.5A) or the protein was transferred to a nitrocellulose membrane, and probed with anti-GST antibodies (Figure 4.5B-C). Protein sizes of GST-MAGI-2 FL and the MAGI-2 domains were estimated using MacVector software, as previously described (Table 4.1). The bands representing GST-MAGI-2 domains (Figure 4.5A-C) were of the apparent molecular weight. The bands representing GST-WW or GST-PDZ domains showed little or no degradation products associated with them and were of the correct estimated molecular weight. GST-GK and GST-GARP had a lot of degradation products, as indicated by their irregular banding pattern and therefore an arrow shows the band corresponding to the most intact protein (Figure 4.5C). The DNA encoding GST-MAGI-2 FL was a truncated version of the full length protein. GST-MAGI-2 FL contained a lot of degradation products, and was not well expressed in prokaryotic cells (Figure 4.5B). Therefore, these GST-MAGI-2 proteins (the WW and PDZ domains) could be used in pull-down assays.

4.2 Limited trypsin digests of GST-MAGI-2 fusion proteins to determine whether isolated MAGI-2 domains could fold properly when fused to GST

In order to determine whether the MAGI-2 domains were folding properly when fused to GST, a limited trypsin digest was performed. Typically, a folded protein will have buried residues inside the protein, protecting these from proteolytic digestion. Once the digested products are resolved by SDS-PAGE and stained with a general protein stain, bands corresponding to the digested protein will be minimal. If a protein is not folding properly, more of these residues will be exposed and sensitive to proteolytic digestion. Therefore, when these products are resolved by SDS-PAGE and stained, the bands corresponding to the unfolded protein will be abundant. For example, a similar experiment was performed on PTEN to distinguish the "open" vs. "closed" conformations (Vazquez *et al.*, 2001). When PTEN is

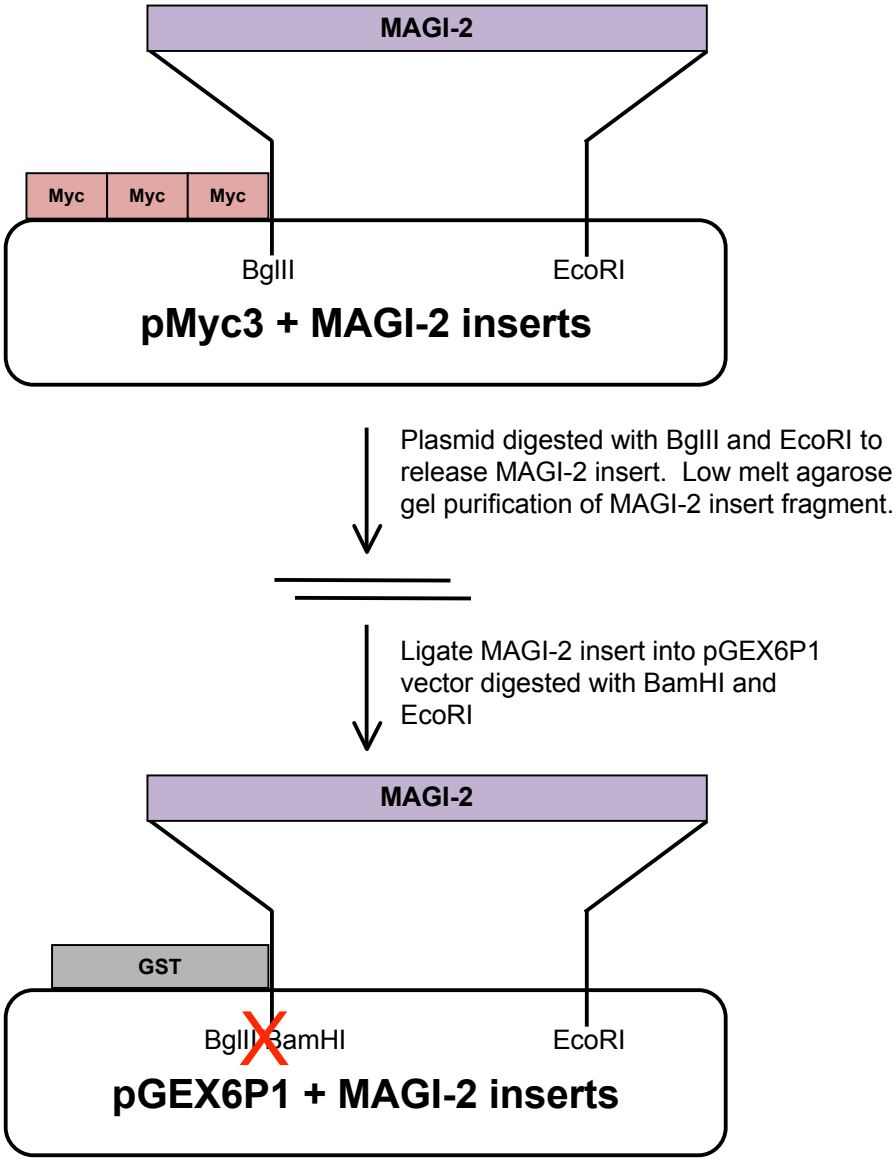

Figure 4.4: Subcloning of the DNA encoding MAGI-2 FL and its respective domains into the pGEX6P1 vector. Subcloning was achieved by digesting the pMyc3 plasmid containing MAGI-2 insert, with BglII and EcoRI. The digested product was then electrophoresed on a low melt 1-1.5% agarose gel and the band size corresponding to the MAGI-2 insert was excised from the gel. The DNA was purified from the gel, using a Gel Purification Kit. MAGI-2 DNA was ligated into the pGEX6P1 vector, previously digested with BamHI and EcoRI. BglII and BamHI have compatible 5' sticky overhangs, however the BamHI/BglII restriction sites are destroyed upon ligation of the insert into the vector. Successful ligations were analyzed by size determination of pGEX6P1 plasmid containing the MAGI-2 insert using EcoRI digestion and also by DNA sequencing.

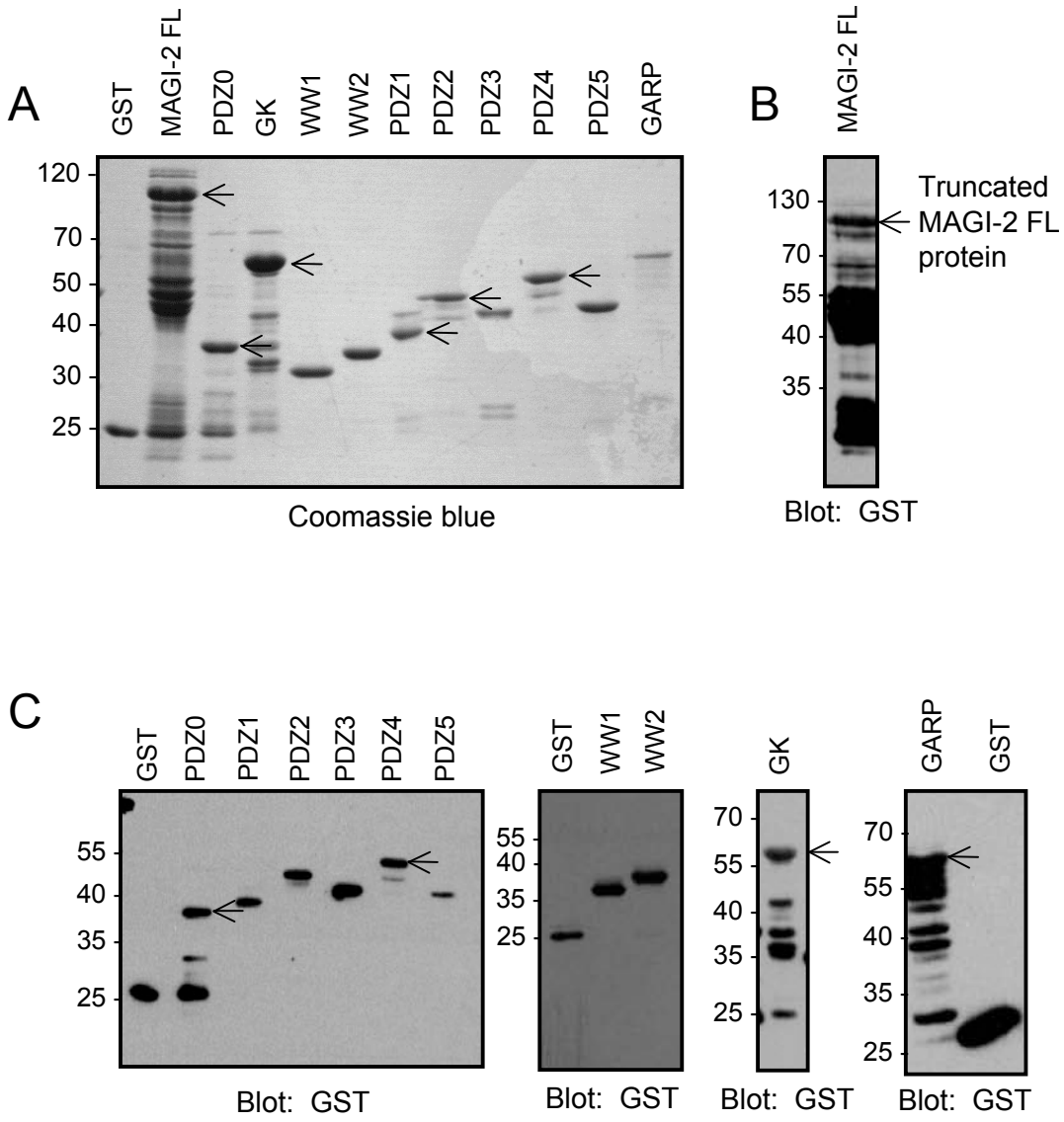

Figure 4.5: Expression and detection of GST-MAGI-2 proteins expressed in BL21 *E. coli* cells. BL21 cells were transformed with plasmid DNA encoding GST-MAGI-2 FL or individual GST-MAGI-2 domain fusion proteins. Cells were induced with IPTG, lysed and GST-MAGI-2 proteins were immobilized on glutathione-Sepharose beads. Purified proteins were resolved by SDS-PAGE and stained with Coomassie blue (**A**) or transferred onto nitrocellulose and immunoblotted with a GST antibody (**B** and **C**), in order to visualize the distinct purified GST-MAGI-2 proteins. Arrows indicate size of expected protein for samples showing multiple bands.

"closed", a limited proteolytic digestion revealed little degradation of the protein when samples were resolved by SDS-PAGE. It is hypothesized that when PTEN is in the "closed" conformation, many of the residues sensitive to proteolytic digestion are buried inside the protein and unavailable for proteolytic digestion (Vazquez *et al.*, 2001). However, an activated, "open" PTEN exposes more of its residues and a limited proteolytic digestion shows more cleavage when the sample is resolved by SDS-PAGE (Vazquez *et al.*, 2001). Therefore, to determine if GST-MAGI-2 proteins were folding properly, MAGI fusion protein was treated with a limited trypsin digest (1:1000 ratio of protease to protein).

The negative control used in this assay was GST (Figure 4.6A), which showed almost no degradation, even after an overnight incubation with trypsin. The purified GST-MAGI-2 FL protein had abundant proteolysis associated with the FL protein product (Figure 4.6B) suggesting that the FL MAGI-2 protein may not fold properly when expressed in bacteria as a GST-MAGI-2 FL protein or that the regions between the various domains may be exposed for trypsin digestion.

WW domains have been shown to fold into stable protein structures (Macias *et al.,* 1996; Macias *et al.,* 2000; Umadevi *et al.,* 2005). GST-WW1 and GST-WW2 domains showed little degradation, indicating that the WW domains fold as stable structures when expressed as a bacterial GST-WW protein (Figure 4.6C). The GK protein is quickly cleaved from the GST portion, within 5 min of trypsin digestion (Figure 4.6D). The linker region between GST and the GK domain may present a site for trypsin digestion. This suggests that GK domain can be cleaved quite easily from the GST portion of the protein; however, it is able to form a stable trypsin-resistant structure on its own (Figure 4.6D). GST-GARP has a small ~15 kDa region that is cleaved soon after the trypsin has been added. This suggests that the C-terminal end of the GARP protein may be sensitive to proteolytic digestion because it is unable to fold into a stable, globular structure (Figure 4.6E).

PDZ domains have also been shown to fold into stable protein structures (Daniels *et al.,* 1998; Doyle *et al.,* 1996; Morais Cabral *et al.,* 1996). All GST-PDZ domains, with the exception of GST-PDZ0, showed little degradation, when subjected to a limited trypsin digest (Figure 4.7). Limited digestion of the PDZ domains occurred one of two ways; either a small portion was degraded at the C-terminal end (approximately 5-10 amino acids removed with

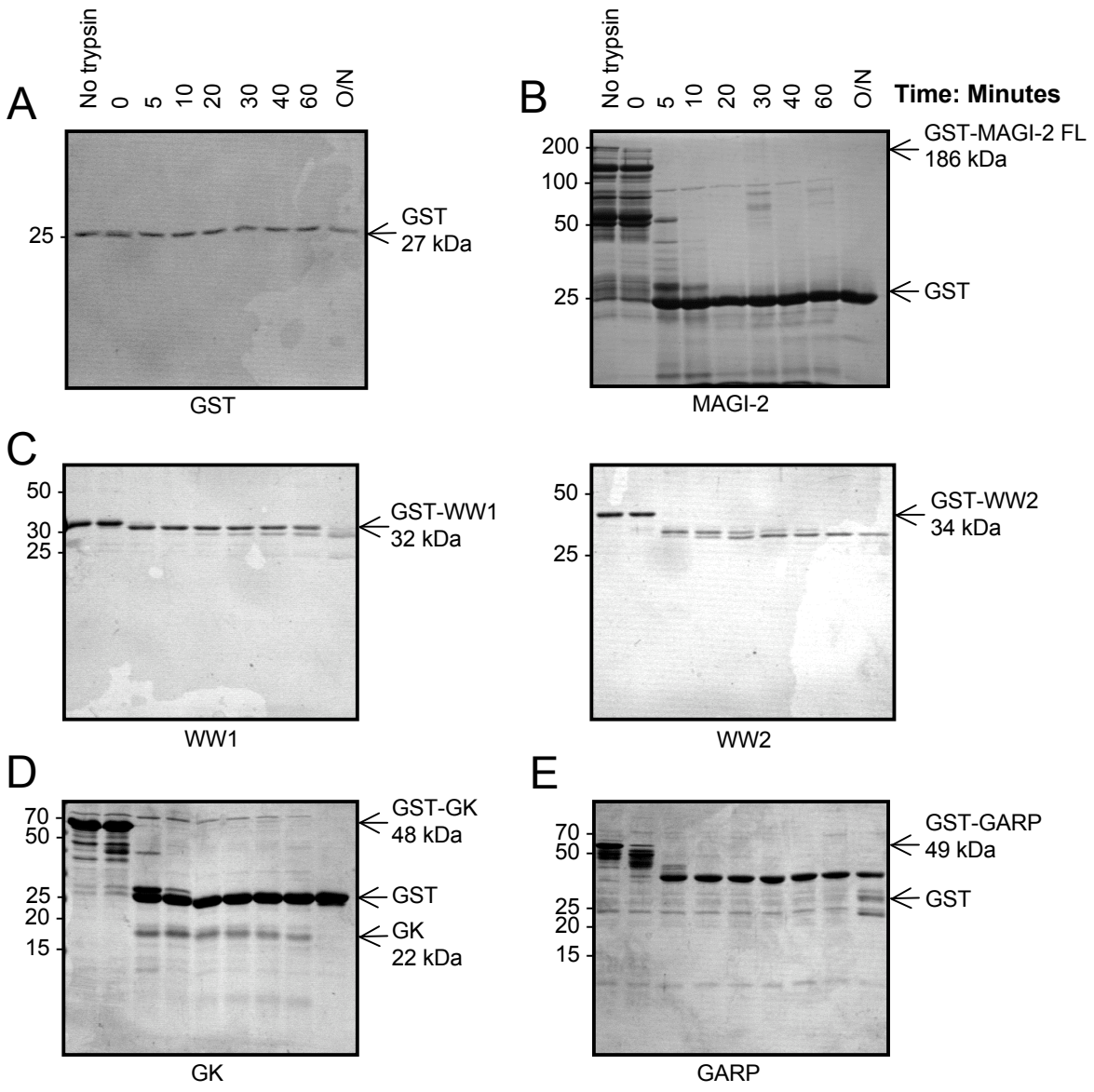

Figure 4.6: Limited trypsin digest of GST-MAGI-2 proteins to determine if the MAGI-2 domains are folding properly while fused to GST. Protein overexpression of GST-MAGI-2 FL and respective domains were induced by IPTG in BL21 cells. Cells were lysed and GST-MAGI-2 proteins were purified on glutathione-Sepharose beads. Purified GST-MAGI-2 proteins were then eluted off of the glutathione-Sepharose beads, using reduced glutathione buffer. Limited trypsin digestion was performed at 37°C where the protease to protein ratio was 1:1000. Protein sizes are estimated based on the amino acid sequence. **A**, GST. **B**, GST-MAGI-2 FL. **C**, GST-WW domains. **D**, GST-GK domain. **E**, GST-GARP domain. Samples were left untreated (no trypsin), treated for the indicated time points (in minutes) or left treated overnight (O/N).

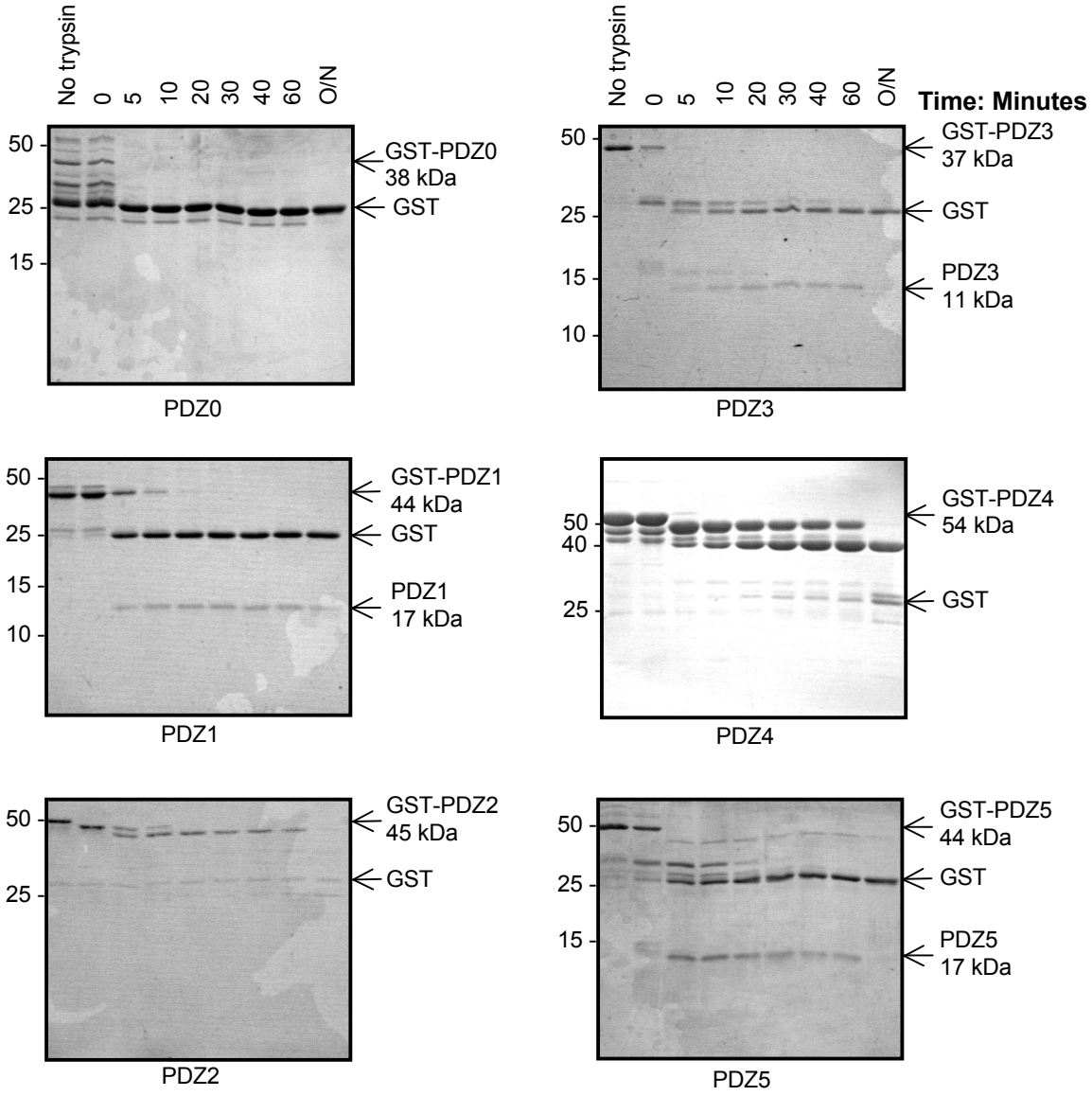

Figure 4.7: Limited trypsin digest of GST-MAGI-2 PDZ proteins to determine if the MAGI-2 domains are folding properly while fused to GST. GST-MAGI-2 PDZ domains were prepared and treated as described in Figure 4.6. Protein sizes are estimated based on the amino acid sequence. Samples were left untreated (no trypsin), treated for the indicated time points (in minutes) or left treated overnight (O/N).

GST-PDZ2 and GST-PDZ4) or the GST portion was cleaved from the stable PDZ portion (GST-PDZ1, GST-PDZ3 and GST-PDZ5). GST-PDZ0 however, was degraded within 5 min upon the addition of trypsin, indicating that this PDZ domain is not able to form a stable structure when expressed in bacteria.

4.3 Pull-down experiments to determine *in vitro* complex formation between various MAGI-2 domains and PTEN, p85, EGFR and PDGFR

4.3.1 MAGI-2 PDZ domains 2 and 5 interact with PTEN

A pull-down experiment was performed to test whether the GST-PDZ domains of MAGI-2 could bind to PTEN. PTEN contains a short, C-terminal amino acid sequence (QI**TKV**-COOH) that contains a consensus class I PDZ binding motif (section 1.4.3 and Table 1.2; reviewed in Jeleń *et al.,* 2003). Previous experiments have shown that the PDZ2 domain of MAGI-2 could bind to PTEN (Hu *et al.,* 2007; Valiente *et al.,* 2005; Vazquez *et al.,* 2001; Wu *et al.,* 2000a) along with other PDZ domains of other scaffolding proteins (Valiente *et al.,* 2005). Therefore we wanted to test our pull-down experimental system, and confirm PTEN binding to PDZ2 of MAGI-2. As a source of PTEN protein, an N-terminal, triple hemagglutinin (HA) tagged, phosphatase dead mutant (C124S) of PTEN was used. The phosphatase dead C124S mutant PTEN has improved stability over the wild type PTEN protein (Das *et al.*, 2003). Briefly, COS-1 cells were transiently transfected with DNA encoding HA-PTEN-C124S (Maehama and Dixon, 1999) and lysates were mixed with 10 µg of GST-PDZ protein domains of MAGI-2 (PDZ0-PDZ5), GST-MAGI-2 FL and GST-GARP or a negative control GST protein, previously immobilized on glutathione-Sepharose beads. Bound complexes were resolved by SDS-PAGE, and proteins were transferred to a nitrocellulose membrane for immunoblot analysis. The immunoblot was probed with anti-PTEN-HRP antibody and visualized by chemiluminescence. PTEN bound to PDZ2 (Hu *et al.,* 2007; as previously shown in Valiente *et al.,* 2005; Vazquez *et al.,* 2001; Wu *et al.,* 2000a), PDZ5 and the truncated MAGI-2 FL (Figure 4.8A). Little or no PTEN bound to GST, GST-GARP and GST-PDZ0, 1, 3 and 4. The result that MAGI-2 PDZ2 domain was able to bind PTEN is in agreement with previous studies and therefore suggests that our pull-down system is working

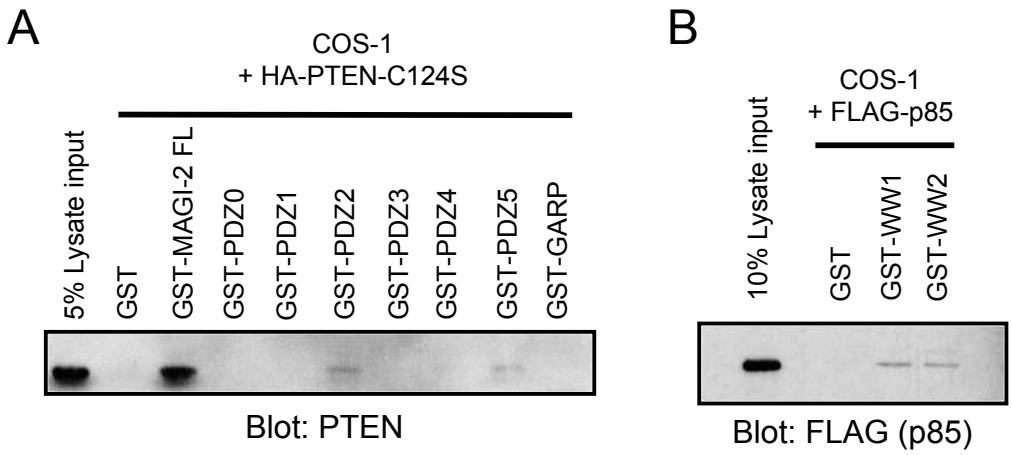

Figure 4.8: MAGI-2 PDZ and WW domains interact with PTEN and p85, respectively. **A**, GST, GST-MAGI-2 FL, GST-PDZ domains and GST-GARP domains of MAGI-2 (10 μg each) were immobilized on glutathione-Sepharose beads. These were incubated for 1 hr at 4°C with lysates from COS-1 cells expressing HA-PTEN-C124S (phosphatase dead mutant of PTEN) in a GST pull-down assay. Unbound protein was washed off and the samples were resolved by SDS-PAGE and transferred to nitrocellulose. Using an immunoblot blot analysis, HA-PTEN-C124S was detected with anti-PTEN antibody conjugated to HRP. Bound proteins were visualized using chemiluminescence. A GST control was used to detect any non-specific binding to the GST protein or the beads. The input lane contains 10 μL of cell lysate, to confirm that PTEN was present in the pull-down system and as a control for the PTEN immunoblot. **B**, GST, and GST-WW domains of MAGI-2, were used in a pull-down assay with lysates from COS-1 cells expressing FLAG-p85, as described for panel A. The immunoblot analysis consisted of a FLAG antibody to detect FLAG-p85 and corresponding secondary antibodies conjugated to HRP. The results shown are typical for at least 3 independent experiments.

correctly. We also show a novel finding where MAGI-2 PDZ5 also has the ability to bind to PTEN. This suggests that MAGI-2 has the potential to interact with PTEN through both its PDZ2 and PDZ5 domains. This result also suggests that the truncated GST-MAGI-2 may have partial binding abilities, regardless of its ability to form an ideally folded full length protein within prokaryotic cells.

4.3.2 MAGI-2 WW domains both interact with p85

A pull-down experiment was performed to test whether the GST-WW domains of MAGI-2 could associate with p85. WW domains, like SH3 domains, are known to bind to Pro rich regions (Kapeller *et al.,* 1994; Nguyen *et al.,* 1998). p85 has two Pro rich sequences; P1: amino acids 82-96 (S**PPTP**KPR**PPRP**LP, class II and III binding motifs, respectively) and P2: amino acids 300-314 (ERQPAPAL**PPKPPKP**, class II binding motifs) (Kapeller *et al.,* 1994) as detailed previously in section 1.4.2 and Table 1.1. It was therefore hypothesized that p85 may have the ability to bind to one, or both, of the WW domains of MAGI-2. Briefly, COS-1 cells were transiently transfected with DNA encoding an N-terminal, triple FLAG-tagged p85 (FLAG-p85) and lysates were mixed with 10 µg GST-WW1 or GST-WW2 proteins, or a negative control GST protein, previously immobilized on glutathione-Sepharose beads. The resultant complexes were resolved by SDS-PAGE and transferred to a nitrocellulose membrane for immunoblot analysis. Bound p85 was detected using anti-FLAG antibodies (Figure 4.8B). The FLAG-p85 protein did not bind to the negative control however, did associate with both WW domains of MAGI-2. These results suggest that both of the WW domains of MAGI-2 have the ability to interact with p85.

4.3.3 MAGI-2 PDZ domains do not associate with the EGFR

Previous studies have shown the C-terminal end of two EGFR family proteins can interact with PDZ domains (Kaech *et al.,* 1998; Lazar *et al.,* 2004). The C-terminal end of the EGFR homologue in *Caenorhabditis elegans* contains a class I PDZ binding motif (KE**TCL**-COOH). It has been shown to bind to the PDZ domain of the LIN-7 PDZ containing scaffolding protein, which is hypothesized to mediate localization to the basolateral membrane and is critical in cell differentiation (Kaech *et al.,* 1998). The MAGI-2 PDZ1 domain has already been shown to associate with the C-terminal class I PDZ binding motif of the human

ErbB4 RTK (RN**TVV**-COOH) (Buxbaum *et al.,* 2008). Therefore, a pull-down experiment was used to test whether the GST-PDZ domains of MAGI-2 could associate with the EGFR. The C-terminal end of the human EGFR contains a class II PDZ binding motif (EF**IGA**-COOH) (based on the *Homo sapiens* EGFR sequence XP_005219). Although the African green monkey (*Cercopithecus aethiops)* EGFR sequence is not known, we hypothesize that it will be conserved and similar to the human EGFR sequence. Briefly, lysates from COS-1 cells that were stimulated with EGF for 5 min or left unstimulated, were mixed with 10 µg of GST, and all GST-PDZ domains of MAGI-2, previously immobilized on glutathione-Sepharose beads. Bound complexes were resolved by SDS-PAGE and immunoblotted with anti-EGFR antibodies. It was shown that EGFR was not pulled down with GST or the GST-PDZ proteins (Figure 4.9A). This result suggests that the monkey EGFR is unable to bind to MAGI-2 through its PDZ domains under the conditions tested. The human EGFR amino acid sequence is identical to the monkey EGFR sequence, the PDZ binding motif of EGFR encodes a class II PDZ domain (Table 1.2). MAGI PDZ domains are predicted to be of the class I variety and therefore may not bind a class II PDZ binding motif.

4.3.4 MAGI-2 PDZ domains do not associate with the PDGFR

Previous studies have shown PDGFR binding to PDZ domains (Demoulin *et al.,* 2003; Maudsley *et al.,* 2000). The C-terminal end of the human PDGFR (ED**SFL**-COOH) can bind to the first PDZ domain of the NHERF scaffold protein (Maudsley *et al.,* 2000). The C-terminal end of the mouse PDGFR contains a class I PDZ binding motif (ED**SFL**-COOH) (based on the *Mus musculus* PDGFR protein sequence NP_032835) and therefore, it is hypothesized to bind to one of the MAGI-2 PDZ domains. A pull-down experiment was used, performed as described above, to determine if MAGI-2 PDZ domains could associate with the PDGFR. The cells that were used in this experiment however, were mouse NIH 3T3 stimulated with PDGF-BB for 5 min or left unstimulated since they express endogenous PDGFRs. The bound complexes were resolved by SDS-PAGE and immunoblotted with anti-PDGFR antibodies. It was shown that PDGFR was not pulled down with the MAGI-2 GST-PDZ

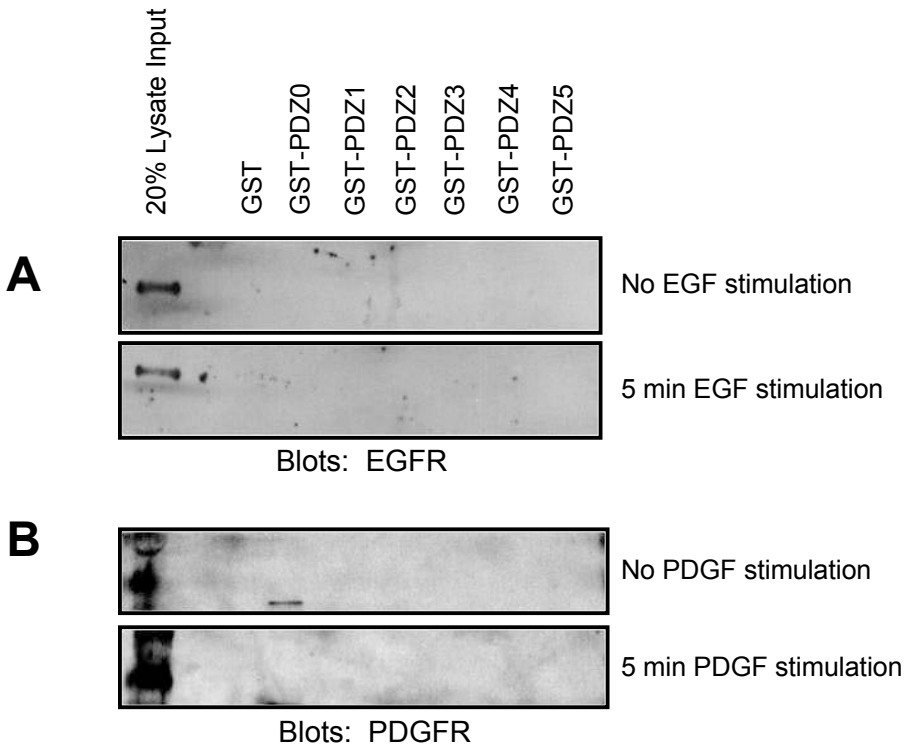

Figure 4.9: MAGI-2 PDZ domains do not associate with endogenous EGFR or PDGFR. **A**, COS-1 cells were stimulated for 5 min with EGF or left unstimulated and lysed. GST and GST-PDZ domains of MAGI-2 (10 μg each) were immobilized onto glutathione-Sepharose beads and incubated for 1 hr at 4°C with lysates from COS-1 cells (expressing endogenous EGFR) in a GST pull-down assay. Unbound protein was washed off and the samples were resolved by SDS-PAGE and transferred to nitrocellulose. Using an immunoblot analysis, EGFR was detected with anti-EGFR antibodies and corresponding secondary antibodies conjugated to HRP. Bound proteins were visualized using chemiluminescence and film. GST control was used to detect any non-specific binding to the GST protein or the beads. **B**, NIH 3T3 cells were either stimulated for 5 min with PDGF-BB or left unstimulated and lysed as described in panel A. GST and GST-PDZ domains of MAGI-2 were used in a pull-down assay with lysates from NIH 3T3 cells (expressing endogenous PDGFR) as described for panel A. An immunoblot analysis was used with PDGFR antibodies, and bound proteins were visualized as described above. The input lane contains 10 μL cell lysate, to confirm that EGFR or PDGFR was present in the system and as a control for the EGFR or PDGFR immunoblots. The results shown are typical for at least 3 independent experiments.

proteins (Figure 4.9B). These results suggest that either the PDGFR is unable to bind MAGI-2 through its PDZ binding domains under the conditions tested.

4.4 Co-immunoprecipitation experiments to determine if MAGI-2 associates with PTEN, EGFR or p85 in cells

4.4.1 MAGI-2 does not consistently co-immunoprecipitate with PTEN

To determine whether MAGI-2 could form a complex with PTEN in cells, a co-immunoprecipitation assay and immunoblot analysis was used. COS-1 cells were co-transfected with Myc-MAGI-2 FL and HA-PTEN-C124S and stimulated with EGF for 5 min, or left unstimulated. Cell lysates were immunoprecipitated separately with anti-Myc (to immunoprecipitate MAGI-2), anti-HA (to immunoprecipitate PTEN) and control immunoglobin G (IgG). These were resolved by SDS-PAGE, transferred to nitrocellulose and the immunoblot was cut in half. The top portion of the immunoblot (containing proteins $\geq$ 100 kDa) was probed with anti-Myc antibody (to detect MAGI-2) (Figure 4.10). The bottom portion of the immunoblot (containing proteins $\leq$ 100 kDa) was probed with anti-PTEN-HRP (Figure 4.10). In the first experiment, PTEN did co-immunoprecipitate with MAGI-2 after 5 min EGF stimulation (Figure 4.10A, lane 6), however, MAGI-2 did not co-immunoprecipitate with PTEN (Figure 4.10A, lanes 3 and 4). Attempts to repeat this experiment showed that PTEN and MAGI-2 did not co-immunoprecipitate (Figure 4.10B). Therefore, these results are inconclusive and may reflect the low abundance and/or the transient nature of any complexes formed.

4.4.2 MAGI-2 does not co-immunoprecipitate with the EGFR

To determine whether MAGI-2 could form a complex with EGFR in cells, COS-1 cells transfected with Myc-MAGI-2 FL and were stimulated with EGF for 5 min, or left unstimulated. Cell lysates were immunoprecipitated separately with anti-Myc (to immunoprecipitate MAGI-2), anti-EGFR and control IgG. The immunoblot was prepared as described previously and the immunoblot was first probed with an anti-Myc antibody (to detect MAGI-2) (Figure 4.11A). The membrane was then stripped and re-probed with an anti-EGFR

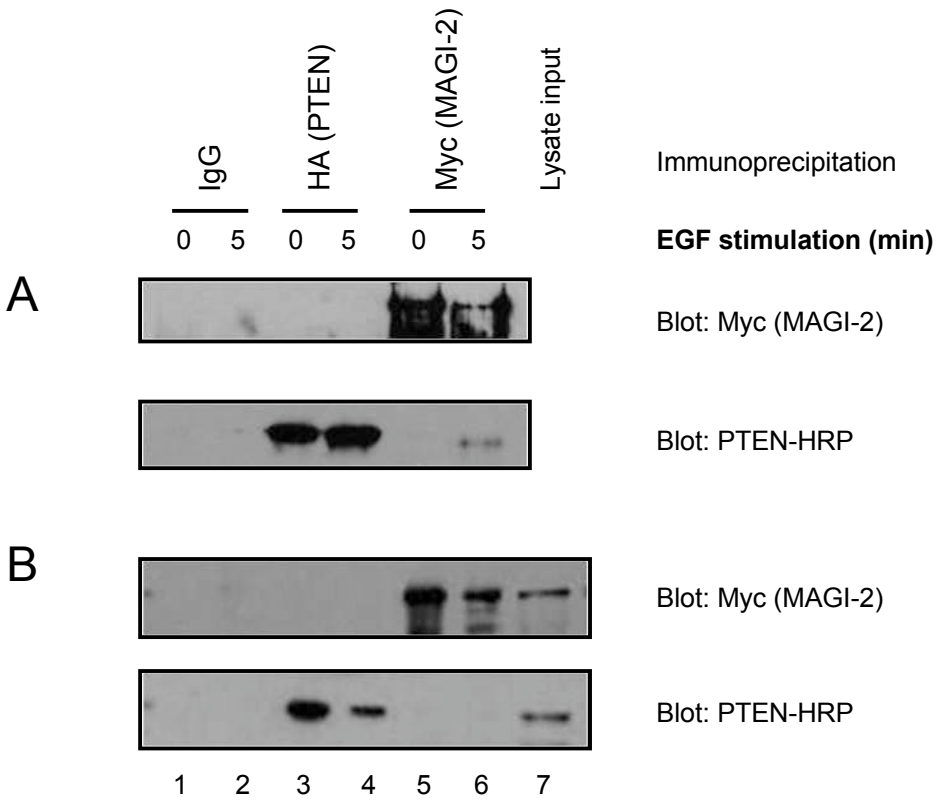

Figure 4.10: MAGI-2 does not consistently associate with PTEN in cells. COS-1 cells were transfected with 3 μg of DNA encoding Myc-MAGI-2 FL and 3 μg of DNA encoding HA-PTEN-C124S. Cells were left unstimulated or stimulated with EGF for 5 min and lysed. Cell lysates were first pre-cleared with mouse and rabbit IgG-AC and protein G beads. The lysates were centrifuged and the supernatant of these lysates were used in a co-immunoprecipitation assay where 10 μg of anti-Myc (lanes 5 and 6) or anti-HA antibody (lanes 3 and 4) were incubated for 1 hr at 4°C with COS-1 cells expressing Myc-MAGI-2 and HA-PTEN-C124S. An IgG immunoprecipitation was also performed to detect any non-specific binding (lanes 1 and 2). Unbound protein was washed off and the samples were resolved by SDS-PAGE and transferred to nitrocellulose. The nitrocellulose membrane was cut at the 100 kDa marker. The upper portion of the immunoblot was probed with anti-Myc (to detect MAGI-2). The bottom portion of the immunoblot was probed with anti-PTEN-HRP antibody. The samples were visualized using chemiluminescence and film. **A**, First experiment showing PTEN co-immunoprecipitates with MAGI-2 after 5 min EGF stimulation. **B**, Attempts to replicate the results of the first experiment showed that PTEN and MAGI-2 did not co-immunoprecipitate in cells. The input lane contains 10 μL cell lysate (lane 7), to confirm that PTEN and Myc-MAGI-2 was present in the system and as a control for PTEN and Myc immunoblots. The result shown in panel B are representative of 5 independent experiments.

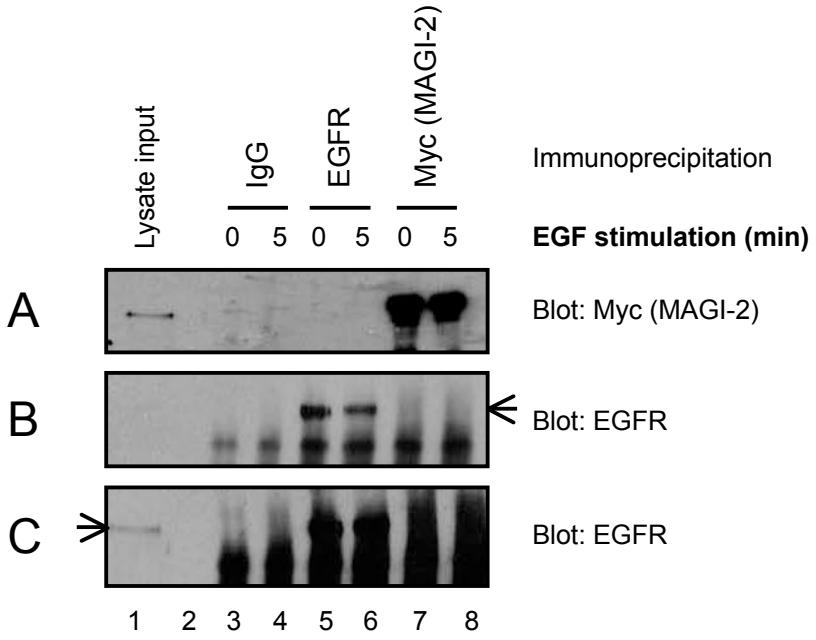

Figure 4.11: MAGI-2 does not associate with EGFR in cells. COS-1 cells were transfected with 3 µg of DNA encoding full length Myc-MAGI-2. Cells were left unstimulated or stimulated with EGF for 5 min and lysed. Cell lysates were pre-cleared with rabbit IgG-AC and protein A beads. The lysates were centrifuged and the supernatant lysates were used in a co-immunoprecipitation assay, where 10 µg of Myc (lanes 7 and 8) or EGFR (lanes 5 and 6) antibody were incubated for 1 hr at 4°C with COS-1 cells expressing Myc-MAGI-2 and endogenous EGFR. An IgG immunoprecipitation was also performed to detect any non-specific binding (lanes 3 and 4). Unbound protein was washed off and the samples were resolved by SDS-PAGE and transferred to nitrocellulose. Using an immunoblot analysis, MAGI-2 and EGFR were detected with anti-Myc and anti-EGFR antibodies, respectively, and corresponding secondary antibodies conjugated to HRP. The samples were visualized using chemiluminescence and film. The membrane was immunoblotted with anti-Myc (**A**) to detect MAGI-2. The membrane was stripped and re-probed with anti-EGFR (**B**). **C**, Longer exposure of panel B to visualize the EGFR band in the lysate input lane. The input lane contains 10 µL (lane 1) cell lysate to confirm that Myc-MAGI-2 and EGFR were present in the system and to control for Myc and EGFR immunoblot. Lane 2 is an empty lane. The results shown for the Myc immunoprecipitation are typical for at least 3 independent experiments. The result shown for the EGFR immunoprecipitation is the result of one experiment.

antibody (Figure 4.11B-C). Myc-MAGI-2 did immunoprecipitate with the anti-Myc and EGFR did immunoprecipitate with anti-EGFR however, no co-immunoprecipitation between MAGI-2 and EGFR were found. These results suggest that MAGI-2 and EGFR do not form a complex in cells under the conditions tested.

4.4.3 MAGI-2 does not co-immunoprecipitate with p85

Because we had determined that p85 could interact with the WW domains of MAGI-2, the next step was to determine whether this interaction could take place in cells. COS-1 cells were co-transfected with Myc-MAGI-2 FL and FLAG-p85 and stimulated with EGF for 5 min or left unstimulated. Cell lysates were used in a co-immunoprecipitation experiment and immunoprecipitated separately with anti-Myc (to immunoprecipitate MAGI-2), anti-FLAG (to immunoprecipitate p85) and control IgG. The immunoblot was prepared as previously described and the upper portion of the immunoblot (containing proteins $\geq$ 100 kDa proteins) was first probed with anti-Myc antibody (to detect MAGI-2, Figure 4.12A). The membrane was then stripped and re-probed with anti-EGFR antibody (Figure 4.12B). The bottom portion of the blot (containing $\leq$ 100 kDa proteins) was probed with anti-FLAG antibody (to detect p85, Figure 4.12C). Myc-MAGI-2 did immunoprecipitate with the anti-Myc, and FLAG-p85 did immunoprecipitate with the anti-FLAG. MAGI-2 did not co-immunoprecipitate p85 or EGFR. The p85 protein did co-immunoprecipitate EGFR upon 5 min stimulation with EGF, as previously shown (Fry and Waterfield, 1993). These results suggests that MAGI-2 and p85 do not form a complex cells under the conditions tested. These results also confirmed the results from Figure 4.11B-C where MAGI-2 and EGFR did not form a complex in cells under the conditions tested. The FLAG immunoblots have non-specific bands in the IgG control lanes and therefore these results are inconclusive. Because the band representing FLAG-p85 in the FLAG immunoprecipitate (Figure 4.12C, lanes 5-6) we speculate that the FLAG immunoprecipitate did in fact immunoprecipitate FLAG-p85 protein. Because the intensity of the non-specific bands in the IgG immunoprecipitation (Figure 4.12C, lanes 3-4) are similar to that of the Myc immunoprecipitation (Figure 4.12C, lanes 7-8), we speculate that the bands in the Myc immunoprecipitation are due to non-specific binding and not actual complex formation between FLAG-p85 and Myc-MAGI-2.

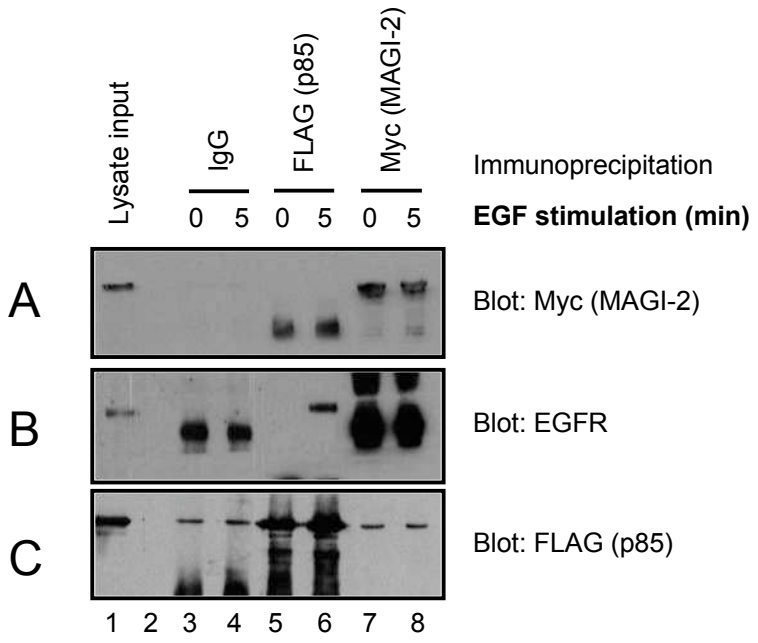

Figure 4.12: MAGI-2 does not associate with p85 in cells. COS-1 cells were co-transfected with 3 μg of DNA encoding Myc-MAGI-2 FL and 3 μg of DNA encoding FLAG-p85. Cells were left unstimulated or stimulated with EGF for 5 min and lysed. Cell lysates were pre-cleared with mouse and rabbit IgG-AC and protein G beads. These lysates were centrifuged and the supernatant was used in an immunoprecipitation assay where 25 μg of Myc (lane 7 and 8) or FLAG (lane 5 and 6) antibody were incubated for 1 hr at 4°C, with COS-1 cells expressing Myc-MAGI-2 and FLAG-p85. IgG immunoprecipitations were also performed to detect any non-specific binding. Unbound protein was washed off and the samples were resolved by SDS-PAGE and transferred to nitrocellulose. Using an immunoblot analysis MAGI-2, EGFR and p85 were detected with anti-Myc, anti-EGFR and anti-FLAG antibodies, respectively, and corresponding secondary antibodies conjugated to HRP. The immunoblot was visualized using chemiluminescence and film. The membrane was cut in half at the 100 kDa mark and the upper membrane (containing protein sizes $\geq$ 100 kDa) was immunoblotted with anti-Myc (**A**) to detect MAGI-2. The upper membrane was then stripped and re-probed with anti-EGFR (**B**). The lower portion of the membrane (containing protein sizes $\leq$ 100 kDa) was probed with anti-FLAG (**C**) to detect p85. Non-specific binding is present in the FLAG immunoblot IgG lanes. The input lane contains 10 μL (lane 1) cell lysate to confirm that Myc-MAGI-2, EGFR and p85 were present in the system and to control for Myc, EGFR and FLAG immunoblot. Lane 2 is an empty lane. The results shown for the Myc immunoprecipitation are typical for at least 3 independent experiments. The result shown for the FLAG immunoprecipitation is the result of one experiment.

4.5 Rabbit polyclonal MAGI-2 antibody can detect Myc-MAGI-2 FL

MAGI-2 is a subfamily of MAGI proteins (MAGI-1 and MAGI-3) which share substantial sequence similarly (Figure 1.6). Most commercially available MAGI-2 antibodies do not specifically detect MAGI-2 since they also detect the other MAGI proteins. Therefore, we generated a rabbit polyclonal antibody that would be specific for MAGI-2. A CUSTLAW sequence alignment shows a unique MAGI-2 C-terminal domain of approximately 200 amino acids (Figure 4.13A) (Wu *et al.,* 2000b). Our lab termed this stretch of amino acids the GARP C-terminal sequence because it is rich in Gly, Ala, Arg and Pro residues. According to a basic local alignment search sequence search, the GARP C-terminal sequence of MAGI-2 (amino acids 1233-1455) had no sequence homology, nor any putative conserved domains detected within this sequence and the GARP C-terminal sequence of MAGI-2 has no known function known to date (Eugene *et al.*, 1990). Therefore, we focused on this unique MAGI-2 sequence to generate the MAGI-2 polyclonal antibody. The GARP protein was purified (Figure 4.13B) (as described in the materials and methods) and used as an antigen injected into a rabbit. The rabbit generated polyclonal antibodies against the unique GARP protein corresponding to the C-terminal end of MAGI-2. A test bleed was performed approximately 3 weeks after antigen injection and crude serum was used to probe an immunoblot containing COS-1 cell lysates expressing Myc-MAGI-2 FL (Figure 4.13C), and compared to a control Myc immunoblot (Figure 4.13D). These results suggest that the MAGI-2 polyclonal antibody, raised against the GARP C-terminal sequence of MAGI-2, has the ability to detect MAGI-2 FL in cells.

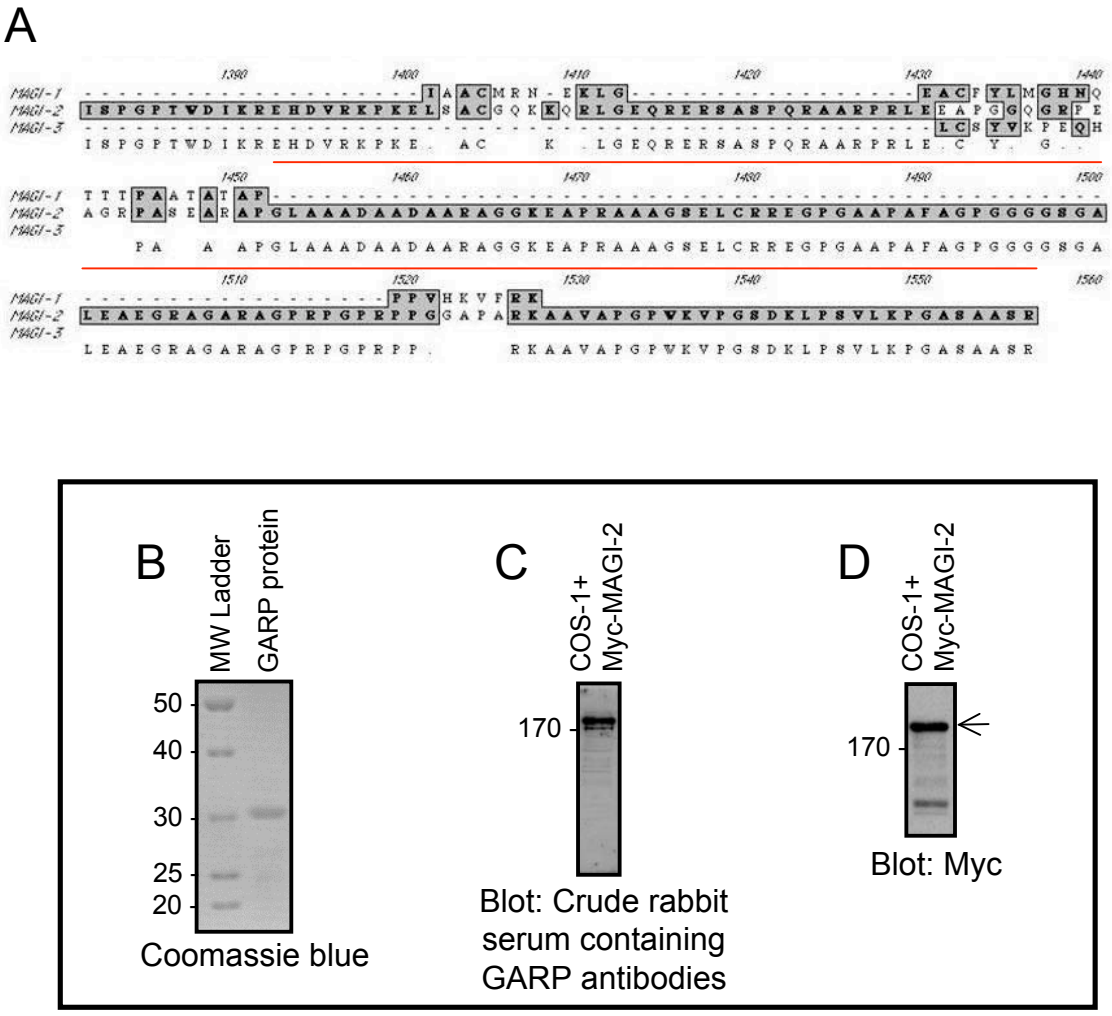

Figure 4.13: Designing the MAGI-2 polyclonal antibody. **A**, C-terminal amino acid sequence alignments of MAGI-1, -2 & -3 showing the unique, approximately 100 amino acid sequence of MAGI-2 representing the GARP C-terminal sequence (outlined in red) (Wu *et al*., 2000b). Protein antigen was generated through PCR amplification of the region encoding amino acids 1233-1455 of the MAGI-2 protein and subcloning it into the pGEX6P1 vector. The plasmid was transformed into BL21 cells and the resulting pGEX6P1-GARP bacterial colony was induced with IPTG to overexpress GST-GARP. BL21 cells were lysed, and GST-GARP protein was isolated on glutathione-Sepharose beads. The GARP protein was cleaved from GST using PreScission protease. **B**, MAGI-2 GARP protein was resolved by SDS-PAGE and visualized by Coomassie blue staining. This GARP protein antigen was used to generate polyclonal antibodies in rabbit. **C**, Transfected COS-1 cells overexpressing Myc-MAGI-2 FL protein immunoblotted with crude rabbit serum expressing the newly generated MAGI-2 GARP antibody/serum. **D**, Myc antibody as a positive control to detect the Myc tag on Myc-MAGI-2 FL (185 kDa).

5.0 DISCUSSION

PTEN is a tumor suppressor protein and its loss of function is correlated with a variety of cancers (Pendaries *et al.,* 2003; Simpson and Parsons, 2001; Sulis and Parsons, 2003). PTEN loss of function is often correlated with the loss of proper attenuation of the Akt signalling pathway, a pathway which promotes cellular survival, cell cycle entry and progression and protein translation for cell growth (Cantley and Neel, 1999; Schlessinger, 2000). PTEN is hypothesized to be recruited to a high molecular weight complex at the plasma membrane, known as the PTEN-associated complex (PAC), and it is suggested to associate with MAGI-2 at this location (Vazquez *et al.,* 2000, 2001). The association of PTEN with MAGI-2 may recruit PTEN to the proper localization of PTEN to its lipid substrates so that it can effectively attenuate Akt signalling (Vazquez *et al.,* 2000, 2001). The goal of this project was to test the ability of MAGI-2 to act as a scaffolding protein to bring together several signalling molecules, including PTEN, and attenuate the PI3K/Akt pathway via PTEN.

5.1 MAGI-2 expression in eukaryotic and prokaryotic cells

In order to study the scaffolding functions of MAGI-2, MAGI-2 FL and its domains were cloned into eukaryotic and prokaryotic expression vectors. These plasmids were transfected or transformed into cells and their encoded proteins were used in protein-protein interaction assays such as immunoprecipitations and pull-down experiments. This allowed us to map some of the domains of MAGI-2 that are involved in binding to proteins involved in the attenuation of PI3K/Akt signalling.

Myc-MAGI-2 proteins are well expressed in eukaryotic cells as little or no degradation products were seen and the proteins were of the appropriate estimated molecular weight (Figure 4.2). The Myc-MAGI-2 FL protein does have degradation products associated with it and this band is seen just under the 130 kDa marker (Figure 4.2A). The Myc-MAGI-2 genes are under the transcriptional control of the cytomegalovirus promoter, a strong promoter that allows abundant gene expression (Bendig 1988; Davis and Huang, 1988). One of the results of overexpression of proteins in eukaryotic cells is the activation of proteases that degrade protein, causing the presence of degraded product in the cells (Bendig 1988). The Myc-MAGI-2 proteins were well expressed in eukaryotic cells and therefore could be used in immunoprecipitation experiments.

GST-MAGI-2 proteins were also well expressed in bacterial cells (Figure 4.5), however did exhibit more degradation. The GST-MAGI-2 protein products had degradation products associated with them, especially the GST-MAGI-2 FL protein (Figure 4.5A-B). Degradation products were also seen with GST-PDZ0, GST-PDZ1, GST-PDZ2 and GST-PDZ4, as well as the GST-GK domain and the GST-GARP (Figure 4.5A-C). MAGI-2 FL protein had abundant degradation product associated with it and a truncated (approximately 120 kDa fragment) of the protein was the largest, reasonably abundant protein observed (Figure 4.5A-B). MAGI-2 may be post-translationally modified in eukaryotic cells, alterations that are not available in bacterial cells. These modifications include Pro *cis/trans* isomerisation, glycosylation, lipidation, phosphorylation, N-terminal residue alteration or protein folding that may require a molecular chaperone (Baneyx and Palumbo, 2003; Bendig 1988; Cereghino and Cregg, 2000; Daly and Hearn, 2005; Palomares *et al.,* 2004; Takano *et al.,* 1999). These post-translational modifications may be important in the proper translation and/or proper folding of the MAGI-2 FL protein (Cereghino and Cregg, 1999; Daly and Hearn, 2005; Frydman, 2001; Palomares *et al.,* 2004). Some MAGUK scaffolding proteins have been shown to be post-translationally modified by palmitoylation, phosphorylation and sumoylation (Chao *et al.,* 2008; Gardoni *et al.,* 2006; Samuels *et al.,* 2007; Topinka and Bredt, 1998). MAGI-2 is not known to be post-translationally modified, however the fact that it is not well expressed in bacterial cells suggests that post-translational modifications or co-expression with a stabilizing chaperone proteins may be necessary for the proper expression of this protein.

A second explanation for the poor quality of expression of MAGI-2 protein in bacterial cells is that the MAGI-2 cDNA sequence encodes a human protein with different codon preferences, as compared to bacterial proteins. Thus, the tRNAs present in the bacterial BL21 cells may not be sufficiently abundant, resulting in truncated proteins (dos Reis *et al.,* 2004; Kuland, 1991; Robinson *et al.,* 1984). Therefore, we could attempt expressing GST-MAGI-2 in *E. coli Rosetta gami* bacterial cells (Novagen), which have six additional tRNAs (for the codons AUA, AGG, AGA, CUA, CCC and GGA), which are limiting in BL21 cells. We could also attempt to express GST-MAGI-2 FL in yeast cells or insect cells (using baculovirus expression) that are of eukaryotic origin and therefore contain transcriptional and translational machinery and support post-translational modifications (Cereghino and Cregg, 1999; Daly and Hearn, 2005; Fleer, 1992; Sudbery, 1996). If we are still unable to express GST-MAGI-2 FL in

cells, it may be beneficial to create two clones, one that encodes the first half of the MAGI-2 protein (PDZ0-WW2) and a second that encodes the second half of the protein (PDZ1-GARP). These proteins may be better expressed in bacterial cells due to the fact that they are not as large as the MAGI-2 FL protein (Kurland and Dong, 1996). MAGI-2 FL expression may not be occurring properly due to a combination of situations such as the lack of post-translational modifications, preferential codon usage by the organism or that the protein is too large for bacterial expression.

To determine if the GST-MAGI proteins were folding properly while fused to GST, a limited trypsin digest was performed (Figure 4.6 and 4.7). Typically, a properly folded protein will have buried residues inside the protein, protecting these from proteolytic digestion, when the digested products are resolved by SDS-PAGE and stained with a general protein stain. The bands representing the digested protein will be minimal if the protein is folded into a stable, tertiary structure. If a protein is not folding properly, more of these residues will be exposed for proteolysis and sensitive to proteolytic digestion. When these products are resolved by SDS-PAGE and stained, the bands representing the unfolded protein will be abundant.

The negative control used in this assay was GST (Figure 4.6A), which showed little or no degradation after an overnight incubation with trypsin. The purified GST-MAGI-2 FL protein had abundant proteolysis associated with it (Figure 4.6B) suggesting that the GST-MAGI-2 FL protein may not fold properly when expressed in bacteria or that the regions between the various domains may be exposed for trypsin digestion. GST-MAGI-2 FL however was used in the PTEN pull-down assay (Figure 4.8A) and the various MAGI-2 fragments were capable of binding to PTEN, thereby suggesting that the MAGI-2 protein retained some binding capabilities.

WW domains have been shown to fold into stable tertiary protein structures (Macias *et al.,* 1996; Macias *et al.,* 2000; Umadevi *et al.,* 2005). GST-WW1 and GST-WW2 domains showed little proteolysis, indicating that the WW domains fold as stable structures when expressed as bacterial GST-WW proteins (Figure 4.6C). A short C-terminal peptide of approximately 10 amino acids is cleaved off of the C-terminal end of the protein. The GK protein is quickly cleaved from the GST portion, within 5 min of trypsin digestion (Figure 4.6D). The linker region between GST and the GK domain and may present an opportunity for trypsin digestion. This suggests that GK domain can be cleaved quite easily from the GST

portion of the protein; however, it is able to form a stable trypsin-resistant structure on its own. GST-GARP has a small ~15 kDa region that is degraded soon after the trypsin has been added. This suggests that the C-terminal end of the GARP protein may be sensitive to proteolytic digestion because it is unable to fold into a stable, globular, tertiary structure (Figure 4.6E). Therefore, GST-MAGI-2 domains form stable structures while fused to GST, whereas the GST-MAGI-2 FL, GST-PDZ0 and GST-GARP fusion proteins may not form stable structures. Perhaps future studies could include transforming yeast cells which may be able to perform necessary post-translational modifications that the protein requires for stable expression in cells.

PDZ domains have also been shown to fold into stable, independent tertiary protein structures (Daniels *et al.,* 1998; Doyle *et al.,* 1996; Morais Cabral *et al.,* 1996). All GST-PDZ domains, with the exception of GST-PDZ0, showed little or no proteolysis when subjected to a limited trypsin digest (Figure 4.7). Limited digestion of the PDZ domains occurred one of two ways; either a small portion was degraded at the C-terminal end (approximately 5-10 amino acids removed with GST-PDZ2 and GST-PDZ4) or the GST portion was cleaved from the stable PDZ portion (GST-PDZ1, GST-PDZ3 and GST-PDZ5). GST-PDZ0 however, was degraded within 5 min upon the addition of trypsin, indicating that this PDZ domain is not able to form a stable structure when expressed in bacteria. The sequence alignment of the MAGI PDZ domains show that PDZ0 is the least conserved of the PDZ domains of MAGI (Figure 1.16). The carboxy binding loop (which is GFGF in the MAGI PDZ domains as opposed to the GLGF motif in most PDZ domains) of the PDZ0 domains of the MAGI proteins is not as well conserved as it is in the rest of the PDZ domains of the MAGI proteins. The GFGF motif is crucial for the structural integrity PDZ domains (Doyle *et al.,* 1996; Morais Cabral *et al.,* 1996) which may explain why the PDZ0 domain of MAGI-2 is unable to form a stable tertiary structure on its own fused to GST. Therefore, the PDZ0 domain of the MAGI proteins may rely on other tertiary structures of the MAGI protein in order for it to gain tertiary stability on its own. Therefore, if we create a mutant that includes the sequences of PDZ0-WW2, we may be able to form a better tertiary folded structure.

One method to reduce the amount of degradation product observed through our limited proteolysis experiment is to restrict the sequences of our mutants to include only the sequences that encode the domains. Amplification of the DNA sequences through PCR included all

residues of the protein therefore we did not restrict the primers to the boundaries of the structural domains (Figure 4.3C). For example, the GK domain contains amino acids 105-260 however in our protein, we included amino acids 105-297. These extra sequences may not form stable, secondary or tertiary structures, thereby being prone to degradation in prokaryotic cells. Therefore, if we restrict the amino acid sequence to the domain itself, and get rid of the excess amino acids flanking the sequence, we may see less degradation products associated with our GST-MAGI-2 proteins.

5.2 MAGI-2 association with PI3K signalling molecules

5.2.1 MAGI association with PTEN

Once the Myc-MAGI-2 FL clone was prepared, we wanted to test whether it could associate with PTEN in cells and whether or not this association was dependent on EGF stimulation. Immunoprecipitation experiments were performed where Myc-MAGI-2 and HA-PTEN-C124S where co-transfected into cells that were stimulated with EGF for 5 min, or left unstimulated. PTEN and MAGI-2 were independently immunoprecipitated and the membrane was immunoblotted with Myc (to detect MAGI-2) and PTEN to determine their presence in the immunoprecipitation complexes. In the HA immunoprecipitation (to immunoprecipitate PTEN), no MAGI-2 was detected (Figure 4.10A lanes 3-4) however, PTEN was detected in the Myc immunoprecipitation after 5 min of EGF stimulation (Figure 4.10A, lanes 6). One of the reasons why we may not detect MAGI-2 in the PTEN immunoprecipitation could be because PTEN is present in many protein complexes in the cell, such as other endogenous PDZ containing scaffolds (Dobrosotskaya *et al.,* 1997; Hu *et al.,* 2007; Kotelevets *et al.,* 2005; Takahashi *et al.,* 2006; Valiente *et al.,* 2005; Wu *et al.,* 2000a), p85 (Chagpar, 2004), lipids (Das *et al.,* 2003; Georgescu, 2008; Murray and Honig, 2002) and in the nucleus (reviewed in Planchon *et al.,* 2008), and therefore only a small percentage of PTEN may be available for MAGI-2 interactions. However, the presence of PTEN in the Myc immunoprecipitation was encouraging because it was in agreement with the hypothesis that MAGI-2 recruitment of PTEN to the PAC is important in attenuating PI3K/Akt signalling in cells. In addition, here we had shown that this recruitment was dependent on EGF stimulation.

Attempts to repeat the above results were unsuccessful and we were unable to detect PTEN in the Myc-MAGI-2 immunoprecipitations (Figure 4.10B). At first, we observed non-specific binding where our IgG control immunoprecipitations appeared to contain some PTEN. Once the non-specific association was cleared through longer pre-clearing steps with anti-IgG antibody and protein G beads, we saw no detection of PTEN in the IgG immunoprecipitation as well as none in the Myc-MAGI-2 immunoprecipitations. We also tried different combinations of transfections of HA-PTEN-C124S with Myc-MAGI-2. Upon EGF stimulation and dephosphorylation of PTEN, PTEN is quickly degraded by the proteosome (Fujita *et al.,* 2006; Georgescu *et al.,* 2000; Torres and Pulido, 2001; Wang *et al.,* 2007). Therefore, we attempted to stimulate cells for 1 min, in addition to 5 min, because the 5 min time point may have a decrease in PTEN levels in the cell due to proteosomal degradation. Unfortunately, we were still unable to detect PTEN upon MAGI-2 immunoprecipitation and our results remain inconclusive.

Further attempts to reproduce results showing PTEN association with MAGI-2 upon EGF stimulation could include decreasing the EGF stimulation time points (ranging between 10-60 secs) because of PTEN sensitivity to degradation upon activation (Fujita *et al.,* 2006; Georgescu *et al.,* 2000; Torres and Pulido, 2001; Wang *et al.,* 2007). Therefore a shorter time point may be required to 'catch' PTEN at the plasma membrane bound to MAGI-2. We could also try using a PTEN mutant [PTEN-C124S-STT/AAA (S380A/T382A/T383A)] (Chagpar, 2004; Das *et al.,* 2003) that is less sensitive to degradation and is in its constitutively open conformation, thereby making PTEN more prone to bind to MAGI-2, which has been shown to work in previous studies (Vazquez *et al.,* 2001). Vazquez and colleagues were also unable to immunoprecipitate wild type PTEN and MAGI-2 concurrently, and they speculated that it was because the PTEN pool available for binding to a MAGI-2 PDZ domain was too low (Vazquez *et al.,* 2001). However, a constitutive open and active PTEN may be degradation sensitive and therefore may be degraded before reaching the plasma membrane (Huang and Wang, 2008; Wang *et al.*, 2007). Therefore, we may need to inhibit PTEN ubiquitination and/or proteosomal degradation in order to see MAGI-2/PTEN association at the plasma membrane. Cells expressing fluorescently tagged PTEN and MAGI-2 are stimulated and PTEN localization to the plasma membrane are analysed using a fluorescence resonance energy transfer approach (Hangaur and Bertozzi, 2008). Live imaging of protein-protein interactions could give a better

idea of a time course to use when stimulating cells for these immunoprecipitation experiments. Further attempts to repeat these experiments may allow us to detect PTEN association with MAGI-2 upon EGF stimulation.

One last explanation as to why the immunoprecipitation experimental results are not consistent is that perhaps our N-terminal tag may be interfering with important protein interaction sites. Therefore, repositioning the N-terminal tag to the C-terminal end may improve binding capabilities. Relocating the N-terminal tag to the C-terminal end however, may also interfere with binding. For example, moving the HA tag on PTEN to its C-terminal end is not advisable because the last 3 amino acids of PTEN contain the PDZ binding motif (Valiente *et al.*, 2005; Vazquez *et al.*, 2000). Therefore, a C-terminal tag at the C-terminal position will almost definitely prevent binding of a PDZ binding motif to a PDZ domain. Therefore, if we suspect that the N-terminal tag is interfering with important binding sites between target proteins, these can be relocated to the C-terminal end of the protein.

Regardless of the fact that PTEN may bind to MAGI-2 upon EGF stimulation, it is well documented that the PDZ2 domain of MAGI-2 can in fact bind to PTEN (Valiente *et al.,* 2005; Vazquez *et al.,* 2001; Wu *et al.,* 2000a), and PTEN and MAGI-2 interactions can better attenuate Akt activation and signalling (Hu *et al.,* 2007; Wu *et al.,* 2000a). A PTEN mutant lacking the C-terminal binding PDZ binding motif can not bind to the PDZ2 domain of MAGI-2, or other MAGI family members, and also does not attenuate Akt activation (Valiente *et al.*, 2005; Wu *et al.*, 2000a, 2000b). Akt attenuation by PTEN through binding to MAGI-2 (or other MAGI proteins) may be due to localizing PTEN to the appropriate microdomain at the plasma membrane in order for PTEN to gain better access to its lipid products (Dobrosotskaya *et al.,* 1997; Wu *et al.,* 2000a, 2000b) or may be due to the fact that PTEN binding to a PDZ domain has been shown to increase PTEN half-life in cells (Wu *et al.,* 2000a, 2000b). Unlike previous studies, we have shown that PTEN can bind to the PDZ5 domain of MAGI-2, in addition to the PDZ2 domain (Figure 4.8A). The fact that MAGI-2 may have the ability to bind to more than one PTEN molecule at a time may be significant in that this may improve the efficiency of the attenuation of Akt signalling by increasing the local concentration of PTEN molecules in the area of PTEN lipid substrate, PI3,4,5P_2. Therefore MAGI-2 may aid the ability of PTEN to decrease Akt signalling by increasing the number of PTEN molecules at appropriate sites for Akt deactivation.

MAGI-2 PDZ2 and PDZ5 domains have been shown to bind to PTEN (Figure 4.8A). A sequence alignment of PDZ2 and PDZ5 shows identities and similarities that are conserved between these two domains, not present in the non-PTEN binding PDZ domains (PDZ1, PDZ3 and PDZ4) (Figure 5.1A, blue). The PDZ2 and PDZ5 domains of MAGI-2 share 24% sequence identities and an additional 25% sequence similarities. Conserved residues which are found in both PDZ2 and PDZ5, but not PDZ1, PDZ3 and PDZ4, of the MAGI proteins may be important in making contact with PTEN (Figure 5.1A, blue). The Gly conserved residue is located in the carboxylate binding loop (Figure 5.1 and 5.2, blue). The conserved negatively charged amino acids are found in both the β1 and the residue following the α1 strand (Figure 5.1 and 5.2, blue). The negatively charged residues are quite close to each other with respect to the folded PDZ domain however, they are outside the carboxylate binding loop that forms the binding pocket of the PDZ domain (Figure 5.2). Therefore, these negatively charged residues may be important in making contact with the PTEN peptide and providing specificity for the PTEN protein. These negatively charged residues are not part of the peptide binding pocket. Similar residues are also conserved in other PDZ domains known to bind PTEN (Figure 5.1B, blue). These residues are conserved in PDZ domains that bind PTEN and therefore may confer specificity towards binding the PTEN protein.

5.2.2 MAGI-2 association with p85

The p85 protein contains two Pro rich regions (Figure 1.4) that may allow it to bind to the WW domains of MAGI-2. Previous studies have shown that p85 may be present in the PAC (Vazquez *et al.,* 2001) and that p85 has the ability to bind to PTEN and increase its lipid phosphatase activity (Chagpar, 2004; Pastor, 2008). Therefore, MAGI-2 may have the ability to bind to p85 and place it in close proximity of PTEN to increase the efficiency of PTEN attenuation of Akt signalling. In a pull-down experiment, we found that p85 can bind to both WW domains of MAGI-2 (Figure 4.8B). MAGI-2 association with p85 could be interpreted in two ways, both of which are not mutually exclusive. p85 has been shown to positively regulate PTEN (Chagpar, 2004; Pastor, 2008) and the function of MAGI-2 may be to bind p85 and place it in close proximity to PTEN. The other interpretation is that MAGI-2 may bind to the PI3K complex bound to the RTK in order to place the MAGI-2/PTEN complex at a specific location of the plasma membrane, near PI3K generated lipid products. An immunoprecipitation

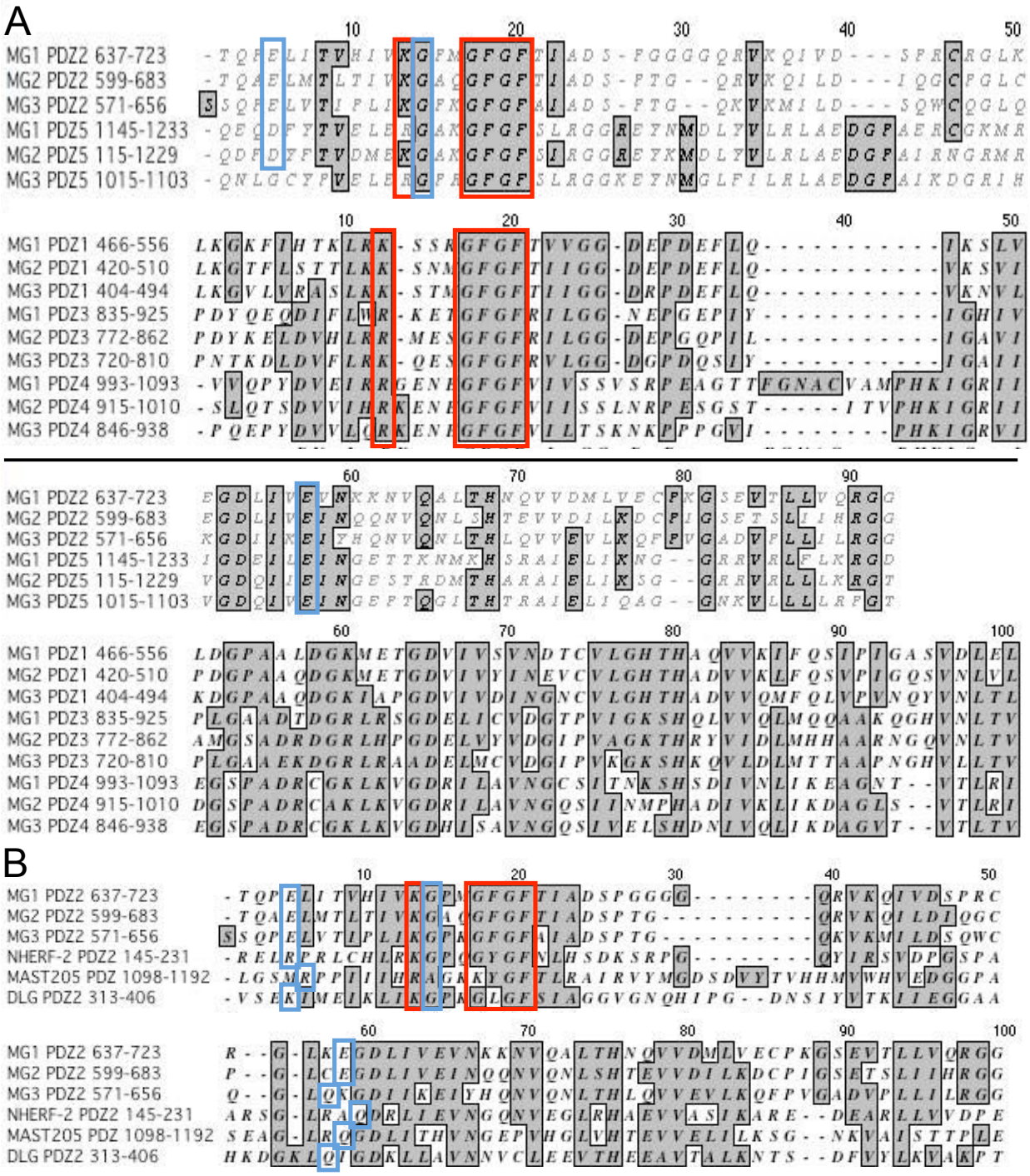

Figure 5.1: Comparison of CUSTLAW sequence alignments of PDZ domain sequences that bind to PTEN with those that do not to identify residues that may confer specificity towards PTEN. **A**, Comparison of the MAGI PDZ domains that bind PTEN (PDZ2 and PDZ5) with other MAGI PDZ domains that do not bind PTEN (PDZ1, PDZ3 and PDZ4). The blue boxes represent amino acids that are conserved in the PDZ2 and PDZ5 domain of MAGI-1 (MG1), MAGI-2 (MG2) and MAGI-3 (MG3). The amino acids representing the carboxylate binding loop are highlighted in red. **B**, PDZ domains from NHERF, MAST205 and DLG that have been shown to bind to PTEN PDZ binding motif.

experiment was performed to determine whether or not p85 could immunoprecipitate with MAGI-2, which showed negative results (Figure 4.12A and C). This experiment was only done once and therefore, additional experiments are required to make conclusive remarks. p85 has been shown to be present in many complexes such as PTEN/p85 (Chagpar, 2004), p85/p110 that constitutes PI3K (reviewed in Zhao and Vogt, 2008) and associated with RTKs (Figure 5.2) (Besset *et al.,* 2000; Claesson-Welsh 1994; Fry and Waterfield, 1993; Zhang and Broxmeyer, 2000). Therefore only a small percentage of p85 may be available for binding to MAGI-2. p85 does have the ability to bind to the WW domains of MAGI-2 and future work is needed and determine if this interaction can also take place in cells. We could optimize the expression of p85 and MAGI-2 levels in cells by transfecting cells with more cDNA encoding these proteins. We could also try stimulating cells with EGF with smaller times points (i.e. 0, 10, 20, 30, 40, 50, 60 seconds as opposed to 0, 1 and 5 min). We could also try a fluorescence resonance energy transfer approach, as mentioned above, to determine better growth factor stimulation time courses to use in our immunoprecipitation assays.

5.2.3 MAGI-2 and does not associate with RTKs

MAGI proteins have been shown to bind to the C-terminal PDZ binding motifs of several cell surface receptors (Figure 1.17). We set out to test the ability of MAGI-2 to interact with the RTKs: EGFR and PDGFR. Both of these receptors have C-terminal PDZ binding motifs and have been shown to interact with PDZ domains (Buxbaum *et al.,* 2008; Demoulin *et al.,* 2003; Kaech *et al.,* 1998; Lazar *et al.,* 2004; Maudsley *et al.,* 2000). Pull-down assays with endogenously expressed EGFR and PDGFR and all of the PDZ domains of MAGI-2 did not reveal any association between these receptors and the individual PDZ domains (Figure 4.9 and 4.11). The use of endogenously expressed RTKs may not provide a high enough signal to detect minute interactions, if they are in fact taking place. These endogenously expressed RTKs may be interacting with other PDZ containing proteins in the cells, thereby limiting the RTKs available for MAGI-2 interaction. Also, we have assumed that the EGFR expressed in COS-1 cells has an identical or similar PDZ binding motif to that of the human EGFR, which may not be the case. Therefore, we could use cell lysate of human origin that expresses EGFR (such as HEK-293 cells). Or we may need to transiently transfect RTKs in cells in order to detect MAGI-2 and RTK binding. One problem with our pull-down system is that more than

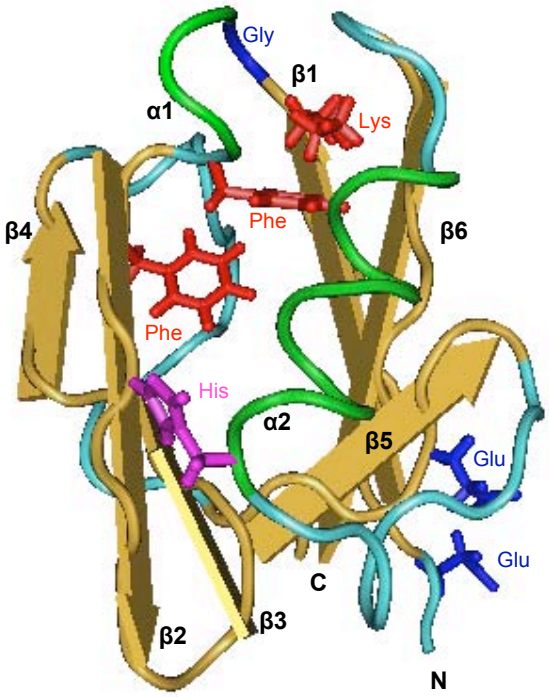

Figure 5.2: NMR solution structure of the PDZ2 domain of MAGI-2 highlighting conserved residues that are hypothesized to make contact with the PTEN protein (PTB ID: 1UJV, Nameki *et al.*, 2003)**.** The conserved residues that may bind PTEN are highlighted in blue. The carboxylate binding loop is highlighted in red, and the His at position α2-1 is highlighted in purple.

one PDZ domain may be required to bind to the dimerized RTK receptor, as it has previously been shown that tandem PDZ domains are required for stronger binding/or higher affinity binding (Mortier *et al.,* 2005; Sugi *et al.,* 2008; Zimmermann *et al.,* 2002, 2005). Since we had problems expressing GST-MAGI-2 FL, it may be beneficial to clone the two halves of the MAGI-2 protein mentioned earlier, in particular, a MAGI-2 protein containing PDZ1-PDZ5 may allow for increased binding opportunities. One last experimental method to detect MAGI-2 PDZ binding to the C-terminal sequence of the EGFR or PDGFR would be to create short peptide sequences that are identical to the EGFR and PDGFR PDZ binding motifs, and test their ability to bind to each of the MAGI-2 PDZ domains. This way we do not need to worry about competitive binding of the purified peptide and PDZ domains. Therefore, we need to continue these experiments in order to confirm MAGI-2 PDZ domain binding, or the lack thereof, to the PDGFR or EGFR.

5.3 The PAC and Akt attenuation

The goal of this project was to determine whether MAGI-2 can act as a scaffolding protein towards PTEN, p85 and RTKs, in order to antagonize PI3K/Akt signalling. This study provides insight into how the PTEN tumor suppressor protein functions in attenuating PI3K/Akt signalling. PTEN is one of the most commonly mutated tumor suppressors in human cancers (Keniry and Parsons, 2008) and therefore it is important to understand its role in PI3K/Akt attenuation. Because MAGI proteins share high sequence similarity and they possess many similar binding partners, understanding the scaffolding function of MAGI-2 may provide a model system for all three MAGI proteins.

MAGI-2 may be responsible for binding to PTEN and bringing it to the plasma membrane at the appropriate location for attenuation of Akt signalling (Figure 5.3). We have shown that MAGI-2 PDZ2 and PDZ5 have the ability to bind to PTEN, thereby potentially increasing the local concentration of PTEN and its ability to attenuate Akt signalling. MAGI-2 WW domains also have the ability to bind to p85, a known positive regulator of PTEN lipid phosphatase activity (Chagpar, 2004; Pastor, 2008). Therefore, MAGI-2 may increase the local concentration of PTEN and p85 at sites important for Akt activation and improve the ability of PTEN to attenuate Akt signalling. MAGI-2 binding to p85 may also provide a mechanism

where MAGI-2 can bind to activated receptor through PI3K (Figure 5.3). As a result, MAGI-2 would be positioned next to PI3K lipid products, thereby making these accessible to PTEN. Therefore, it is currently hypothesized that MAGI-2 recruits PTEN and p85 to the PAC and increases the efficiency of Akt attenuation through PTEN regulation.

5.4 MAGI-2 specific polyclonal antibody

The MAGI group of MAGUK scaffolding proteins share high sequence similarity (Figure 1.6) (Wu *et al.,* 2000b) however, MAGI-2 contains a unique C-terminal sequence (Figure 4.13A) that we termed the GARP C-terminal sequence. We raised a rabbit polyclonal antibody that would recognize the GARP C-terminal sequence of MAGI-2. Many of the published studies on MAGI proteins have used commercially available antibodies that do not distinguish between the MAGI group of scaffolding proteins (Hu *et al.,* 2007; Subauste *et al.,* 2005; Wood *et al.,* 1998; Wu *et al.,* 2000a). Additionally, much of the published work also generated N-terminally tagged MAGI proteins so that they could detect their protein of interest, much like we have done in this project (Figure 4.3). However, N-terminally tagged proteins are transfected and expressed in cells and the overexpression of a protein in cells may show artificial results (Bendig 1988). Therefore, generating a MAGI-2 specific antibody that has the potential to detect endogenous protein could be a useful reagent to provide physiological insights into MAGI-2 function.

We have successfully generated a GARP antigen (Figure 4.13B) that was injected into a rabbit. A dilution of the crude serum had the ability to detect Myc-MAGI-2 expressed in COS-1 cell lysates (Figure 4.13C) and cell lysate control (Figure 4.13D). The next steps we must take with this antibody is to purify it from the crude serum and test its ability to specifically detect endogenous MAGI-2 and not MAGI-1 or MAGI-3.

5.5 Future studies

The goal of future studies is to continue to determine how MAGI-2 affects PTEN attenuation of PI3K/Akt signalling. Now that we have determined that MAGI-2 has the ability to bind to PTEN and p85 *in vitro*, the next step would be to determine if these interactions are also found in cells and has physiological relevance. We could continue studies on determining whether or not PTEN association is dependent on EGF stimulation. Determining the

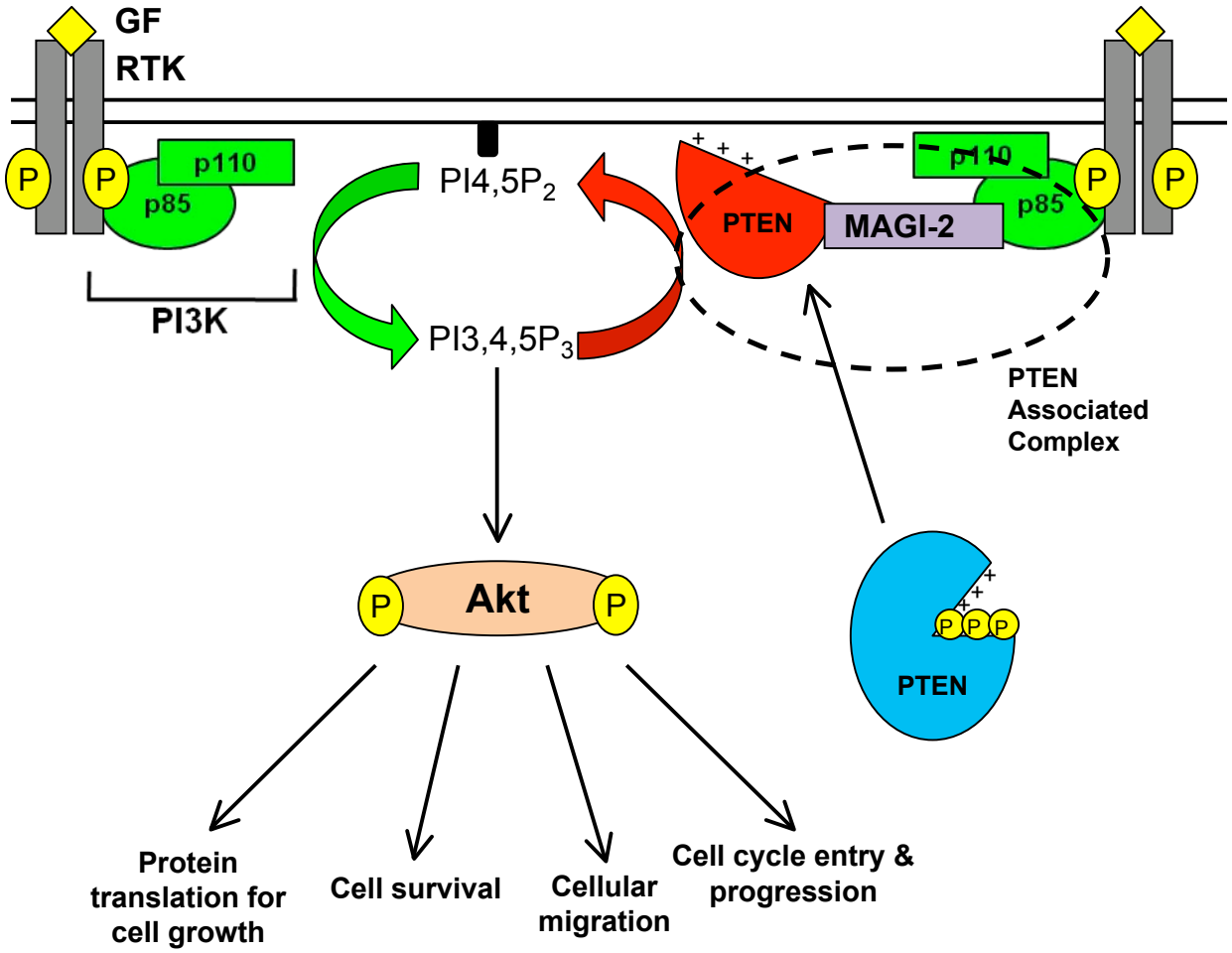

Figure 5.3: The hypothesized role of the PAC in the attenuation of RTK activated Akt signalling. Upon growth factor (GF) stimulation, RTK subunits dimerize and autophosphorylation occurs on the tyrosines. Phosphorylated receptor recruits the PI3K complex to the plasma membrane by binding to the RTK. PI3K phosphorylates $PI4,5P_2$ to $PI3,4,5P_3$ which recruits and activates the Ser/Thr kinase Akt, which in turn activates proteins that promote anti-apoptotic signalling, cell cycle entry and cellular survival. PTEN is present in the cytosol of quiescent cells in its closed conformation. Upon growth factor stimulation, PTEN is believed to localize to the plasma membrane through electrostatic interactions with the plasma membrane and through binding of the PDZ binding motif with PDZ2 and PDZ5 of MAGI-2. The ability of MAGI-2 to bind to two PTEN molecules may enable MAGI-2 to increase the local concentration of PTEN and increase the attenuation efficiency of Akt. The binding of p85 to MAGI-2 may act two fold: to localize MAGI-2 to the appropriate site of PI3K product and to bring together p85 with PTEN, to increase PTEN lipid phosphatase activity towards $PI3,4,5P_2$. Therefore MAGI-2 may act as a scaffolding protein towards the proteins involved in the attenuation of the Akt signalling pathway.

transfection ratio of HA-PTEN and Myc-MAGI-2 that gives optimal expression of both proteins could aid in our immunoprecipitation experiments. We could also determine whether the PDZ and PTEN association are direct by purifying GST-PDZ and His_6-PTEN and performing a pull-down experiment with these purified proteins. Similar transfections experiments could be performed to determine if the WW domains of MAGI-2 and p85 interact in cells and whether this interaction is dependent on EGF stimulation. Similarly, we could purify GST-WW domains and used them in a pull-down assay with His_6-p85 purified protein. We could also generate peptide sequences of the Pro rich sequences within the two Pro rich regions of p85 and perform pull-down assay with purified GST-WW domains to determine which Pro rich sequences have the potential to bind the WW domains of MAGI-2.

To determine if MAGI-2 has the ability to bind to more than one PTEN molecule at a time would be worth pursuing. PDZ domains can only interact with one peptide at a time because the binding pocket can only accommodate the C-terminal end of one peptide (Doyle *et al.,* 1996; Morais Cabral *et al.,* 1996). Therefore, if two PTEN molecules can interact with the MAGI-2 protein, more than one PDZ domain would be involved. To answer the question of whether or not MAGI-2 can bind to more than one PTEN molecule at the same time, an *in vitro* assay could be used (Figure 5.3). We could clone PTEN into a His_6-PTEN expressing plasmid, isolate this fusion protein on a nickel column (Figure 5.4A), pour a purified truncated version of GST-MAGI-2 encoding the PDZ1-PDZ5 sequence (Figure 5.4B) followed by another incubation of a fused maltose binding protein (MBP)-PTEN protein (Figure 5.4C). We would then elute the complex off of the column and resolve the mixture by SDS-PAGE and transfer to nitrocellulose membrane. An immunoblot analysis could be used to detect for the presence of the MBP-PTEN with an MBP antibody. If MAGI-2 can only interact with one PTEN molecule, there would be no detection of the MBP-PTEN (Figure 5.4C). If however MAGI-2 can interact with two PTEN molecules simultaneously, MBP-PTEN will be present (Figure 5.4C). An experiment in the absence of GST-MAGI-2 would be necessary to ensure that His_6-PTEN and MBP-PTEN do not have the ability to associate. If MAGI-2 can interact with two PTEN proteins simultaneously, the MAGI-2 scaffolding protein may be important in increasing the local concentration of PTEN, thereby amplifying the attenuation of Akt signalling. Because we have shown that p85 can associate with both WW domains of MAGI-2, we could test the similar hypothesis that two p85 proteins may bind MAGI-2 simultaneously.

Currently, work is being done on the crystallization of MAGI-2 PDZ2 and PDZ5 domains, and a C-terminal peptide of PTEN that encodes the PDZ binding motif. Once this complex is crystallized, we can determine the important interacting residues between PTEN and the PDZ2 and PDZ5 domains of MAGI-2. From here, we could make more informed decisions on the important contact points between the two proteins and generate mutants that abolish binding between the two. These mutational analyses would be useful in determining important interactions between MAGI-2 and PTEN and its importance in the attenuation of the Akt signalling pathway.

Mutations that can abolish binding of the MAGI-2 scaffolding protein with its respective ligand are important in order to study the importance of the interaction between cell signalling intermediates in signal transduction pathways. Although knockdown and knockout studies have proven to be very useful, small, discrete interruptions through mutational analysis may provide a more accurate picture of what is going on. For example, if we were to knockout or knockdown MAGI proteins, we may see a disruption in the maintenance of cell junctions and the results seen may be a reflection of cell junction interruption and not specifically due to MAGI-2 effects in the attenuation of PI3K/Akt signalling. Also, a knockdown in MAGI proteins may disrupt PTEN stability thereby decreasing PTEN expression in cells. Therefore the reason why PTEN may not be attenuating Akt signalling would not be due to its association and localization with MAGI-2 however, but due to the lack of stability of the protein. Therefore, discrete mutational analysis that disrupts protein-protein interactions may provide useful information on providing a role for MAGI-2 and its binding partners in Akt signalling.

Future work on this project would be to study the scaffolding effects of MAGI-2 and its role in the PTEN attenuation of PI3K/Akt signalling pathway. We have shown that MAGI-2 PDZ2 and PDZ5 have the ability to bind to PTEN and this may increase the local concentration of PTEN at areas of the plasma membrane that is high in $PI3,4,5P_2$ in order to efficiently attenuate Akt signalling. MAGI-2 may also have the ability to bind to p85 and this interaction may work twofold: One, to increase the local concentration of p85, a positive PTEN regulator, in order to increase the ability of PTEN to attenuate Akt signalling, and two, to localize MAGI-2 next to PI3K and its products, $PI3,4,5P_2$, in order to bring PTEN to close proximity to its lipid products. Future work is needed in order to confirm these findings and to test this model in cells and to determine if these interactions are dependent on EGF stimulation.

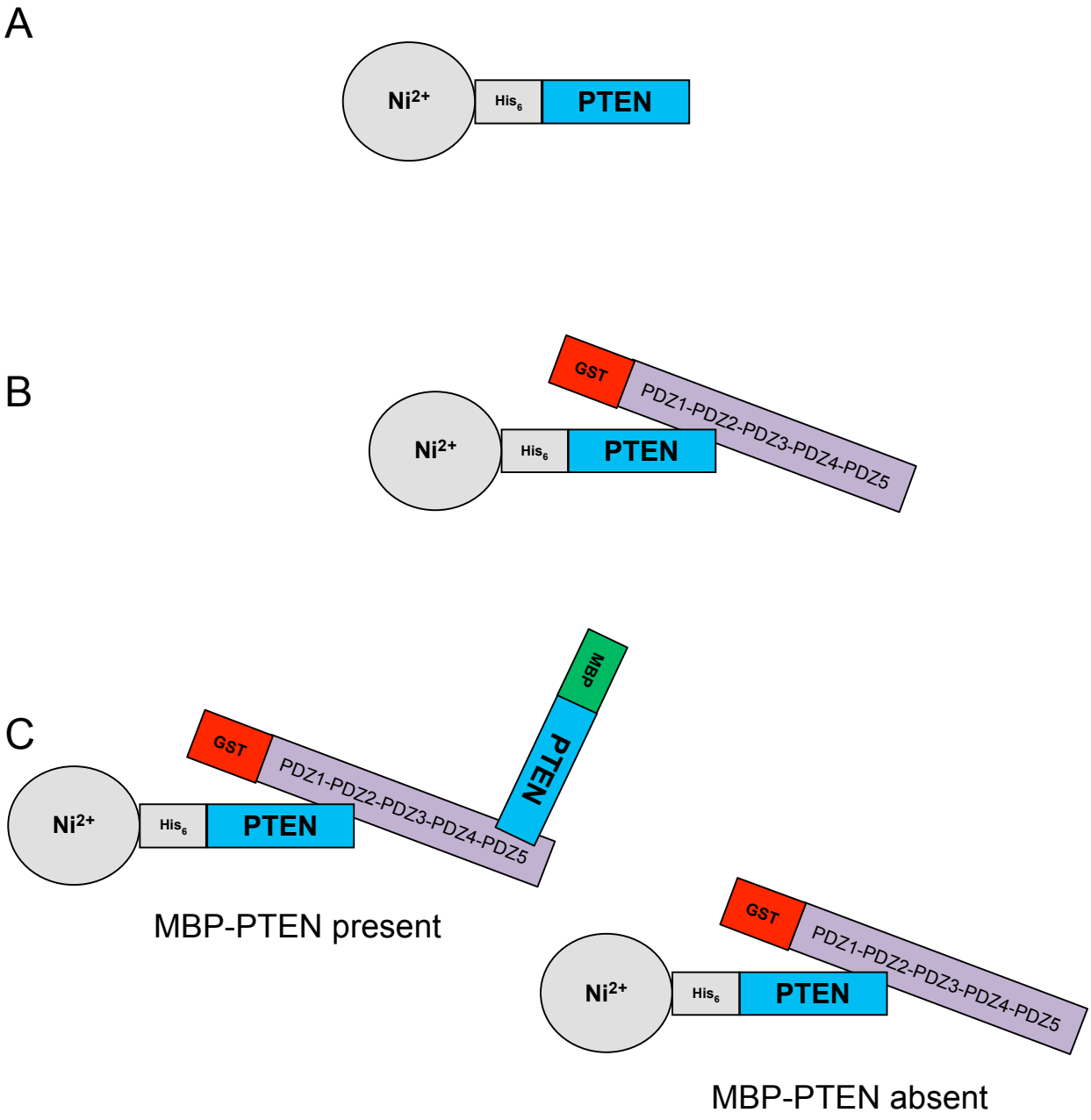

Figure 5.4: Hypothesized experiment to determine if MAGI-2 can bind to two PTEN protein molecules simultaneously. **A**, First, purified His_6-PTEN will be immobilized onto a Ni^{2+} column. **B**, Purified GST-MAGI-2 will be poured into the column and allowed to associate with His_6-PTEN. **C**, Purified MBP-PTEN will be poured on the column to allow binding to MAGI-2. These complexes will be eluted and the elutant will be resolved by SDS-PAGE. Proteins will be transferred to a nitrocellulose membrane and immunobloted with an MBP antibody. If MBP-PTEN is detected, MAGI-2 can interact with two PTEN proteins simultaneously. If MBP-PTEN is absent, MAGI-2 can interact with one PTEN molecule at a time. GST tag is red, His_6 tag is grey and MBP tag is green.

6.0 REFERENCES

Adamsky K., Arnold K., Sabanay H. and Peles E. (2003). Junctional protein MAGI-3 interacts with receptor tyrosine phosphatase beta (RPTP beta) and tyrosine-phosphorylated proteins. J. Cell. Sci. *116,* 1279-1289.

Adell T., Gamulin V., Perović-Ottstadt S., Wiens M., Korzhev M., Müller I. and Müller W.E. (2004). Evolution of metazoan cell junction proteins: The scaffold protein MAGI and the transmembrane receptor tetraspanin in the demosponge *Suberites domuncula*. J. Mol. Evol. *59,* 41-50.

Altschul S.F., Gish W., Miller W., Myers E.W. and Lipman D.J. (1990). Basic local alignment search tool. J. Mol. Biol. *215,* 403-410.

Baneyx F. and Palumbo J.L. (2003). Improving heterologous protein folding via molecular chaperone and foldase co-expression. Meth. Mol. Biol. *205,* 171-197.

Barber D., Alvarado-Kristensson M., González-García A., Pulido R. and Carrera A. (2006). PTEN regulation, a novel function for the p85 subunit of phosphoinositide 3-kinase. Science *2006*, 49-51.

Bastola D., Pahwa G., Lin M.F. and Cheng P.W. (2002). Downregulation of PTEN/MMAC/TEP1 expression in human prostate cancer cell line DU145 by growth stimuli. Mol. Cell. Biochem. *236,* 75-81.

Bendig M.M. (1988). The production of foreign proteins in mammalian cells. Genet. Eng. *7,* 91-127.

Besset V., Scott R.P. and Ibanez C.F. (2000). Signaling complexes and protein-protein interactions involved in the activation of the ras and phosphatidylinositol 3-kinase pathways by the c-ret receptor tyrosine kinase. J. Biol. Chem. *275,* 39159-39166.

Bezprozvanny I. and Maximov A. (2001). Classification of PDZ domains. FEBS Lett. *509,* 457-462.

Birrane G., Chung J. and Ladias J.A. (2003). Novel mode of ligand recognition by the erbin PDZ domain. J. Biol. Chem. *278,* 1399-1402.

Blot V., Perugi F., Gay B., Prévost M., Briant L., Tangy F., Abriel H., Staub O., Dokhélar M. and Pique C. (2004). Nedd4.1-mediated ubiquitination and subsequent recruitment of Tsg101 ensure HTLV-1 gag trafficking towards the multivesicular body pathway prior to virus budding. J. Cell. Sci. *117,* 2357-2367.

Borrell-Pagès M., Fernández-Larrea J., Borroto A., Rojo F., Baselga J. and Arribas J. (2000). The carboxy-terminal cysteine of the tetraspanin L6 antigen is required for its interaction with SITAC, a novel PDZ protein. Mol. Biol. Cell. *11,* 4217-4225.

Brône B. and Eggermont J. (2005). PDZ proteins retain and regulate membrane transporters in polarized epithelial cell membranes. Am. J. Physiol. Cell Physiol. *288,* C20-29.

Bryant P.J. and Woods D.F. (1992). A major palmitoylated membrane protein of human erythrocytes shows homology to yeast guanylate kinase and to the product of a drosophila tumor suppressor gene. Cell *68,* 621-622.

Buxbaum J.D., Georgieva L., Young J.J., Plescia C., Kajiwara Y., Jiang Y., Moskvina V., Norton N., Peirce T., Williams H., Craddock N.J., Carroll L., Corfas G., Davis K.L., Owen M.J., Harroch S., Sakurai T. and O'Donovan M.C. (2008). Molecular dissection of NRG1-ERBB4 signaling implicates PTPRZ1 as a potential schizophrenia susceptibility gene. Mol. Psych. *13,* 162-172.

Cantley L.C. and Neel B.G. (1999). New insights into tumor suppression: PTEN suppresses tumor formation by restraining the phosphoinositide 3-kinase/AKT pathway. Proc. Natl. Acad. Sci. U.S.A. *96,* 4240-4245.

Cereghino G.P. and Cregg J.M. (1999). Applications of yeast in biotechnology: Protein production and genetic analysis. Curr. Opin. Biotechnol. *10,* 422-427.

Cereghino J.L. and Cregg J.M. (2000). Heterologous protein expression in the methylotrophic yeast *Pichia pastoris*. FEMS Microbiol. Rev. *24,* 45-66.

Chagpar R.B. (2004). Role of A-raf and p85 in regulation of the PTEN/PI3K signaling axis. M. Sc. Thesis. *Univeristy of Saskatchewan,* Saskatoon.

Chamberlain M.D., Berry T.R., Pastor M.C. and Anderson D.H. (2004). The p85alpha subunit of phosphatidylinositol 3'-kinase binds to and stimulates the GTPase activity of rab proteins. J. Biol. Chem. *279,* 48607-48614.

Chao H.W., Hong C.J., Huang T.N., Lin Y.L. and Hsueh Y.P. (2008). SUMOylation of the MAGUK protein CASK regulates dendritic spinogenesis. J. Cell Biol. *182,* 141-155.

Chen H.I. and Sudol M. (1995). The WW domain of yes-associated protein binds a Pro-rich ligand that differs from the consensus established for src homology 3-binding modules. Proc. Natl. Acad. Sci. U.S.A. *92,* 7819-7923.

Chi C.N., Engström A., Gianni S., Larsson M. and Jemth P. (2006). Two conserved residues govern the salt and pH dependencies of the binding reaction of a PDZ domain. J. Biol. Chem. *281,* 36811-36818.

Chong, P.A., Lin, H., Wrana, J.L. and Forman-Kay,J.D. (2006). An expanded WW domain recognition motif revealed by the interaction between Smad7 and the E3 ubiquitin ligase Smurf2. J. Biol. Chem. *281*, 17069-17075.

Claesson-Welsh L. (1994). Signal transduction by the PDGF receptors. Prog. Growth Factor Res. *5,* 37-54.

Colledge M., Dean R.A., Scott G.K., Langeberg L.K., Huganir R.L. and Scott J.D. (2000). Targeting of PKA to glutamate receptors through a MAGUK-AKAP complex. Neuron. *27,* 107-119.

Dahia P.L., Aguiar R.C., Alberta J., Kum J.B., Caron S., Sill H., Marsh D.J., Ritz J., Freedman A., Stiles C. and Eng C. (1999). PTEN is inversely correlated with the cell survival factor Akt/PKB and is inactivated via multiple mechanisms in haematological malignancies. Hum. Mol. Genet. *8,* 185-193.

Daly R. and Hearn M.T.W. (2005). Expression of heterologous proteins in *Pichia pastoris*: A useful experimental tool in protein engineering and production. J. Mol. Recognit. *18,* 119-138.

Daniels D.L., Cohen A.R., Anderson J.M. and Brünger A.T. (1998). Crystal structure of the hCASK PDZ domain reveals the structural basis of class II PDZ domain target recognition. Nat. Struct. Biol. *5,* 317-325.

Das S., Cho W. and Dixon J. (2003). Membrane-binding and activation mechanism of PTEN. Proc. Natl. Acad. Sci. U.S.A. *100,* 7491-7496.

Davis M.G. and Huang E.S. (1988). Transfer and expression of plasmids containing human cytomegalovirus immediate-early gene 1 promoter-enhancer sequences in eukaryotic and prokaryotic cells. Biotechnol. Appl. Biochem. *10,* 6-12.

Demoulin J., Seo J.K., Ekman S., Grapengiesser E., Hellman U., Rönnstrand L. and Heldin C. (2003). Ligand-induced recruitment of Na+/H+ exchanger regulatory factor to the PDGF (platelet-derived growth factor) receptor regulates actin cytoskeleton reorganization by PDGF. Biochem. J. *376,* 505-510.

Deng F., Price M.G., Davis C.F., Mori M. and Burgess D.L. (2006). Stargazin and other transmembrane AMPA receptor regulating proteins interact with synaptic scaffolding protein MAGI-2 in brain. J. Neurosci. *26,* 7875-7884.

Dev K.K. (2004). Making protein interactions druggable: Targeting PDZ domains. Nat. Rev. Drug. Discov. *3,* 1047-1056.

Dimitratos S.D., Woods D.F., Stathakis D.G. and Bryant P.J. (1999). Signaling pathways are focused at specialized regions of the plasma membrane by scaffolding proteins of the MAGUK family. BioEssays *21,* 912-921.

Dobrosotskaya I., Guy R.K. and James G.L. (1997). MAGI-1, a membrane-associated guanylate kinase with a unique arrangement of protein-protein interaction domains. J. Biol. Chem. *272,* 31589-31597.

Dobrosotskaya I.Y. (2001). Identification of mNET1 as a candidate ligand for the first PDZ domain of MAGI-1. Biochem. Biophys. Res. Commun. *283,* 969-975.

Dobrosotskaya I.Y. and James G.L. (2000). MAGI-1 interacts with beta-catenin and is associated with cell-cell adhesion structures. Biochem. Biophys. Res. Commun. *270,* 903-909.

dos Reis M., Savva R. and Wernisch L. (2004). Solving the riddle of codon usage preferences: A test for translational selection. Nucleic Acids Res. *32,* 5036-5044.

Doyle D.A., Lee A., Lewis J., Kim E., Sheng M. and MacKinnon R. (1996). Crystal structures of a complexed and peptide-free membrane protein-binding domain: Molecular basis of peptide recognition by PDZ. Cell *85,* 1067-1076.

Elias G.M. and Nicoll R.A. (2007). Synaptic trafficking of glutamate receptors by MAGUK scaffolding proteins. Trends Cell Biol. *17,* 343-352.

Espanel X., Navin N., Kato Y., Tanokura M. and Sudol M. (2003). Probing WW domains to uncover and refine determinants of specificity in ligand recognition. Cytotech. *43,* 105-111.

Ferguson K.M. (2008). Structure-based view of epidermal growth factor receptor regulation. Annu. Rev. Biophys. *37,* 353.

Fleer R. (1992). Engineering yeast for high level expression. Curr. Opin. Biotechnol. *3,* 486-496.

Fouladkou F., Landry T., Kawabe H., Neeb A., Lu C., Brose N., Stambolic V. and Rotin D. (2008). The ubiquitin ligase Nedd4-1 is dispensable for the regulation of PTEN stability and localization. Proc. Natl. Acad. Sci. U.S.A. *105,* 8585-8590.

Franklin J.L., Yoshiura K., Dempsey P.J., Bogatcheva G., Jeyakumar L., Meise K.S., Pearsall R.S., Threadgill D. and Coffey R.J. (2005). Identification of MAGI-3 as a transforming growth factor-alpha tail binding protein. Exp. Cell Res. *303,* 457-470.

Fry M.J. and Waterfield M.D. (1993). Structure and function of phosphatidylinositol 3-kinase: A potential second messenger system involved in growth control. Philos. Trans. R. Soc. Lon. B. Biol. Sci. *340,* 337-344.

Frydman J. (2001). Folding of newly translated proteins in vivo: The role of molecular chaperones. Annu. Rev. Biochem. *70,* 603-647.

Fujii K., Furukawa F. and Matsuyoshi N. (1996). Ligand activation of overexpressed epidermal growth factor receptor results in colony dissociation and disturbed E-cadherin function in HSC-1 human cutaneous squamous carcinoma cells. Exp. Cell Res. *223,* 50-62.

Fujita T., Doihara H., Washio K., Kawasaki K., Takabatake D., Takahashi H., Tsukuda K., Ogasawara Y. and Shimizu N. (2006). Proteasome inhibitor bortezomib increases PTEN expression and enhances trastuzumab-induced growth inhibition in trastuzumab-resistant cells. Anticancer Drugs. *17,* 455-462.

Funke L., Dakoji S. and Bredt D. (2005). Membrane-associated guanylate kinases regulate adhesion and plasticity at cell junctions. Annu. Rev. Biochem. *74,* 219-245.

Gardoni F., Polli F., Cattabeni F. and Di Luca M. (2006). Calcium-calmodulin-dependent protein kinase II phosphorylation modulates PSD-95 binding to NMDA receptors. Eur. J. Neurosci. *24,* 2694-2704.

Garrett T.P., McKern N.M., Lou M., Frenkel M.J., Bentley J.D., Lovrecz G.O., Elleman T.C., Cosgrove L.J. and Ward C.W. (1998). Crystal structure of the first three domains of the type-1 insulin-like growth factor receptor. Nature *394,* 395-399.

Garrett T.P.J., McKern N.M., Lou M., Elleman T.C., Adams T.E., Lovrecz G.O., Zhu H., Walker F., Frenkel M.J., Hoyne P.A., Jorissen R.N., Nice E.C., Burgess A.W. and Ward C.W. (2002). Crystal structure of a truncated epidermal growth factor receptor extracellular domain bound to transforming growth factor alpha. Cell *110,* 763-773.

Gee S.H., Quenneville S., Lombardo C.R. and Chabot J. (2000). Single-amino acid substitutions alter the specificity and affinity of PDZ domains for their ligands. Biochem. *39,* 14638-14646.

Geering, B., Cutillas, P.R. and Vanhaesebroeck, B. (2007). Regulation of class I PI3Ks: Is there a role for monomeric PI3K subunits? Biochem. Soc. Trans. *35,* 199-203.

Georgescu M.M. (2008). NHERF1: Molecular brake on the PI3K pathway in breast cancer. Breast Cancer Res. *10,* 106-107.

Georgescu M.M., Kirsch K.H., Kaloudis P., Yang H., Pavletich N.P. and Hanafusa H. (2000). Stabilization and productive positioning roles of the C2 domain of PTEN tumor suppressor. Cancer Res. *60,* 7033-7038.

Godreau D., Neyroud N., Vrancks R. and Hatem S. (2004). [MAGUKs: Beyond ionic channel anchoring]. Med. Sci. *20,* 84-88.

Gonzalez-Mariscal L., Betanzos A. and Avila-Flores A. (2000). MAGUK proteins: Structure and role in the tight junction. Semin. Cell Dev. Biol. *11,* 315-324.

Gregorc U., Ivanova S., Thomas M., Guccione E., Glaunsinger B., Javier R., Turk V., Banks L. and Turk B. (2007). Cleavage of MAGI-1, a tight junction PDZ protein, by caspases is an important step for cell-cell detachment in apoptosis. Apoptosis *12,* 343-354.

Hanada T., Lin L., Tibaldi E.V., Reinherz E.L. and Chishti A.H. (2000). GAKIN, a novel kinesin-like protein associates with the human homologue of the drosophila discs large tumor suppressor in T lymphocytes. J. Biol. Chem. *275,* 28774-28784.

Hangauer M.J. and Bertozzi C.R. (2008). A FRET-based fluorogenic phosphine for live-cell imaging with the staudinger ligation. Agnew. Chem. Int. Ed. Engl. *47,* 2394-2397.

Harpur A.G., Layton M.J., Das P., Bottomley M.J., Panayotou G., Driscoll P.C. and Waterfield M.D. (1999). Intermolecular interactions of the p85alpha regulatory subunit of phosphatidylinositol 3-kinase. J. Biol. Chem. *274,* 12323-12332.

Harris B.Z., Lau F.W., Fujii N., Guy R.K. and Lim W.A. (2003). Role of electrostatic interactions in PDZ domain ligand recognition. Biochem. *42,* 2797-2805.

Harrison S.C. (1996). Peptide-surface association: The case of PDZ and PTB domains. Cell. *86,* 341-343.

Hazan R.B. and Norton L. (1998). The epidermal growth factor receptor modulates the interaction of E-cadherin with the actin cytoskeleton. J. Biol. Chem. *273,* 9078-9084.

He J. (2006). Proteomic analysis of beta1-adrenergic receptor interactions with PDZ scaffold proteins. J. Biol. Chem. *281,* 2820-2827.

Henry P., Kanelis V., O'Brien M.C., Kim B., Gautschi I., Forman-Kay J., Schild L. and Rotin D. (2003). Affinity and specificity of interactions between Nedd4 isoforms and the epithelial Na+ channel. J. Biol. Chem. *278,* 20019-20028.

Hirano T. and Nishida K. (2003). The role of gab family scaffolding adapter proteins in the signal transduction of cytokine and growth factor receptors. Cancer Sci. *94,* 1029-1033.

Hirao K., Hata Y., Ide N., Takeuchi M., Irie M., Yao I., Deguchi M., Toyoda A., Sudhof T.C. and Takai Y. (1998). A novel multiple PDZ domain-containing molecule interacting with N-methyl-D-aspartate receptors and neuronal cell adhesion proteins. J. Biol. Chem. *273,* 21105-21110.

Hlobilková A., Knillová J., Bártek J., Lukás J. and Kolár Z. (2003). The mechanism of action of the tumour suppressor gene PTEN. Biomed. Pap. Med. Fac. Univ. Palacky Olomouc Czech Repub. *147,* 19-25.

Hock B., Bohme B., Karn T., Feller S., Rubsamen-Waigmann H. and Strebhardt K. (1998). Tyrosine-614, the major autophosphorylation site of the receptor tyrosine kinase HEK2, functions as multi-docking site for SH2-domain mediated interactions. Oncogene *17,* 255-260.

Hoelz A., Janz J.M., Lawrie S.D., Corwin B., Lee A. and Sakmar T.P. (2006). Crystal structure of the SH3 domain of betaPIX in complex with a high affinity peptide from PAK2. J. Mol. Biol. *358,* 509-522.

Hofmann K. and Bucher P. (1995). The rsp5-domain is shared by proteins of diverse functions. FEBS Lett. *358,* 153-157.

Hoover K.B., Liao S.Y. and Bryant P.J. (1998). Loss of the tight junction MAGUK ZO-1 in breast cancer: Relationship to glandular differentiation and loss of heterozygosity. Am. J. Pathol. *153,* 1767-1773.

Hoschuetzky H., Aberle H. and Kemler R. (1994). Beta-catenin mediates the interaction of the cadherin-catenin complex with epidermal growth factor receptor. J. Cell Biol. *127,* 1375-1380.

Hoskins R., Hajnal A.F., Harp S.A. and Kim S.K. (1996). The *C. elegans* vulval induction gene lin-2 encodes a member of the MAGUK family of cell junction proteins. Dev. *122,* 97-111.

Hsueh Y.P., Wang T.F., Yang F.C. and Sheng M. (2000). Nuclear translocation and transcription regulation by the membrane-associated guanylate kinase CASK/LIN-2. Nature *404,* 298-302.

Hu Y., Li Z., Guo L., Wang L., Zhang L., Cai X., Zhao H. and Zha X. (2007). MAGI-2 inhibits cell migration and proliferation via PTEN in human hepatocarcinoma cells. Arch. Biochem. Biophys. *467,* 1-9.

Huang X., Poy F., Zhang R., Joachimiak A., Sudol M. and Eck M.J. (2000). Structure of a WW domain containing fragment of dystrophin in complex with beta-dystroglycan. Nat. Struct. Biol. *7,* 634-638.

Ide N., Hata Y., Deguchi M., Hirao K., Yao I. and Takai Y. (1999). Interaction of S-SCAM with neural plakophilin-related armadillo-repeat protein/delta-catenin. Biochem. Biophys. Res. Commun. *256,* 456-461.

Im Y.J., Park S.H., Rho S., Lee J.H., Kang G.B., Sheng M., Kim E. and Eom S.H. (2003). Crystal structure of GRIP1 PDZ6-peptide complex reveals the structural basis for class II PDZ target recognition and PDZ domain-mediated multimerization. J. Biol. Chem. *278,* 8501-8507.

Ingham R.J., Colwill K., Howard C., Dettwiler S., Lim C.S., Yu J., Hersi K., Raaijmakers J., Gish G., Mbamalu G., Taylor L., Yeung B., Vassilovski G., Amin M., Chen F., Matskova L., Winberg G., Ernberg I., Linding R., O'donnell P., Starostine A., Keller W., Metalnikov P.,

Stark C. and Pawson T. (2005). WW domains provide a platform for the assembly of multiprotein networks. Mol. Cell Biol. *25,* 7092-7106.

Izawa I., Nishizawa M., Hayashi Y. and Inagaki M. (2008). Palmitoylation of ERBIN is required for its plasma membrane localization. Genes to cells *13,* 691-701.

Jeleń F., Oleksy A., Smietana K. and Otlewski J. (2003). PDZ domains - common players in the cell signaling. Acta Biochim. Pol. *50,* 985-1017.

Jemth P. and Gianni S. (2007). PDZ domains: Folding and binding. Biochem. *46,* 8701-8708.

Jin W., Ge W., Xu J., Cao M., Peng L., Yung W., Liao D., Duan S., Zhang M. and Xia J. (2006). Lipid binding regulates synaptic targeting of PICK1, AMPA receptor trafficking, and synaptic plasticity. J. Neurosci. *26,* 2380-2890.

Kachel N., Erdmann K.S., Kremer W., Wolff P., Gronwald W., Heumann R. and Kalbitzer H.R. (2003). Structure determination and ligand interactions of the PDZ2b domain of PTP-bas (hPTP1E): Splicing-induced modulation of ligand specificity. J. Mol. Biol. *334,* 143-155.

Kaech S.M., Whitfield C.W. and Kim S.K. (1998). The LIN-2/LIN-7/LIN-10 complex mediates basolateral membrane localization of the *C. elegans* EGF receptor LET-23 in vulval epithelial cells. Cell *94,* 761-771.

Kanelis V., Bruce M.C., Skrynnikov N.R., Rotin D. and Forman-Kay J.D. (2006). Structural determinants for high-affinity binding in a Nedd4 WW3* domain-comm PY motif complex. Struct. *14,* 543-553.

Kang B.S., Cooper D.R., Devedjiev Y., Derewenda U. and Derewenda Z.S. (2003). Molecular roots of degenerate specificity in syntenin's PDZ2 domain: Reassessment of the PDZ recognition paradigm. Struct. *11,* 845-853.

Kapeller R., Prasad K.V., Janssen O., Hou W., Schaffhausen B.S., Rudd C.E. and Cantley L.C. (1994). Identification of two SH3-binding motifs in the regulatory subunit of phosphatidylinositol 3-kinase. J. Biol. Chem. *269,* 1927-1933.

Kato Y., Miyakawa T., Kurita J. and Tanokura M. (2006). Structure of FBP11 WW1-PL ligand complex reveals the mechanism of proline-rich ligand recognition by group II/III WW domains. J. Biol. Chem. *281,* 40321-40329.

Kato Y., Nagata K., Takahashi M., Lian L., Herrero J.J., Sudol M. and Tanokura M. (2004). Common mechanism of ligand recognition by group II/III WW domains: Redefining their functional classification. J. Biol. Chem. *279,* 31833-31841.

Katsube T., Takahisa M., Ueda R., Hashimoto N., Kobayashi M. and Togashi S. (1998). Cortactin associates with the cell-cell junction protein ZO-1 in both drosophila and mouse. J. Biol. Chem. *273,* 29672-29677.

Kawajiri A., Itoh N., Fukata M., Nakagawa M., Yamaga M., Iwamatsu A. and Kaibuchi K. (2000). Identification of a novel beta-catenin-interacting protein. Biochem. Biophys. Res. Commun. *273,* 712-717.

Kay B.K. and Kehoe J.W. (2004). PDZ domains and their ligands. Chem. Biol. *11,* 423-425.

Keniry M. and Parsons R. (2008). The role of PTEN signaling perturbations in cancer and in targeted therapy. Oncogene *27,* 5477.

Kim E., Naisbitt S., Hsueh Y.P., Rao A., Rothschild A., Craig A. and Sheng M. (1997). GKAP, a novel synaptic protein that interacts with the guanylate kinase-like domain of the PSD-95/SAP90 family of channel clustering molecules. J. Cell Biol. *136,* 669-678.

Kim E. and Sheng M. (2004). PDZ domain proteins of synapses. Nat. Rev. Neurosci. *5,* 771.

Kistner U., Garner C.C. and Linial M. (1995). Nucleotide binding by the synapse associated protein SAP90. FEBS Lett. *359,* 159-163.

Kornau H.C. (2006). GABA(B) receptors and synaptic modulation. Cell Tissue Res. *326,* 517-533.

Kotelevets L., van Hengel J., Bruyneel E., Mareel M., van Roy F. and Chastre E. (2005). Implication of the MAGI-1b/PTEN signalosome in stabilization of adherens junctions and suppression of invasiveness. FASEB J. *19,* 115-117.

Kubota Y., Angelotti T., Niederfellner G., Herbst R. and Ullrich A. (1998). Activation of phosphatidylinositol 3-kinase is necessary for differentiation of FDC-P1 cells following stimulation of type III receptor tyrosine kinases. Cell Growth Differ. *9,* 247-256.

Kuhlendahl S., Spangenberg O., Konrad M., Kim E. and Garner C.C. (1998). Functional analysis of the guanylate kinase-like domain in the synapse-associated protein SAP97. Eur. J. Biochem. *252,* 305-313.

Kurland C.G. (1991). Codon bias and gene expression. FEBS Lett. *285,* 165-169.

Kurland C.G. and Dong H. (1996). Bacterial growth inhibition by overproduction of protein. Mol. Microbiol. *21,* 1-4.

Laemmli U.K. (1970). Cleavage of structural proteins during the assembly of the head of bacteriophage T4. Nature *227,* 680-685.

Lahey T., Gorczyca M., Jia X.X. and Budnik V. (1994). The drosophila tumor suppressor gene dlg is required for normal synaptic bouton structure. Neuron. *13,* 823-835.

Laura R.P., Ross S., Koeppen H. and Lasky L.A. (2002). MAGI-1: A widely expressed, alternatively spliced tight junction protein. Exp. Cell Res. *275,* 155-170.

Lazar C.S., Cresson C.M., Lauffenburger D.A. and Gill G.N. (2004). The Na+ exchanger regulatory factor stabilizes epidermal growth factor receptors at the cell surface. Mol. biol. Cell *15,* 5470-5480.

Lehtonen S., Ryan J.J., Kudlicka K., Iino N., Zhou H. and Farquhar M.G. (2005). Cell junction-associated proteins IQGAP1, MAGI-2, CASK, spectrins, and alpha-actinin are components of the nephrin multiprotein complex. Proc. Natl. Acad. Sci. U.S.A. *102,* 9814-9819.

Li Y., Spangenberg O., Paarmann I., Konrad M. and Lavie A. (2002). Structural basis for nucleotide-dependent regulation of membrane-associated guanylate kinase-like domains. J. Biol. Chem. *277,* 4159-4165.

Li Y., Zhang Y. and Yan H. (1996). Kinetic and thermodynamic characterizations of yeast guanylate kinase. J. Biol. Chem. *271,* 28038-28044.

Liu X. and Pawson T. (1994). Biochemistry of the src protein-tyrosine kinase: Regulation by SH2 and SH3 domains. Recent Prog. Horm. Res. *49,* 149-160.

Loll P.J., Swain E., Chen Y., Turner B.T. and Zhang J. (2008). Structure of the SH3 domain of rat endophilin A2. Acta Crystallogr. Sect. F. Struct. Biol. Cryst. Commun. *64,* 243-246.

Macias M.J., Gervais V., Civera C. and Oschkinat H. (2000). Structural analysis of WW domains and design of a WW prototype. Nat. Struct. Biol. *7,* 375-379.

Macias M.J., Hyvönen M., Baraldi E., Schultz J., Sudol M., Saraste M. and Oschkinat H. (1996). Structure of the WW domain of a kinase-associated protein complexed with a proline-rich peptide. Nature *382,* 646-649.

Madsen K.L., Beuming T., Niv M.Y., Chang C., Dev K.K., Weinstein H. and Gether U. (2005). Molecular determinants for the complex binding specificity of the PDZ domain in PICK1. J. Biol. Chem. *280,* 20539-20548.

Maehama T. and Dixon J.E. (1999). PTEN: A tumour suppressor that functions as a phospholipid phosphatase. Trends Cell Biol. *9,* 125-128.

Martin-García J.M., Luque I., Mateo P.L., Ruiz-Sanz J. and Cámara-Artigas A. (2007). Crystallographic structure of the SH3 domain of the human c-yes tyrosine kinase: Loop flexibility and amyloid aggregation. FEBS Lett. *581,* 1701-1076.

Maudsley S., Zamah A.M., Rahman N., Blitzer J.T., Luttrell L.M., Lefkowitz R.J. and Hall R.A. (2000). Platelet-derived growth factor receptor association with Na(+)/H(+) exchanger regulatory factor potentiates receptor activity. Mol. Cell. Biol. *20,* 8352-8363.

Maximov A., Südhof T.C. and Bezprozvanny I. (1999). Association of neuronal calcium channels with modular adaptor proteins. J. Biol. Chem. *274,* 24453-24456.

McGee A.W. and Bredt D.S. (1999). Identification of an intramolecular interaction between the SH3 and guanylate kinase domains of PSD-95. J. Biol. Chem. *274,* 17431-17436.

McGee A.W., Dakoji S.R., Olsen O., Bredt D.S., Lim W.A. and Prehoda K.E. (2001). Structure of the SH3-guanylate kinase module from PSD-95 suggests a mechanism for regulated assembly of MAGUK scaffolding proteins. Mol. Cell. *8,* 1291-1301.

Mino A., Ohtsuka T., Inoue E. and Takai Y. (2000). Membrane-associated guanylate kinase with inverted orientation (MAGI)-1/brain angiogenesis inhibitor 1-associated protein (BAP1) as a scaffolding molecule for rap small G protein GDP/GTP exchange protein at tight junctions. Genes to Cells *5,* 1009-1016.

Morais-Cabral J.H., Petosa C., Sutcliffe M.J., Raza S., Byron O., Poy F., Marfatia S.M., Chishti A.H. and Liddington R.C. (1996). Crystal structure of a PDZ domain. Nature *382,* 649-652.

Mortier E., Wuytens G., Leenaerts I., Hannes F., Heung M.Y., Degeest G., David G. and Zimmermann P. (2005). Nuclear speckles and nucleoli targeting by PIP2-PDZ domain interactions. EMBO J. *24,* 2556-2565.

Murray D. and Honig B. (2002). Electrostatic control of the membrane targeting of C2 domains. Mol. Cell. *9,* 145-154.

Nadolski M. and Linder M. (2007). Protein lipidation. FEBS J. *274,* 5202-5210.

Nameki, N., Koshiba, S., Kigawa, T. And Yokiyama, S. (2003). Solution structure of the second PDZ domain of human membrane associated guanylate kinase-inverted (Magi-2). RSGI.

Nguyen J.T., Turck C.W., Cohen F.E., Zuckermann R.N. and Lim W.A. (1998). Exploiting the basis of proline recognition by SH3 and WW domains: Design of N-substituted inhibitors. Science *282,* 2088-2092.

Niethammer M., Valtschanoff J.G., Kapoor T.M., Allison D.W., Weinberg R.J., Craig A.M. and Sheng M. (1998). CRIPT, a novel postsynaptic protein that binds to the third PDZ domain of PSD-95/SAP90. Neuron. *20,* 693-707.

Nix S.L., Chishti A.H., Anderson J.M. and Walther Z. (2000). hCASK and hDlg associate in epithelia, and their src homology 3 and guanylate kinase domains participate in both intramolecular and intermolecular interactions. J. Biol. Chem. *275,* 41192-41200.

Nourry C., Grant S.G. and Borg J.P. (2003). PDZ domain proteins: Plug and play! Science *2003*, 7-18

Novak K.A., Fujii N. and Guy R.K. (2002). Investigation of the PDZ domain ligand binding site using chemically modified peptides. Bioorg. Med. Chem. Lett. *12,* 2471-2474.

Ogiso H., Ishitani R., Nureki O., Fukai S., Yamanaka M., Kim J., Saito K., Sakamoto A., Inoue M., Shirouzu M. and Yokoyama S. (2002). Crystal structure of the complex of human epidermal growth factor and receptor extracellular domains. Cell *110,* 775.

Ogura K., Nobuhisa I., Yuzawa S., Takeya R., Torikai S., Saikawa K., Sumimoto H. and Inagaki F. (2006). NMR solution structure of the tandem src homology 3 domains of p47phox complexed with a p22phox-derived proline-rich peptide. J. Biol. Chem. *281,* 3660-3668.

Paarmann I., Spangenberg O., Lavie A. and Konrad M. (2002). Formation of complexes between Ca^{2+} calmodulin and the synapse-associated protein SAP97 requires the SH3 domain-guanylate kinase domain-connecting HOOK region. J. Biol. Chem. *277,* 40832-40838.

Palomares L.A., Estrada-Mondaca S. and Ramírez O.T. (2004). Production of recombinant proteins: Challenges and solutions. Meth. Mol. Biol. *267,* 15-52.

Pan L., Wu H., Shen C., Shi Y., Jin W., Xia J. and Zhang M. (2007). Clustering and synaptic targeting of PICK1 requires direct interaction between the PDZ domain and lipid membranes. EMBO J. *26,* 4576-4587.

Pastor M.C. (2008). Altered regulation of PTEN by mutagenesis and p85 binding. M. Sc. Thesis. *Univeristy of Saskatchewan,* Saskatoon.

Pawson T. (1994). SH2 and SH3 domains in signal transduction. Adv. Cancer Res. *64,* 87-110.

Pawson T., Olivier P., Rozakis-Adcock M., McGlade J. and Henkemeyer M. (1993). Proteins with SH2 and SH3 domains couple receptor tyrosine kinases to intracellular signalling pathways. Philos. Trans. R. Soc. Biol. Sci. *340,* 279-285.

Pawson T. and Schlessingert J. (1993). SH2 and SH3 domains. Curr. Biol. *3,* 434-442.

Pawson T. and Scott J.D. (2005). Protein phosphorylation in signaling--50 years and counting. Trends Biochem. Sci. *30,* 286-290.

Pawson T. and Scott J.D. (1997). Signaling through scaffold, anchoring, and adaptor proteins. Science *278,* 2075-2080.

Pawson T. and Nash P. (2003). Assembly of cell regulatory systems through protein interaction domains. Science *300,* 445-452.

Pendaries C., Tronchre H., Plantavid M. and Payrastre B. (2003). Phosphoinositide signaling disorders in human diseases. FEBS Lett. *546,* 25-31.

Peng T., Zintsmaster J.S., Namanja A.T. and Peng J.W. (2007). Sequence-specific dynamics modulate recognition specificity in WW domains. Nat. Struct. Mol. Biol. *14,* 325-331.

Pires J.R., Parthier C., Aido-Machado R.d., Wiedemann U., Otte L., Böhm G., Rudolph R. and Oschkinat H. (2005). Structural basis for APPTPPPLPP peptide recognition by the FBP11WW1 domain. J. Mol. Biol. *348,* 399-408.

Pisabarro M.T., Serrano L. and Wilmanns M. (1998). Crystal structure of the abl-SH3 domain complexed with a designed high-affinity peptide ligand: Implications for SH3-ligand interactions. J. Mol. Biol. *281,* 513-521.

Planchon S.M., Waite K.A. and Eng C. (2008). The nuclear affairs of PTEN. J. Cell. Sci. *121,* 249-253.

Pleiman C.M., Hertz W.M. and Cambier J.C. (1994). Activation of phosphatidylinositol-3' kinase by src-family kinase SH3 binding to the p85 subunit. Science *263,* 1609-1612.

Rahdar M., Inoue T., Meyer T., Zhang J., Vazquez F. and Devreotes P. (2009). A phosphorylation-dependent intramolecular interaction regulates the membrane association and activity of the tumor suppressor PTEN. Proc. Natl. Acad. Sci. U.S.A. *106,* 480-485.

Reczek D., Berryman M. and Bretscher A. (1997). Identification of EBP50: A PDZ-containing phosphoprotein that associates with members of the ezrin-radixin-moesin family. J. Cell Biol. *139,* 169-179.

Robinson M., Lilley R., Little S., Emtage J.S., Yarranton G., Stephens P., Millican A., Eaton M. and Humphreys G. (1984). Codon usage can affect efficiency of translation of genes in *Escherichia coli*. Nucleic Acids Res. *12,* 6663-6671.

Ross A.H. and Gericke A. (2009). Phosphorylation keeps PTEN phosphatase closed for business. Proc. Natl. Acad. Sci. U.S.A. *106,* 1297-1298.

Samuels B., Hsueh Y.P., Shu T., Liang H., Tseng H.C., Hong C.J., Su S., Volker J., Neve R., Yue D. and Tsai L.H. (2007). Cdk5 promotes synaptogenesis by regulating the subcellular distribution of the MAGUK family member CASK. Neuron. *56,* 823-837.

Schlessinger J. (2000). Cell signaling by receptor tyrosine kinases. Cell *103,* 211-225.

Schlessinger J. (2002). Ligand-induced, receptor-mediated dimerization and activation of EGF receptor. Cell *110,* 669-672.

Schultz J., Copley R.R., Doerks T., Ponting C.P. and Bork P. (2000). SMART: A web-based tool for the study of genetically mobile domains. Nucleic Acids Res. *28,* 231-234.

Shen W., Balajee A., Wang J., Wu H., Eng C., Pandolfi P. and Yin Y. (2007). Essential role for nuclear PTEN in maintaining chromosomal integrity. Cell *128,* 157-170.

Shin H., Hsueh Y.P., Yang F.C., Kim E. and Sheng M. (2000). An intramolecular interaction between src homology 3 domain and guanylate kinase-like domain required for channel clustering by postsynaptic density-95/SAP90. J. Neurosci. *20,* 3580-3587.

Shoji H., Tsuchida K., Kishi H., Yamakawa N., Matsuzaki T., Liu Z., Nakamura T. and Sugino H. (2000). Identification and characterization of a PDZ protein that interacts with activin type II receptors. J. Biol. Chem. *275,* 5485-5492.

Sierralta J. and Mendoza C. (2004). PDZ-containing proteins: Alternative splicing as a source of functional diversity. Brain Res. Rev. *47,* 105-115.

Simpson R. and Parsons L. (2001). PTEN: Life as a tumor suppressor. Exp. Cell Res. *264,* 29-41.

Songyang Z., Fanning A.S., Fu C., Xu J., Marfatia S.M., Chishti A.H., Crompton A., Chan A.C., Anderson J.M. and Cantley L.C. (1997). Recognition of unique carboxyl-terminal motifs by distinct PDZ domains. Science *275,* 73-77.

Subauste M.C., Nalbant P., Adamson E.D. and Hahn K.M. (2005). Vinculin controls PTEN protein level by maintaining the interaction of the adherens junction protein beta-catenin with the scaffolding protein MAGI-2. J. Biol. Chem. *280,* 5676-5681.

Sudbery P.E. (1996). The expression of recombinant proteins in yeasts. Curr. Opin. Biotechnol. *7,* 517-524.

Sudol M. (1996). The WW module competes with the SH3 domain? Trends Biochem. Sci. *21,* 161-163.

Sugi T., Oyama T., Morikawa K. and Jingami H. (2008). Structural insights into the PIP2 recognition by syntenin-1 PDZ domain. Biochem. Biophys. Res. Commun. *366,* 373-378.

Sulis M. and Parsons R. (2003). PTEN: From pathology to biology. Trends Cell Biol. *13,* 478-483.

Sumita K., Sato Y., Iida J., Kawata A., Hamano M., Hirabayashi S., Ohno K., Peles E. and Hata Y. (2007). Synaptic scaffolding molecule (S-SCAM) membrane-associated guanylate kinase

with inverted organization (MAGI)-2 is associated with cell adhesion molecules at inhibitory synapses in rat hippocampal neurons. J. Neurochem. *100,* 154-166.

Suzuki A., de la Pompa J.L., Stambolic V., Elia A.J., Sasaki T., del Barco Barrantes I., Ho A., Wakeham A., Itie A., Khoo W., Fukumoto M. and Mak T.W. (1998). High cancer susceptibility and embryonic lethality associated with mutation of the PTEN tumor suppressor gene in mice. Curr. Biol. *8,* 1169-1178.

Takahashi Y., Morales F., Kreimann E. and Georgescu M. (2006). PTEN tumor suppressor associates with NHERF proteins to attenuate PDGF receptor signaling. EMBO J. *25,* 910-920.

Takano K., Tsuchimori K., Yamagata Y. and Yutani K. (1999). Effect of foreign N-terminal residues on the conformational stability of human lysozyme. Eur. J. Biochem. *266,* 675-682.

Takeuchi M., Hata Y., Hirao K., Toyoda A., Irie M. and Takai Y. (1997). SAPAPs. A family of PSD-95/SAP90-associated proteins localized at postsynaptic density. J. Biol. Chem. *272,* 11943-11951.

Tanemoto M. (2008). MAGI-1a functions as a scaffolding protein for the distal renal tubular basolateral K channels. J. Biol. Chem. *283,* 12241-12247.

Taniguchi C., Aleman J., Ueki K., Luo J., Asano T., Kaneto H., Stephanopoulos G., Cantley L. and Kahn C.R. (2007). The p85alpha regulatory subunit of phosphoinositide 3-kinase potentiates c-jun N-terminal kinase-mediated insulin resistance. Mol. Cell. Biol. *27,* 2830-2840.

Tavares G.A., Panepucci E.H. and Brunger A.T. (2001). Structural characterization of the intramolecular interaction between the SH3 and guanylate kinase domains of PSD-95. Mol. Cell *8,* 1313-1325.

te Velthuis A.J.W., Admiraal J.F. and Bagowski C.P. (2007). Molecular evolution of the MAGUK family in metazoan genomes. BMC Evol. Biol. *7,* 129-139.

Tepass U. and Knust E. (1993). Crumbs and stardust act in a genetic pathway that controls the organization of epithelia in drosophila melanogaster. Dev. Biol. *159,* 311-326.

Tepass U., Theres C. and Knust E. (1990). Crumbs encodes an EGF-like protein expressed on apical membranes of drosophila epithelial cells and required for organization of epithelia. Cell *61,* 787-799.

Tochio H., Zhang Q., Mandal P., Li M. and Zhang M. (1999). Solution structure of the extended neuronal nitric oxide synthase PDZ domain complexed with an associated peptide. Nat. Struct. Biol. *6,* 417-421.

Tolkacheva T., Boddapati M., Sanfiz A., Tsuchida K., Kimmelman A.C. and Chan A.M. (2001). Regulation of PTEN binding to MAGI-2 by two putative phosphorylation sites at threonine 382 and 383. Cancer Res. *61,* 4985-4989.

Tonikian R., Zhang Y., Sazinsky S.L., Currell B., Yeh J., Reva B., Held H.A., Appleton B.A., Evangelista M., Wu Y., Xin X., Chan A.C., Seshagiri S., Lasky L.A., Sander C., Boone C., Bader G.D. and Sidhu S.S. (2008). A specificity map for the PDZ domain family. PLoS Biol. *6,* 2043-2059.

Topinka J.R. and Bredt D.S. (1998). N-terminal palmitoylation of PSD-95 regulates association with cell membranes and interaction with K channel Kv1.4. Neuron. *20,* 125-134.

Torres J. and Pulido R. (2001). The tumor suppressor PTEN is phosphorylated by the protein kinase CK2 at its C terminus. Implications for PTEN stability to proteasome-mediated degradation. J. Biol. Chem. *276,* 993-998.

Trotman L., Alimonti A., Scaglioni P., Koutcher J., Cordon-Cardo C. and Pandolfi P. (2006). Identification of a tumour suppressor network opposing nuclear akt function. Nature *441,* 523-527.

Ueki K., Fruman D., Brachmann S., Tseng Y., Cantley L. and Kahn C.R. (2002). Molecular balance between the regulatory and catalytic subunits of phosphoinositide 3-kinase regulates cell signaling and survival. Mol. Cell. Biol. *22,* 965-977.

Umadevi N., Kumar S. and Narayana N. (2005). Crystallization and preliminary X-ray diffraction studies of the WW4 domain of the Nedd4-2 ubiquitin-protein ligase. Acta Crystallogr. Sect. F Struct. Biol. Cryst. Commun. *61,* 1084-1086.

Vaccaro P., Brannetti B., Montecchi-Palazzi L., Philipp S., Helmer Citterich M., Cesareni G. and Dente L. (2001). Distinct binding specificity of the multiple PDZ domains of INADL, a human protein with homology to INAD from drosophila melanogaster. J. Biol. Chem. *276,* 42122-42130.

Valiente M., Andrés-Pons A., Gomar B., Torres J., Gil A., Tapparel C., Antonarakis S.E. and Pulido R. (2005). Binding of PTEN to specific PDZ domains contributes to PTEN protein stability and phosphorylation by microtubule-associated serine/threonine kinases. J. Biol. Chem. *280,* 28936-28943.

van Ijzendoorn S.C., Mostov K. and Hoekstra D. (2003). Role of rab proteins in epithelial membrane traffic. Int. Rev. Cytol. *232,* 59-88.

van Themsche C., Leblanc V., Parent S. and Asselin E. (2009). XIAP regulates PTEN ubiquitination, content and compartmentalization. J. Biol. Chem. *[ahead of print]*

Vazquez F., Grossman S.R., Takahashi Y., Rokas M.V., Nakamura N. and Sellers W.R. (2001). Phosphorylation of the PTEN tail acts as an inhibitory switch by preventing its recruitment into a protein complex. J. Biol. Chem. *276,* 48627.

Vazquez F., Ramaswamy S., Nakamura N. and Sellers W.R. (2000). Phosphorylation of the PTEN tail regulates protein stability and function. Mol. Cell. Biol. *20,* 5010-5018.

Wang X. and Jiang X. (2008). Post-translational regulation of PTEN. Oncogene *27,* 5454-5463.

Wang X., Trotman L., Koppie T., Alimonti A., Chen Z., Gao Z., Wang J., Erdjument-Bromage H., Tempst P., Cordon-Cardo C., Pandolfi P. and Jiang X. (2007). NEDD4-1 is a proto-oncogenic ubiquitin ligase for PTEN. Cell *128,* 129-139.

Wiesner S., Stier G., Sattler M. and Macias M.J. (2002). Solution structure and ligand recognition of the WW domain pair of the yeast splicing factor Prp40. J. Mol. Biol. *324,* 807-822.

Willott E., Balda M.S., Fanning A.S., Jameson B., van Itallie C. and Anderson J.M. (1993). The tight junction protein ZO-1 is homologous to the drosophila discs-large tumor suppressor protein of septate junctions. Proc. Natl. Acad. Sci. U.S.A. *90,* 7834-7838.

Wisniewska M., Bossenmaier B., Georges G., Hesse F., Dangl M., Knkele K., Ioannidis I., Huber R. and Engh R. (2005). The 1.1 A resolution crystal structure of the p130cas SH3 domain and ramifications for ligand selectivity. J. Mol. Biol. *347,* 1005-1014.

Wood J.D., Yuan J., Margolis R.L., Colomer V., Duan K., Kushi J., Kaminsky Z., Kleiderlein J.J., Sharp A.H. and Ross C.A. (1998). Atrophin-1, the DRPLA gene product, interacts with two families of WW domain-containing proteins. Mol. Cell. Neurosci. *11,* 149-160.

Woodfield R.J., Hodgkin M.N., Akhtar N., Morse M.A., Fuller K.J., Saqib K., Thompson N.T. and Wakelam M.J. (2001). The p85 subunit of phosphoinositide 3-kinase is associated with beta-catenin in the cadherin-based adhesion complex. Biochem. J. *360,* 335-344.

Woods D.F. and Bryant P.J. (1991). The discs-large tumor suppressor gene of drosophila encodes a guanylate kinase homolog localized at septate junctions. Cell *66,* 451-464.

Woods D.F., Hough C., Peel D., Callaini G. and Bryant P.J. (1996). Dlg protein is required for junction structure, cell polarity, and proliferation control in drosophila epithelia. J.Cell Biol. *134,* 1469-1482.

Wu H., Feng W., Chen J., Chan L., Huang S. and Zhang M. (2007). PDZ domains of par-3 as potential phosphoinositide signaling integrators. Mol. Cell. *28,* 886-898.

Wu X., Hepner K., Castelino-Prabhu S., Do D., Kaye M.B., Yuan X.J., Wood J., Ross C., Sawyers C.L. and Whang Y.E. (2000a). Evidence for regulation of the PTEN tumor suppressor

by a membrane-localized multi-PDZ domain containing scaffold protein MAGI-2. Proc. Natl. Acad. Sci. U.S.A. *97,* 4233-4238.

Wu Y., Dowbenko D., Spencer S., Laura R., Lee J., Gu Q. and Lasky L.A. (2000b). Interaction of the tumor suppressor PTEN/MMAC with a PDZ domain of MAGI3, a novel membrane-associated guanylate kinase. J. Biol. Chem. *275,* 21477-21485.

Xu J., Paquet M., Lau A.G., Wood J.D., Ross C.A. and Hall R.A. (2001). Beta 1-adrenergic receptor association with the synaptic scaffolding protein membrane-associated guanylate kinase inverted-2 (MAGI-2) differential regulation of receptor internalization by MAGI-2 and PSD-95. J. Biol. Chem. *276,* 41310-41317.

Xu J. and Xia J. (2006). Structure and function of PICK1. Neuro-Signals *15,* 190-201.

Zhang M. and Wang W. (2003). Organization of signaling complexes by PDZ-domain scaffold proteins. Acc. Chem. Res. *36,* 530-538.

Zhang S. and Broxmeyer H.E. (2000). Flt3 ligand induces tyrosine phosphorylation of gab1 and gab2 and their association with shp-2, grb2, and PI3 kinase. Biochem. Biophys. Res. Commun. *277,* 195-199.

Zhao L. and Vogt P.K. (2008). Class I PI3K in oncogenic cellular transformation. Oncogene *27,* 5486-5496.

Zimmermann P. (2006). The prevalence and significance of PDZ domain-phosphoinositide interactions. Biochim. Biophys. Acta. *1761,* 947-956.

Zimmermann P., Meerschaert K., Reekmans G., Leenaerts I., Small J.V., Vandekerckhove J., David G. and Gettemans J. (2002). PIP(2)-PDZ domain binding controls the association of syntenin with the plasma membrane. Mol. Cell. *9,* 1215-1225.

Zimmermann P., Zhang Z., Degeest G., Mortier E., Leenaerts I., Coomans C., Schulz J., N'Kuli F., Courtoy P.J. and David G. (2005). Syndecan recycling is controlled by syntenin-PIP2 interaction and Arf6. Dev. Cell *9,* 377-388.